

AD-A258 918



①

AFIT/GE/ENG/92D-32

RADAR CROSS SECTION MODELS FOR
LIMITED ASPECT ANGLE WINDOWS

THESIS

Mark Clayton Robinson
Captain, USAFR

AFIT/GE/ENG/92D-32

DTIC
ELECTE
JAN 07 1993
S B D

93-00103

Approved for public release; distribution unlimited

93 1 04 157

AFIT/GE/ENG/92D-32

**RADAR CROSS SECTION MODELS FOR
LIMITED ASPECT ANGLE WINDOWS**

THESIS

**Presented to the Faculty of the School of Engineering
of the Air Force Institute of Technology
Air University
In Partial Fulfillment of the
Requirements for the Degree of
Master of Science in Electrical Engineering**

**Mark Clayton Robinson, B.S.
Captain, USAFR**

December, 1992

Approved for public release; distribution unlimited

Acknowledgements

I thank my thesis advisor, Dr Vittal Pyati for his patience and advice throughout this project. I also thank coworkers Capt Chaz Daly and Mr. Alan Buterbaugh for making valuable suggestions. I especially thank my wife Carla and my sons Sean, Dusty, and Kyle for putting up with me this last year and a half. This thesis is sponsored by the Radar Target Scattering range (RATSCAT) at Holloman AFB, NM and ESC/YV.

Mark C. Robinson

DTIC QUALITY INSPECTED 1

| | |
|----------------------|--|
| Accession For | |
| NTIS GRA&I | <input checked="checked" type="checkbox"/> |
| DTIC TAB | <input type="checkbox"/> |
| Unannounced | <input type="checkbox"/> |
| Justification | |
| By _____ | |
| Distribution/ | |
| Availability Codes | |
| Dist | Avail and/or Special |
| A-1 | |

Table of Contents

| | Page |
|---|------------|
| Table of Contents | iii |
| List of Figures | vii |
| List of Tables | xii |
| Abstract | xiv |
| I. Introduction | 1-1 |
| 1.1 Overview | 1-1 |
| 1.2 Problem Statement | 1-1 |
| 1.3 Assumptions | 1-2 |
| 1.4 Scope | 1-2 |
| 1.5 Approach | 1-3 |
| 1.6 Sequence of Presentation | 1-3 |
| II. Background | 2-1 |
| 2.1 Overview | 2-1 |
| 2.2 RCS Characteristics | 2-1 |
| 2.3 Modeling RCS with Probability Density Functions | 2-3 |
| 2.4 Parameter Estimation | 2-4 |
| 2.5 Goodness-Of-Fit | 2-6 |
| 2.6 Radar Detection | 2-8 |
| 2.7 Summary | 2-12 |

| | Page |
|---|----------------|
| III. Methodology | 3-1 |
| 3.1 Introduction | 3-1 |
| 3.2 Parameter Determination | 3-1 |
| 3.2.1 Rayleigh | 3-1 |
| 3.2.2 Rayleigh Squared | 3-2 |
| 3.2.3 One-Dominant-Plus-Rayleigh | 3-4 |
| 3.2.4 Lognormal | 3-4 |
| 3.2.5 Normal | 3-6 |
| 3.2.6 Beta | 3-7 |
| 3.2.7 Weibull | 3-9 |
| 3.3 Data Inputs | 3-11 |
| 3.4 ASPECT Program Operation | 3-12 |
| 3.4.1 Step 1: Input Prompts | 3-12 |
| 3.4.2 Step 2: Generation of Statistics | 3-12 |
| 3.4.3 Step 3: Parameter Determination | 3-13 |
| 3.4.4 Step 4: PDF and CDF Plots | 3-13 |
| 3.4.5 Step 5: Goodness-of-Fit | 3-14 |
| 3.4.6 Step 6: Optimum Model Determination | 3-15 |
| 3.5 Summary | 3-15 |
| IV. Determination of Optimum RCS Models for Window vs. Full- Range Sample Sets | 4-1 |
| 4.1 Introduction | 4-1 |
| 4.2 Parameter Types | 4-1 |
| 4.2.1 Normal | 4-2 |
| 4.2.2 Lognormal | 4-3 |
| 4.2.3 Weibull | 4-3 |
| 4.2.4 Beta | 4-3 |

| | Page |
|---|---------|
| 4.2.5 Rayleigh Class | 4-5 |
| 4.3 Test Results for Window vs. Full-Range RCS Models | 4-5 |
| 4.3.1 Nose-On Fighter: $\theta = 90^\circ$ | 4-6 |
| 4.3.2 Nose-On Fighter: $\theta = 90^\circ \pm 5^\circ$ | 4-7 |
| 4.3.3 Nose-On Missile: $\theta = 90^\circ$ | 4-8 |
| 4.3.4 Broadside Fighter: $\theta = 90^\circ$ | 4-15 |
| 4.3.5 Broadside Fighter: $\theta = 90^\circ \pm 5^\circ$ | 4-15 |
| 4.3.6 Broadside Missile: $\theta = 90^\circ$ | 4-15 |
| 4.3.7 Tail-On Fighter: $\theta = 90^\circ$ | 4-22 |
| 4.3.8 Tail-On Fighter: $\theta = 90^\circ \pm 5^\circ$ | 4-22 |
| 4.3.9 Tail-On Missile: $\theta = 90^\circ$ | 4-22 |
| 4.4 Summary of Window vs. Full-Range RCS Models | 4-23 |
| V. Determination of Optimum Model for Window vs. Window Comparisons | 5-1 |
| 5.1 Introduction | 5-1 |
| 5.2 Test Results for Window vs. Window RCS Models | 5-1 |
| 5.2.1 Nose-On Fighter: $\theta = 90^\circ$ | 5-1 |
| 5.2.2 Nose-On Fighter: $\theta = 90^\circ \pm 5^\circ$ | 5-2 |
| 5.2.3 Nose-On Missile: $\theta = 90^\circ$ | 5-2 |
| 5.2.4 Broadside Fighter: $\theta = 90^\circ$ | 5-9 |
| 5.2.5 Broadside Fighter: $\theta = 90^\circ \pm 5^\circ$ | 5-9 |
| 5.2.6 Broadside Missile: $\theta = 90^\circ$ | 5-9 |
| 5.2.7 Tail-On Fighter: $\theta = 90^\circ$ | 5-15 |
| 5.2.8 Tail-On Fighter: $\theta = 90^\circ \pm 5^\circ$ | 5-15 |
| 5.2.9 Tail-On Missile: $\theta = 90^\circ$ | 5-16 |
| 5.3 Analysis of Window vs. Window RCS Models | 5-16 |
| 5.3.1 PDF Performance | 5-16 |

| | Page |
|--|-------------|
| 5.3.2 Parameter Estimation | 5-18 |
| 5.3.3 Sample Set Behaviour | 5-18 |
| 5.4 Summary | 5-18 |
| VI. Conclusions and Recommendations | 6-1 |
| 6.0.1 Conclusions | 6-1 |
| 6.0.2 Recommendations | 6-1 |
| Appendix A. Test Statistics and Levels of Significance | A-1 |
| Appendix B. ASPECT RCS Modeling Program | B-1 |
| Bibliography | BIB-1 |

List of Figures

| Figure | Page |
|---|------|
| 2.1. Neyman-Pearson Decision Test | 2-9 |
| 4.1. Normal pdf's response to changes in μ and σ | 4-2 |
| 4.2. Lognormal pdf's response to changes in μ and σ | 4-4 |
| 4.3. Weibull pdf's response to changes in α and β | 4-4 |
| 4.4. Beta pdf's response to changes in α and β | 4-5 |
| 4.5. Rayleigh pdf's response to changes in α | 4-6 |
| 4.6. Top KGFT and CGFT CDF of Fighter Data at Nose-On $\pm 5^\circ$, 0.5° sample interval, $\theta = 90^\circ$, $\theta - \theta$ polarization, 1 GHz Full-Scale | 4-9 |
| 4.7. Top KGFT and CGFT PDF of Fighter Data at Nose-On $\pm 5^\circ$, 0.5° sample interval, $\theta = 90^\circ$, $\theta - \theta$ polarization, 1 GHz Full-Scale | 4-9 |
| 4.8. Top CGFT CDF of Fighter Data at Nose-On $\pm 5^\circ$, 0.5° sample interval, $\theta = 90^\circ$, $\theta - \theta$ polarization, 1 GHz Full-Scale | 4-10 |
| 4.9. Top CGFT PDF of Fighter Data at Nose-On $\pm 5^\circ$, 0.5° sample interval, $\theta = 90^\circ$, $\theta - \theta$ polarization, 1 GHz Full-Scale | 4-10 |
| 4.10. Top KGFT CDF of Fighter Data at Nose-On $\pm 5^\circ$, 0.5° sample interval, $\theta = 90^\circ \pm 5^\circ$, $\theta - \theta$ polarization, 1 GHz Full-Scale | 4-11 |
| 4.11. Top KGFT PDF of Fighter Data at Nose-On $\pm 5^\circ$, 0.5° sample interval, $\theta = 90^\circ \pm 5^\circ$, $\theta - \theta$ polarization, 1 GHz Full-Scale | 4-11 |
| 4.12. Top CGFT CDF of Fighter Data at Nose-On $\pm 5^\circ$, 0.5° sample interval, $\theta = 90^\circ \pm 5^\circ$, $\theta - \theta$ polarization, 1 GHz Full-Scale | 4-12 |
| 4.13. Top CGFT PDF of Fighter Data at Nose-On $\pm 5^\circ$, 0.5° sample interval, $\theta = 90^\circ \pm 5^\circ$, $\theta - \theta$ polarization, 1 GHz Full-Scale | 4-12 |
| 4.14. Top KGFT and CGFT CDF of Missile Data at Nose-On $\pm 5^\circ$, 0.5° sample interval, $\theta = 90^\circ$, $\theta - \theta$ polarization, 18 GHz Full-Scale | 4-13 |
| 4.15. Top KGFT and CGFT PDF of Missile Data at Nose-On $\pm 5^\circ$, 0.5° sample interval, $\theta = 90^\circ$, $\theta - \theta$ polarization, 18 GHz Full-Scale | 4-13 |

| Figure | Page |
|---|------|
| 4.16. Top CGFT CDF of Missile Data at Nose-On $\pm 5^\circ$, 0.5° sample interval, $\theta = 90^\circ$, $\theta - \theta$ polarization, 18 GHz Full-Scale | 4-14 |
| 4.17. Top CGFT PDF of Missile Data at Nose-On $\pm 5^\circ$, 0.5° sample interval, $\theta = 90^\circ$, $\theta - \theta$ polarization, 18 GHz Full-Scale | 4-14 |
| 4.18. Top KGFT and CGFT CDF of Fighter Data at Broadside $\pm 5^\circ$, 0.5° sam- ple interval, $\theta = 90^\circ$, $\theta - \theta$ polarization, 1 GHz Full-Scale | 4-17 |
| 4.19. Top KGFT and CGFT PDF of Fighter Data at Broadside $\pm 5^\circ$, 0.5° sam- ple interval, $\theta = 90^\circ$, $\theta - \theta$ polarization, 1 GHz Full-Scale | 4-17 |
| 4.20. Top CGFT CDF of Fighter Data at Broadside $\pm 5^\circ$, 0.5° sample interval, $\theta = 90^\circ$, $\theta - \theta$ polarization, 1 GHz Full-Scale | 4-18 |
| 4.21. Top CGFT PDF of Fighter Data at Broadside $\pm 5^\circ$, 0.5° sample interval, $\theta = 90^\circ$, $\theta - \theta$ polarization, 1 GHz Full-Scale | 4-18 |
| 4.22. Top KGFT and CGFT CDF of Fighter Data at Nose-On $\pm 5^\circ$, 0.5° sample interval, $\theta = 90^\circ \pm 5^\circ$, $\theta - \theta$ polarization, 1 GHz Full-Scale | 4-19 |
| 4.23. Top KGFT and CGFT PDF of Fighter Data at Nose-On $\pm 5^\circ$, 0.5° sample interval, $\theta = 90^\circ \pm 5^\circ$, $\theta - \theta$ polarization, 1 GHz Full-Scale | 4-19 |
| 4.24. Top KGFT and CGFT CDF of Missile Data at Broadside $\pm 5^\circ$, 0.5° sample interval, $\theta = 90^\circ$, $\theta - \theta$ polarization, 18 GHz Full-Scale | 4-20 |
| 4.25. Top KGFT and CGFT PDF of Missile Data at Broadside $\pm 5^\circ$, 0.5° sample interval, $\theta = 90^\circ$, $\theta - \theta$ polarization, 18 GHz Full-Scale | 4-20 |
| 4.26. Top CGFT CDF of Missile Data at Broadside $\pm 5^\circ$, 0.5° sample interval, $\theta = 90^\circ$, $\theta - \theta$ polarization, 18 GHz Full-Scale | 4-21 |
| 4.27. Top CGFT PDF of Missile Data at Broadside $\pm 5^\circ$, 0.5° sample interval, $\theta = 90^\circ$, $\theta - \theta$ polarization, 18 GHz Full-Scale | 4-21 |
| 4.28. Top KGFT and CGFT CDF of Fighter Data at Tail-On $\pm 5^\circ$, 0.5° sample interval, $\theta = 90^\circ$, $\theta - \theta$ polarization, 1 GHz Full-Scale | 4-25 |
| 4.29. Top KGFT and CGFT PDF of Fighter Data at Tail-On $\pm 5^\circ$, 0.5° sample interval, $\theta = 90^\circ$, $\theta - \theta$ polarization, 1 GHz Full-Scale | 4-25 |
| 4.30. Top CGFT CDF of Fighter Data at Tail-On $\pm 5^\circ$, 0.5° sample interval, $\theta = 90^\circ$, $\theta - \theta$ polarization, 1 GHz Full-Scale | 4-26 |

| Figure | Page |
|--|------|
| 4.31. Top CGFT PDF of Fighter Data at Tail-On $\pm 5^\circ$, 0.5° sample interval, $\theta = 90^\circ$, $\theta - \theta$ polarization, 1 GHz Full-Scale | 4-26 |
| 4.32. Top KGFT CDF of Fighter Data at Tail-On $\pm 5^\circ$, 0.5° sample interval, $\theta = 90^\circ \pm 5^\circ$, $\theta - \theta$ polarization, 1 GHz Full-Scale | 4-27 |
| 4.33. Top KGFT PDF of Fighter Data at Tail-On $\pm 5^\circ$, 0.5° sample interval, $\theta = 90^\circ \pm 5^\circ$, $\theta - \theta$ polarization, 1 GHz Full-Scale | 4-27 |
| 4.34. Top CGFT CDF of Fighter Data at Tail-On $\pm 5^\circ$, 0.5° sample interval, $\theta = 90^\circ \pm 5^\circ$, $\theta - \theta$ polarization, 1 GHz Full-Scale | 4-28 |
| 4.35. Top CGFT PDF of Fighter Data at Tail-On $\pm 5^\circ$, 0.5° sample interval, $\theta = 90^\circ \pm 5^\circ$, $\theta - \theta$ polarization, 1 GHz Full-Scale | 4-28 |
| 4.36. Top KGFT and CGFT CDF of Missile Data at Tail-On $\pm 5^\circ$, 0.5° sample interval, $\theta = 90^\circ$, $\theta - \theta$ polarization, 18 GHz Full-Scale | 4-29 |
| 4.37. Top KGFT and CGFT PDF of Missile Data at Tail-On $\pm 5^\circ$, 0.5° sample interval, $\theta = 90^\circ$, $\theta - \theta$ polarization, 18 GHz Full-Scale | 4-29 |
| 4.38. Top CGFT CDF of Missile Data at Tail-On $\pm 5^\circ$, 0.5° sample interval, $\theta = 90^\circ$, $\theta - \theta$ polarization, 18 GHz Full-Scale | 4-30 |
| 4.39. Top CGFT PDF of Missile Data at Tail-On $\pm 5^\circ$, 0.5° sample interval, $\theta = 90^\circ$, $\theta - \theta$ polarization, 18 GHz Full-Scale | 4-30 |
| 5.1. Top KGFT CDF of Fighter Data at Nose-On $\pm 5^\circ$, 0.5° sample interval, $\theta = 90^\circ$, $\theta - \theta$ polarization, 1 GHz Full-Scale | 5-4 |
| 5.2. Top KGFT PDF of Fighter Data at Nose-On $\pm 5^\circ$, 0.5° sample interval, $\theta = 90^\circ$, $\theta - \theta$ polarization, 1 GHz Full-Scale | 5-4 |
| 5.3. Top CGFT CDF of Fighter Data at Nose-On $\pm 5^\circ$, 0.5° sample interval, $\theta = 90^\circ$, $\theta - \theta$ polarization, 1 GHz Full-Scale | 5-5 |
| 5.4. Top CGFT PDF of Fighter Data at Nose-On $\pm 5^\circ$, 0.5° sample interval, $\theta = 90^\circ$, $\theta - \theta$ polarization, 1 GHz Full-Scale | 5-5 |
| 5.5. Top KGFT CDF of Fighter Data at Nose-On $\pm 5^\circ$, 0.5° sample interval, $\theta = 90^\circ \pm 5^\circ$, $\theta - \theta$ polarization, 1 GHz Full-Scale | 5-6 |
| 5.6. Top KGFT PDF of Fighter Data at Nose-On $\pm 5^\circ$, 0.5° sample interval, $\theta = 90^\circ \pm 5^\circ$, $\theta - \theta$ polarization, 1 GHz Full-Scale | 5-6 |

| Figure | Page |
|--|------|
| 5.7. Top CGFT CDF of Fighter Data at Nose-On $\pm 5^\circ$, 0.5° sample interval, $\theta = 90^\circ \pm 5^\circ$, $\theta - \theta$ polarization, 1 GHz Full-Scale | 5-7 |
| 5.8. Top CGFT PDF of Fighter Data at Nose-On $\pm 5^\circ$, 0.5° sample interval, $\theta = 90^\circ \pm 5^\circ$, $\theta - \theta$ polarization, 1 GHz Full-Scale | 5-7 |
| 5.9. Top KGFT and CDFT CDF of Missile Data at Nose-On $\pm 5^\circ$, 0.5° sample interval, $\theta = 90^\circ$, $\theta - \theta$ polarization, 18 GHz Full-Scale | 5-8 |
| 5.10. Top KGFT and CGFT PDF of Missile Data at Nose-On $\pm 5^\circ$, 0.5° sample interval, $\theta = 90^\circ$, $\theta - \theta$ polarization, 18 GHz Full-Scale | 5-8 |
| 5.11. Top KGFT CDF of Fighter Data at Broadside $\pm 5^\circ$, 0.5° sample interval, $\theta = 90^\circ$, $\theta - \theta$ polarization, 1 GHz Full-Scale | 5-11 |
| 5.12. Top KGFT PDF of Fighter Data at Broadside $\pm 5^\circ$, 0.5° sample interval, $\theta = 90^\circ$, $\theta - \theta$ polarization, 1 GHz Full-Scale | 5-11 |
| 5.13. Top CGFT CDF of Fighter Data at Broadside $\pm 5^\circ$, 0.5° sample interval, $\theta = 90^\circ$, $\theta - \theta$ polarization, 1 GHz Full-Scale | 5-12 |
| 5.14. Top CGFT PDF of Fighter Data at Broadside $\pm 5^\circ$, 0.5° sample interval, $\theta = 90^\circ$, $\theta - \theta$ polarization, 1 GHz Full-Scale | 5-12 |
| 5.15. Top KGFT and CGFT CDF of Fighter Data at Broadside $\pm 5^\circ$, 0.5° sample interval, $\theta = 90^\circ \pm 5^\circ$, $\theta - \theta$ polarization, 1 GHz Full-Scale | 5-13 |
| 5.16. Top KGFT and CGFT PDF of Fighter Data at Broadside $\pm 5^\circ$, 0.5° sample interval, $\theta = 90^\circ \pm 5^\circ$, $\theta - \theta$ polarization, 1 GHz Full-Scale | 5-13 |
| 5.17. Top KGFT and CGFT CDF of Missile Data at Broadside $\pm 5^\circ$, 0.5° sample interval, $\theta = 90^\circ$, $\theta - \theta$ polarization, 18 GHz Full-Scale | 5-14 |
| 5.18. Top KGFT and CGFT PDF of Missile Data at Broadside $\pm 5^\circ$, 0.5° sample interval, $\theta = 90^\circ$, $\theta - \theta$ polarization, 18 GHz Full-Scale | 5-14 |
| 5.19. Top KGFT and CGFT CDF of Fighter Data at Tail-On $\pm 5^\circ$, 0.5° sample interval, $\theta = 90^\circ$, $\theta - \theta$ polarization, 1 GHz Full-Scale | 5-19 |
| 5.20. Top KGFT and CGFT PDF of Fighter Data at Tail-On $\pm 5^\circ$, 0.5° sample interval, $\theta = 90^\circ$, $\theta - \theta$ polarization, 1 GHz Full-Scale | 5-19 |
| 5.21. Top CGFT CDF of Fighter Data at Tail-On $\pm 5^\circ$, 0.5° sample interval, $\theta = 90^\circ$, $\theta - \theta$ polarization, 1 GHz Full-Scale | 5-20 |

| Figure | Page |
|--|------|
| 5.22. Top CGFT PDF of Fighter Data at Tail-On $\pm 5^\circ$, 0.5° sample interval, $\theta = 90^\circ$, $\theta - \theta$ polarization, 1 GHz Full-Scale | 5-20 |
| 5.23. Top KGFT CDF of Fighter Data at Tail-On $\pm 5^\circ$, 0.5° sample interval, $\theta = 90^\circ \pm 5^\circ$, $\theta - \theta$ polarization, 1 GHz Full-Scale | 5-21 |
| 5.24. Top KGFT PDF of Fighter Data at Tail-On $\pm 5^\circ$, 0.5° sample interval, $\theta = 90^\circ \pm 5^\circ$, $\theta - \theta$ polarization, 1 GHz Full-Scale | 5-21 |
| 5.25. Top CGFT CDF of Fighter Data at Tail-On $\pm 5^\circ$, 0.5° sample interval, $\theta = 90^\circ \pm 5^\circ$, $\theta - \theta$ polarization, 1 GHz Full-Scale | 5-22 |
| 5.26. Top CGFT PDF of Fighter Data at Tail-On $\pm 5^\circ$, 0.5° sample interval, $\theta = 90^\circ \pm 5^\circ$, $\theta - \theta$ polarization, 1 GHz Full-Scale | 5-22 |
| 5.27. Top KGFT and CGFT CDF of Missile Data at Tail-On $\pm 5^\circ$, 0.5° sample interval, $\theta = 90^\circ$, $\theta - \theta$ polarization, 18 GHz Full-Scale | 5-23 |
| 5.28. Top KGFT and CGFT PDF of Missile Data at Tail-On $\pm 5^\circ$, 0.5° sample interval, $\theta = 90^\circ$, $\theta - \theta$ polarization, 18 GHz Full-Scale | 5-23 |

List of Tables

| Table | Page |
|--|------|
| 2.1. Probability Density Functions | 2-4 |
| A.1. Fighter: $\theta = 90^\circ$ Kolmogorov Levels of Significance for Window vs. Full-Range, n =number of samples, T_1 =Test Statistic, $W_p=1-\alpha$ Quantile . . | A-2 |
| A.2. Fighter: $\theta = 90^\circ$ Chi-Square Levels of Significance for Window vs. Full-Range, n =number of samples, DoF= Degrees of Freedom, T_1 =Test Statistic, $W_p=1-\alpha$ Quantile | A-3 |
| A.3. Missile: $\theta = 90^\circ$ Kolmogorov Levels of Significance for Window vs. Full-Range, n =number of samples, T_1 =Test Statistic, $W_p=1-\alpha$ Quantile . . | A-4 |
| A.4. Missile: $\theta = 90^\circ$ Chi-Square Levels of Significance for Window vs. Full-Range, n =number of samples, DoF= Degrees of Freedom, T_1 =Test Statistic, $W_p=1-\alpha$ Quantile | A-5 |
| A.5. Fighter: $\theta = 90^\circ \pm 5^\circ$ Kolmogorov Levels of Significance for Window vs. Full-Range, n =number of samples, T_1 =Test Statistic, $W_p=1-\alpha$ Quantile | A-6 |
| A.6. Fighter: $\theta = 90^\circ \pm 5^\circ$ Chi-Square Levels of Significance for Window vs. Full-Range, n =number of samples, DoF= Degrees of Freedom, T_1 =Test Statistic, $W_p=1-\alpha$ Quantile | A-7 |
| A.7. Fighter: $\theta = 90^\circ$ Kolmogorov Levels of Significance for Window vs. Window, n =number of samples, T_1 =Test Statistic, $W_p=1-\alpha$ Quantile | A-8 |
| A.8. Fighter: $\theta = 90^\circ$ Chi-Square Levels of Significance for Window vs. Window, n =number of samples, DoF= Degrees of Freedom, T_1 =Test Statistic, $W_p=1-\alpha$ Quantile | A-9 |
| A.9. Missile: $\theta = 90^\circ$ Kolmogorov Levels of Significance for Window vs. Window, n =number of samples, T_1 =Test Statistic, $W_p=1-\alpha$ Quantile | A-10 |
| A.10. Missile: $\theta = 90^\circ$ Chi-Square Levels of Significance for Window vs. Window, n =number of samples, DoF= Degrees of Freedom, T_1 =Test Statistic, $W_p=1-\alpha$ Quantile | A-11 |
| A.11. Fighter: $\theta = 90^\circ \pm 5^\circ$ Kolmogorov Levels of Significance for Window vs. Window, n =number of samples, T_1 =Test Statistic, $W_p=1-\alpha$ Quantile . | A-12 |

| Table | Page |
|--|------|
| A.12.Fighter: $\theta = 90^\circ \pm 5^\circ$ Chi-Square Levels of Significance for Window vs. Window, n =number of samples, DoF= Degrees of Freedom, T_1 =Test Statistic, $W_p=1-\alpha$ Quantile | A-13 |

Abstract

This thesis presents a method for building static Radar Cross Section (RCS) models of aircraft based on static data taken from limited aspect angle windows. These models statistically characterize static RCS. This is done to show that a limited number of samples can be used to effectively characterize static aircraft RCS.

The aspect angles that the data are taken from are nose-on ($0^\circ \pm 5^\circ$), broadside ($90^\circ \pm 5^\circ$), and tail-on ($180^\circ \pm 5^\circ$). These aspects are chosen because they have the greatest probability of being presented to the point defense radar. However, any aspect angle with any window size can be modeled with the method presented here.

The optimum models are determined by performing both a Kolmogorov and a Chi-Square goodness-of-fit test comparing the static RCS data with a variety of probability density functions (pdf) that are known to be effective at approximating the static RCS of aircraft. The optimum parameter estimator is also determined by the goodness-of-fit tests if there is a difference in pdf parameters obtained by the Maximum Likelihood Estimator (MLE) and the Method of Moments (MoM) estimators. If solving for the MLE results in transcendental equations, numerical methods are used to obtain the parameter estimate.

RADAR CROSS SECTION MODELS FOR LIMITED ASPECT ANGLE WINDOWS

I. Introduction

1.1 Overview

In the problem of detection of aircraft by a radar, statistical models of the radar cross section (RCS) are necessary (Skolnick, 1980:46). The models must take into account the high rate of RCS fluctuation and the large magnitude of the fluctuations that complex shapes, such as aircraft, exhibit as a function of aspect angle. The fluctuating characteristic of RCS can be treated as a random variable and therefore, probability density functions (pdf) can be used to model aircraft RCS (Dowdy, 1991:164). The parameters of the pdfs can be estimated using either measured RCS data from the aircraft itself or theoretical RCS data generated from the electromagnetic reflections of combinations of simple point scatterers (Maffett, 1989:239).

A high rate of amplitude fluctuations requires a correspondingly high sampling rate to model lobe pattern. The Radar Target Scattering range (RATSCAT, Holloman AFB, NM), an Air Force organization responsible for measuring the RCS of aircraft, and the sponsor of this research, is currently required to sample the RCS of static aircraft every 0.1° to meet characterization requirements. RATSCAT would like to determine if the total number of samples can be reduced without affecting the characterization. This thesis will show that good RCS models can be built from limited aspect windows, thus drastically reducing the total number of data samples required.

1.2 Problem Statement

The goals of this thesis are to derive a method for building RCS models using a minimum number of data samples and to determine if there is a consistently superior method of parameter estimation for the models. Minimizing the value of the test statistic

in goodness-of-fit tests, for both parameter estimators of pdfs and the pdfs themselves, should result in acceptable RCS models.

1.3 Assumptions

1. The aircraft RCS data used is from a scale model of a jet fighter, coated with metallic paint. It is assumed that the aircraft is completely symmetrical, so only 180° (one side) of the aircraft is sampled. The missile RCS data is obtained from an actual AIM-9 missile. However, measurement errors distorted the amplitude of one side of the missile relative to the other side.

2. The sampling intervals are assumed to be adequate for RATSCAT standards. The aircraft data is sampled at 0.5° intervals, the missile is sampled at 0.25° intervals.

3. The Maximum Likelihood Estimator (MLE) and the Method of Moments (MoM) are the two most effective parameter estimators.

4. The aircraft and missile data are representative of their class of object. Data from more than one type of jet fighter or missile would be helpful in validating the effectiveness of the results, but were unavailable.

1.4 Scope

This study will investigate the sampling requirements for building a static RCS model. No account of dynamic properties effecting RCS such as wing flutter, pitch and roll, or atmospheric conditions will be taken into account.

The parameters will be estimated using the Maximum Likelihood Estimator and the Method of Moments.

The study will consider two types of targets: a jet fighter aircraft and an air-to-air missile. This will be done to compare the statistical characteristics of the two types of targets.

1.5 Approach

A computer program will form the pdfs using RCS data. The program will compute the MoM and MLE parameters. Theoretical values for MoM and MLE parameters will be determined in Chapter III.

The program will also determine the test statistics for the Kolmogorov and Chi-Square goodness-of-fit tests. Tables are then used to determine the Level of Significance for the parameter estimates, pdfs, and data sets.

Trends in success of types of pdfs and parameter estimators in relation to sample statistics will be analyzed in Chapters IV and V.

1.6 Sequence of Presentation

Chapter II presents background material related to the thesis topic. The chapter also provides support for some of the limitations stated here.

Chapter III outlines the methodology used and specific assumptions implicit in computations required to determine best fit.

Chapter IV provides analysis of RCS models built from limited aspect window versus full-range sample sets.

Chapter V provides analysis of RCS models built from limited aspect window versus limited aspect window sample sets.

Chapter VI presents conclusions drawn from the study and recommends topics for further study.

II. Background

2.1 Overview

This chapter provides a background of radar and statistical concepts used in the topic development in the following chapters.

The radar range equation is the primary means of evaluating radar performance based on the power of the transmitted signal, the gain of the antenna, the wavelength of the transmitted signal, the power of the received signal, and the radar cross section (RCS) of the target. Of all the parameters of the radar range equation, the RCS is the most difficult to specify because it is constantly fluctuating in a random manner. RCS depends upon the size and surface of the target, aspect angle of the target to the radar, motion of the target relative to the radar, frequency of the transmitted signal, and so on (Skolnik, 1980:41).

A radar system can detect and classify an unknown target by comparing characteristics of the received signal with a dictionary of optimized statistical models of various types of targets. The statistical models are developed from RCS data of static models of the aircraft. Statistical characteristics of the data are used to estimate the parameters of probability density functions (pdf).

This chapter will review RCS characteristics, types of probability density functions used to make RCS models, methods of parameter estimation, goodness-of-fit tests, and radar detection techniques.

2.2 RCS Characteristics

When an electromagnetic wave travelling through one medium strikes the surface of a second medium, a portion of the energy of the wave is refracted into the second medium, and the rest of the energy is reflected back into the first medium. The amount of energy that enters each medium depends on two variables: the angle of incidence the wave has with the tangent line of the point of incidence on the second medium and the impedance of the two mediums. Snell's law of reflection states that the angle of reflection from the line

perpendicular to the tangent of the point of incidence equals the angle of incidence to the tangent. However, the angle of reflection refers to the opposite side of the perpendicular line from the angle of incidence. Therefore, the only time energy will be reflected back toward the origin of the wave (the radar) will be if it strikes the second medium perpendicularly. This reflected energy would be the signal a monostatic (one antenna) radar would receive.

For a perpendicular wave, the magnitude of the reflected electrical field is

$$E_r = \frac{(Z_2 - Z_1)E_i}{Z_2 + Z_1}, \quad (2.1)$$

where E_r is the reflected electromagnetic field, E_i is the incident electromagnetic field, Z_2 is the impedance of the second medium, and Z_1 is the impedance of the first medium. A negative value indicates a wave travelling toward the origin of the incident wave (Kraus: 1984, Ch. 10 and 12). For a radar signal, the first medium is air and the second medium is the target (aircraft). Most aircraft have a metallic (low impedance) skin. Air has a high impedance. Therefore, most of the electromagnetic wave is reflected away from the aircraft. Link states that "the Radar Cross Section (RCS) of a target, simply put, is a measure of the electromagnetic energy reflected from the target divided by the electromagnetic energy incident upon the target" (Link, 1983:I-1). A complex target, such as an aircraft, has a variety of surface types. An electromagnetic wave incident upon it will be scattered in many directions. Some portion of the scattering surfaces will reflect the wave back toward the radar. The variety of types of surfaces and distances from the radar of the individual scattering surfaces will cause the reflected waves to possess different phases and amplitudes.

Skolnik states

The relative phases and amplitudes of the echo signals from the individual scattering objects as measured at the radar receiver determine the total cross section. The phases and amplitudes of the individual signals might add to give a large total cross section, or the relationships with one another might result in total cancellation (Skolnik, 1980:38).

The interaction of the multiple scattering surfaces causes the phase of the received signal to fluctuate much more rapidly than the magnitude, as aspect angle is changed

(Knott, et al., 1985:180). For this reason, the phase of the received signal is usually modeled as a random variable having a uniform pdf over the interval $[0, 2\pi]$ (Crispin and Seigel, 1968:395), (Maffett, 1989:218), though this is not always the case (Sandhu and Saylor, 1984:490-507). Assuming a uniform phase distribution and independent scattering surfaces, each surface's phase may be averaged over individually. RCS fluctuates at a slower rate, but it is still practical to treat it as a random variable (Skolnik, 1980:46).

2.3 Modeling RCS with Probability Density Functions

Certain types of pdfs have been found that do a good job of modeling the RCS. The most popular pdfs are Rayleigh functions Swerling used in his four fluctuation models (Swerling, 1960:268-308). One pdf modeled a complex target consisting of many independent scatterers of approximately equal echoing areas:

$$p(x|\alpha) = \frac{x}{\alpha^2} \exp\left(\frac{-x^2}{2\alpha^2}\right), \quad (2.2)$$

$$x \geq 0, \quad (2.3)$$

where x is the RCS and α is a parameter that will be estimated from the RCS statistics. The other pdf modeled one large reflector together with other small reflectors and is named the One-Dominant-Plus-Rayleigh:

$$p(x|\alpha) = \frac{9x^3}{2\alpha^4} \exp\left(\frac{-3x^2}{2\alpha^2}\right), \quad (2.4)$$

$$x \geq 0. \quad (2.5)$$

(DiFranco and Rubin, 1980:Ch. 11). These pdfs are modifications of the chi-square density function of degree of freedom 2 and 4 respectively.

Other pdfs that have been found to exhibit good fit to experimental data are the Beta, Lognormal, Normal, Rayleigh Squared, and Weibull (Maffett, 1989:255), (Dowdy, 1991:165) and are listed in Table 2.1. In this table, x is RCS, y is RCS squared, and α , β , μ , and σ are parameters which are estimated from the RCS statistics.

| Name | PDF | Range |
|------------------|--|--|
| Beta | $p(x \alpha, \beta) = \frac{\Gamma(\alpha+\beta)}{\Gamma(\alpha)\Gamma(\beta)} x^{\alpha-1} (1-x)^{\beta-1}$ | $0 \leq x \leq 1$ $\alpha, \beta > 0$ |
| Lognormal | $p(x \sigma, \mu) = \frac{1}{(x\sigma(2\pi)^{\frac{1}{2}})} \exp[-\frac{(\ln x - \mu)^2}{2\sigma^2}]$ | $\sigma \geq 0$ |
| Normal | $p(x \sigma, \mu) = \frac{1}{\sigma(2\pi)^{\frac{1}{2}}} \exp[-\frac{(x-\mu)^2}{2\sigma^2}]$ | $-\infty \leq x \leq \infty$ |
| Rayleigh Squared | $p(y \alpha) = \frac{1}{2\alpha^2} \exp(-\frac{y^2}{2\alpha^2})$ | $y \geq 0$ |
| Weibull | $p(x \alpha, \beta) = \alpha\beta^{-\alpha} x^{\alpha-1} \exp(-\frac{x}{\beta})^{\alpha}$ | $x > 0$ $\alpha, \beta > 0$ |

Table 2.1. Probability Density Functions

2.4 Parameter Estimation

To optimize the fit of pdfs to the data, the parameters of the pdfs must be optimized. The job of a parameter estimator is to estimate $\bar{\theta}$ (the parameter of the pdf) by determining $\hat{\bar{\theta}}$ (the parameter of the observed data). Two of the most common methods used to estimate parameters are the Method of Moments (MoM) and the Maximum Likelihood Estimator (MLE). The MLE method declares $\hat{\bar{\theta}}$ to be the values of $\bar{\theta}$ that gives the likelihood function $p(\bar{x}|\bar{\theta})$ its maximum value. This is done by taking the first derivative of the likelihood function and setting it equal to zero:

$$\frac{\partial p(\bar{x}|\bar{\theta})}{\partial \bar{\theta}} = 0, \quad (2.6)$$

and solving for $\bar{\theta}$ (Cramer, 1946:499). The second derivative should be examined to determine whether $\bar{\theta}$ is actually a maximum or a minimum. Cramer states

The importance of the method is clearly shown by the two following propositions:

If an efficient estimate $\hat{\bar{\theta}}$ of $\bar{\theta}$ exists, the likelihood equation will have a unique solution equal to $\hat{\bar{\theta}}$.

If a sufficient estimate $\hat{\bar{\theta}}$ of $\bar{\theta}$ exists, any solution of the likelihood equation will be a function of $\hat{\bar{\theta}}$ (Cramer, 1946:499).

An efficient estimate is an unbiased estimate that satisfies the following equation:

$$\frac{\partial \ln p(x|\bar{\theta})}{\partial \bar{\theta}} = k(\hat{\theta} - \bar{\theta}) \quad (2.7)$$

where k is a non-zero function of $\bar{\theta}$. A sufficient estimate is an unbiased estimate that satisfies the following equation:

$$\frac{\partial \ln p(x|\bar{\theta})}{\partial \bar{\theta}} = 0. \quad (2.8)$$

Since the maximum of $\ln p(x|\bar{\theta})$ occurs for the same value of $\bar{\theta}$ as the maximum of $p(x|\bar{\theta})$, the $\hat{\theta}_{MLE}$ will be an efficient and sufficient estimator of $\bar{\theta}$ if $\hat{\theta}_{MLE}$ is unbiased. An estimator is unbiased if the expected value of $\hat{\theta}$ is $\bar{\theta}$:

$$E(\hat{\theta}) = \bar{\theta}. \quad (2.9)$$

Law and Kelton list these desirable statistical properties of MLEs:

1. For most of the common distributions, the MLE is unique; that is, $L(\hat{\beta})$ is strictly greater than $L(\beta)$ for any other value of β ($L(\beta)$ is the likelihood function of β).
2. Although MLEs need not be unbiased, in general, the asymptotic distribution (as $n \rightarrow \infty$) of $\hat{\theta}$ has mean equal to θ (see property 4 below).
3. MLEs are invariant; i.e., if $\phi = h(\theta)$ for some function h , then the MLE of ϕ is $h(\hat{\theta})$. (Unbiasedness is not invariant). For example, the variance of an $\exp(\beta)$ random variable is β^2 , so that the MLE of this variance is $[\bar{x}(n)]^2$.
4. MLEs are asymptotically normally distributed; i.e., $\sqrt{n}(\hat{\theta} - \theta) \xrightarrow{D} N(0, v(\theta))$, where $v(\theta) = \frac{-1}{E(\frac{\partial^2 l}{\partial \theta^2})}$ (the expectation is with respect to x_i , assuming that x_i has the hypothesized distribution) and \xrightarrow{D} denotes convergence in distribution. Furthermore if $\tilde{\theta}$ is any other estimator such that $\sqrt{n}(\tilde{\theta} - \theta) \xrightarrow{D} N(0, \sigma^2)$, then $v(\theta) \leq \sigma^2$. (Thus, MLEs are called best asymptotically normal.)
5. MLEs are strongly consistent; that is, $\lim_{n \rightarrow \infty} \hat{\theta} = \theta$ (with probability of 1) (Law and Kelton, 1982:191).

The Method of Moments determines $\hat{\theta}_i$ by determining the first i moments of the density function (μ_i) and equating each of those moments to the corresponding sample

moments (m_i) of the data. n multiple parameters can be determined by solving n equations simultaneously. The MoM is widely used mainly because it is easy to implement. However, it was shown by Fisher that the asymptotic efficiency of the MoM is not very good (Fisher, 1921:309). This would indicate that the MoM does not generally give parameters with the smallest possible variance from the true parameters (Cramer, 1946:490). The superior efficiency of the MLE would tend to indicate that the MLE should be chosen over the MoM as an estimator if possible. However, for pdfs with multiple parameters, the MLE often results in transcendental equations, in which case numerical methods must be used to determine the parameters. The MoM can then be used as the initial value of an iteration process (Shenton and Bowman, 1977:162). Also, if the MLE parameters are arrived at numerically, depending on the procedure, the arrived at parameters may not have an efficiency as high as the actual MLE estimate. The MoM by itself may then give a better estimate. Finally, there are many pdfs for which the MoM and the MLE give an identical value of $\hat{\theta}$.

2.5 Goodness-Of-Fit

In the last section, parameter variance was mentioned as a tool for determining, a priori, what method of parameter estimation to use to fit a pdf to the observed data. To determine if the observed data really could have been obtained by sampling from the fitted pdf, a goodness-of-fit test is used. This test shows how well a fitted pdf fits the observed data (Lewis and Orav, 1989:140). A goodness-of-fit test works by performing a hypothesis test on the pdf with a null hypothesis of:

H_0 : The x_i 's are independent identically distributed (IID) random variables with distribution function \hat{F} .

The test then finds a test statistic by making some type of comparison between the fitted distribution and the observed data. The test statistic is compared with a range of possible values of the test statistic for a given number of samples. Where the actual test statistic falls in the range determines the level of significance α , which is the maximum probability of rejecting the null hypothesis. Therefore, a higher value of α corresponds to a better cor-

relation between the data and the distribution. There are no set rules for determining what an appropriate Level of Significance is, but a commonly accepted figure is 5% (Otnes and Enochson, 1978:61), (Conover, 1980:Chapters 4 and 5), (Law and Kelton, 1982: Chapter 5).

The two most commonly used goodness-of-fit tests are the Chi-Square and the Kolmogorov tests. The Chi-Square test groups the ordered data into frequency histograms. The test statistic is given by

$$T = \sum_{i=1}^n \frac{(O_i - E_i)^2}{E_i}, \quad (2.10)$$

where O_i is the actual number of observations in bin i and E_i is the expected number of observations. Although the optimum number of histogram intervals has not been determined, Law and Kelton recommend that the probability of an observation occurring in an interval should be as close to identical as possible for all intervals. This is done to make the test unbiased. They also recommend that the expected number of observations E_i be greater than or equal to 5, so that the agreement between the true distribution of T and its asymptotic Chi-Square distribution will not be too small. This is desirable because, if the null hypothesis is true, T converges with the Chi-Square distribution as $n \rightarrow \infty$. The Chi-Square test's chief asset is its applicability to any type of distribution function (Law and Kelton, 1982:197).

The Kolmogorov goodness-of-fit test is the appropriate name of the Kolmogorov-Smirnov goodness-of-fit test when it is applied to comparisons between distributions and observed data. The test statistic is the maximum vertical distance between the observed data and the hypothesized distribution:

$$T = \sup_x |F(x) - S(x)|, \quad (2.11)$$

where $F(x)$ is the hypothesized distribution, $S(x)$ is the empirical distribution of the observed data, and \sup_x indicates the supremum over all x (Conover, 1980:296). The chief advantage of the Kolmogorov test over the Chi-Square test is that it gives exact answers regardless of the sample size, while the Chi-Square test only asymptotically approaches

exactness as the number of samples approaches infinity. Therefore, the Kolmogorov test is particularly useful for small sample sets (Conover, 1980:296).

Unfortunately, Law and Kelton state that the Kolmogorov goodness-of-fit test is , in general, only applicable to hypothesized distributions whose parameters are determined independently of the observed data. One notable exception is the Weibull distribution function (Law and Kelton, 1982:202). However, Law and Kelton further state, "the effect of this misapplication (using the Kolmogorov test for a distribution with parameters estimated from data) is not well understood" (Law and Kelton, 1982:199). In addition, Breiman states

The effect that this has on the level of the test is not well known. The evidence we have is that the effect is not very important. For moderate to large sample size, it is probably safe to ignore the fact that θ was estimated (Breiman, 1973:213).

There are also many examples of the Kolmogorov test being applied to distributions with estimated parameters (Dowdy, 1991:164), (Maffett, 1989:Ch.12). Because the test is valid for the Weibull distribution and evidently does not cause big problems for other distributions, the results of the Kolmogorov test will be determined along with the Chi-Square test in this study.

2.6 *Radar Detection*

This section demonstrates how RCS models using pdfs are used in radar detection determination. Radar detection is an application of statistical decision theory. DiFranco and Rubin state

The basic elements of a statistical decision problem are: (1) a set of hypotheses that characterize the possible true states of nature; (2) a test in which data are obtained from which we wish to infer the truth; (3) a decision rule that operates on the data to decide in an optimal fashion which hypothesis in fact best describes the true state of nature; (4) a criterion of optimality that reflects the cost of correct and incorrect decisions.

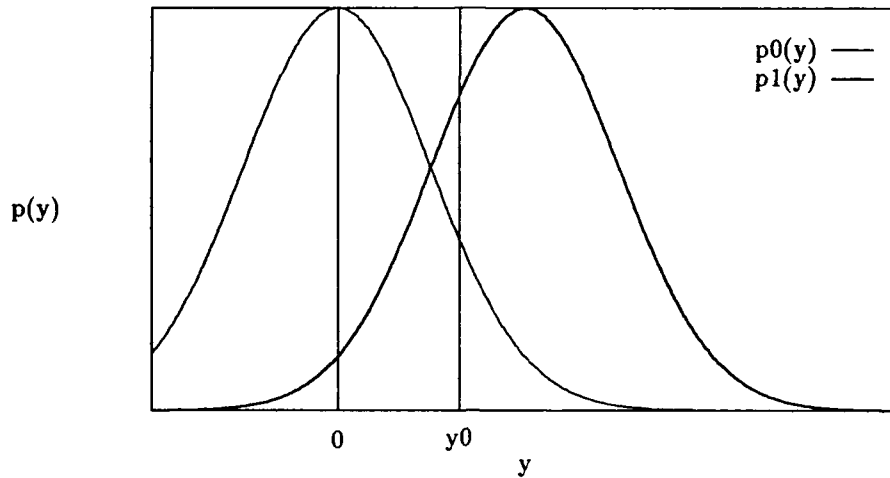


Figure 2.1. Neyman-Pearson Decision Test

(DiFranco and Rubin, 1980:253). For a radar detection problem, the hypotheses are usually

H_0 : Noise only present

H_1 : Signal plus noise is present

There could be further hypotheses if a distinction is to be made over the type of signal present.

The test used to determine which hypothesis is true is called the Likelihood Ratio Test. In this test, a likelihood ratio is formed by the pdfs of the two hypotheses and is compared with a threshold. If the ratio is larger than the threshold, the hypothesis whose pdf formed the numerator of the ratio is declared to be true. If the ratio is less than the threshold, the other hypothesis is declared to be true (Melsa, 1978:25).

There are a variety of methods to determine what the threshold should be. For radar applications, the Neyman-Pearson Test is usually used. This test chooses a value that maximizes the probability of detection P_d , for a given probability of false alarm P_{fa} (Maffett, 1989:275). This method can be understood by examining Figure 1. Assume $p_1(y)$

is the pdf of a signal present plus noise. Assume $p_0(y)$ is the pdf of just noise. If P_{fa} is given a value of α_0 , then

$$\alpha_0 = \int_{y_0}^{\infty} p_0(y) dy \quad (2.12)$$

where y is the magnitude of the received waveform. α_0 and $p_0(y)$ are known, so y_0 can be solved for. The value of the threshold λ is then

$$\lambda = \frac{p_1(y_0)}{p_0(y_0)}, \quad (2.13)$$

and the complete Neyman-Pearson test is

$$\Lambda(y) = \frac{p_1(y)}{p_0(y)} \stackrel{H_1}{\underset{H_0}{\gtrless}} \lambda, \quad (2.14)$$

where $\Lambda(y)$ represents the likelihood ratio test (LRT). This test reads: choose H_1 if the LRT is greater than λ , choose H_0 if the LRT is less than λ . P_d can be found by integrating $p_1(y)$ over the region of P_{fa} :

$$P_d = \int_{y_0}^{\infty} p_1(y) dy \quad (2.15)$$

(Maffett, 1989:275-277).

If the a priori probabilities of the two hypotheses ($P[H_0]$ and $P[H_1]$) are known, a method called the Bayes Risk test can be used to determine the threshold. Besides $P[H_0]$ and $P[H_1]$, the costs of each of the four possible choices from Figure 1 must be known. The variables for the possible costs are as follows:

- C_{00} : Cost of correct no target
- C_{01} : Cost of miss
- C_{10} : Cost of false alarm
- C_{11} : Cost of correct target present

Usually, C_{00} and C_{11} have a cost of 0. If $C_{00} = C_{11} = 0$ and $C_{01} = C_{10}$, the test is called the ideal observer test. The objective of the Bayes Risk criterion is to minimize Bayes Cost (B):

$$B = C_{00}P[d_0, H_0] + C_{01}P[d_0, H_1] + C_{10}P[d_1, H_0] + C_{11}P[d_1, H_1] \quad (2.16)$$

Assuming $C_{11} = C_{00} = 0$, Melsa and Cohn show the LRT for the Bayes Risk is

$$\Lambda(y) = \frac{p(y|H_1)}{p(y|H_0)} \underset{H_0}{\overset{H_1}{>}} \frac{C_{10}P[H_0]}{C_{01}P[H_1]} \quad (2.17)$$

(Melsa and Cohn, 1978:45). The idea behind the test is that even though the received signal's amplitude would indicate one hypothesis, it is much more important to correctly identify the other hypothesis, so the threshold is skewed to compensate. As an example, assume the job of the LRT is to perform target identification and the two hypotheses are

H_0 : Target is a missile

H_1 : Target is a fighter

The cost variable would then be

C_{00} : Cost of correctly deciding missile

C_{01} : Cost of deciding missile present when fighter present

C_{10} : Cost of deciding fighter present when missile present

C_{11} : Cost of correctly deciding fighter

Assume the cost of incorrectly identifying a missile (C_{10}) is five times higher than the cost of incorrectly identifying a fighter (C_{01}), and that $C_{00} = C_{11} = 0$. Also, assume the a priori probabilities of H_1 and H_0 are equal. Then the LRT would be

$$\Lambda(y) = \frac{p(y|H_1)}{p(y|H_0)} \underset{H_0}{\overset{H_1}{>}} 5. \quad (2.18)$$

Most radar receivers are designed to perform target detection based on a number of observations of a randomly fluctuating waveform. The receivers are usually designed to optimize detection of waveforms that behave according to one of the four Swerling cases for randomly fluctuating waveforms (Skolnik, 1980:46):

Swerling I: Amplitude of an entire pulse train is constant but behaves as a single random variable with a Rayleigh pdf, from scan-to-scan. The phase of each pulse is assumed to be a statistically independent random variable with a uniform pdf.

Swerling II: Similar to Swerling I except the amplitude of each pulse in the pulse train is a statistically independent random variable with a Rayleigh pdf.

Swerling III: Similar to Swerling I except the amplitude of the pulse train is a random variable with a one-dominant-plus-Rayleigh pdf.

Swerling IV: Similar to Swerling III except the amplitude of each pulse in the pulse train is a statistically independent random variable with a one-dominant-plus-Rayleigh pdf.

DiFranco and Rubin show that the optimum detection receiver for these waveforms is a single pulse matched filter followed by an envelope detector, a sampler, an integrator, and finally, a threshold comparator (DiFranco and Rubin, 1980:Ch.10 and 11). Kulp, Maffett, and Dowdy each show that the Rayleigh and the one-dominant-plus-Rayleigh pdfs are not always the optimum pdfs for the Swerling cases (Kulp, 1984:165-183), (Maffett, 1989:280-285), (Dowdy, 1991:167).

2.7 Summary

This chapter presented a description of the nature of RCS and how it is used in radar detection systems. In doing so, the importance of the pdf was demonstrated, along with methods of optimizing the pdf in the Likelihood Ratio Test.

III. Methodology

3.1 Introduction

This chapter introduces a method to determine the optimum pdf and parameter estimator for any range of aspect angle needed. Assumptions made will be explained as they arise. The MoM and MLE estimators will be determined for all pdfs considered in this thesis. The RCS model generating program "ASPECT" is presented along with the required inputs.

3.2 Parameter Determination

As explained in Chapter II, parameters will be estimated for the Rayleigh, One-Dominant-Plus-Rayleigh, Rayleigh Squared (negative exponential), Lognormal, Normal, Beta, and Weibull pdfs.

3.2.1 Rayleigh The Rayleigh pdf for n independent identically distributed (IID) data samples is defined as (DiFranco and Rubin, 1968:376)

$$p(x_1, x_2, \dots, x_n | \alpha) = \prod_{i=1}^n \frac{x_i}{\alpha^2} \exp\left(\frac{-x_i^2}{2\alpha^2}\right) \quad (3.1)$$

for $x \geq 0$. To determine the MLE estimate of α , a sufficient statistic is found by taking the natural logarithm of both sides of the equation, giving:

$$\ln p(x_1, x_2, \dots, x_n | \alpha) = \ln\left(\sum_{i=1}^n x_i\right) - 2n \ln \alpha - \frac{1}{2\alpha^2} \sum_{i=1}^n x_i^2. \quad (3.2)$$

Taking the first derivative with respect to α and setting it equal to zero gives:

$$\frac{\partial \ln p(x_1, x_2, \dots, x_n | \alpha)}{\partial \alpha} = \frac{-2n}{\alpha} + \frac{1}{\alpha^3} \sum_{i=1}^n x_i^2 \quad (3.3)$$

$$= 0.$$

Solving for α gives:

$$\hat{\alpha}_{MLE} = \left(\frac{1}{2n} \sum_{i=1}^n x_i^2 \right)^{\frac{1}{2}}. \quad (3.4)$$

The MoM estimate of α is found by first determining the second moment of the single sample pdf:

$$\mu_2 = \int_0^{\infty} \frac{x^3}{\alpha^2} \exp\left(\frac{-x^2}{2\alpha^2}\right) dx. \quad (3.5)$$

The solution to this definite integral is found using the CRC integral #662:

$$\int_0^{\infty} x^n \exp(-ax^p) dx = \frac{\Gamma(k)}{pa^k}, \quad (3.6)$$

where $n > -1$, $p > 0$, $a > 0$, and $k = \frac{n+1}{p}$. Thus,

$$\mu_2 = \left(\frac{1}{\alpha^2} \right) \frac{\Gamma(2)}{2\left(\frac{1}{2\alpha^2}\right)^2} \quad (3.7)$$

$$= 2\alpha^2. \quad (3.8)$$

Setting μ_2 equal to the sampled second moment and solving for α gives:

$$\hat{\alpha}_{MoM} = \left(\frac{1}{2n} \sum_{i=1}^n x_i^2 \right)^{\frac{1}{2}}, \quad (3.9)$$

which is identical to $\hat{\alpha}_{MLE}$.

3.2.2 Rayleigh Squared This pdf is found by transforming the random variable x to the random variable $y = x^2$. This is done by substituting y into the Rayleigh pdf for x and multiplying the result by the Jacobian of the transformation,

$$p(y_1, y_2, \dots, y_n | \alpha) = \prod_{i=1}^n \frac{y_i}{\alpha^2} \exp\left(\frac{-y_i^2}{2\alpha^2}\right) \left| \frac{\partial y}{\partial x} \right| \quad (3.10)$$

$$= \prod_{i=1}^n \frac{1}{2\alpha^2} \exp\left(\frac{-y_i^2}{2\alpha^2}\right) \quad (3.11)$$

The MLE estimate of α is found by taking the natural logarithm of both sides, which is

$$\ln p(x_1, x_2, \dots, x_n | \alpha) = -n \ln 2 - 2n \ln \alpha - \frac{1}{2\alpha^2} \sum_{i=1}^n y_i^2. \quad (3.12)$$

Taking the first derivative with respect to α and setting the result equal to zero gives:

$$\frac{\partial \ln p(x_1, x_2, \dots, x_n | \alpha)}{\partial \alpha} = \frac{-2n}{\alpha} + \frac{1}{\alpha^3} \sum_{i=1}^n y_i^2 \quad (3.13)$$

$$= 0.$$

Solving for α gives:

$$\hat{\alpha}_{MLE} = \left(\frac{1}{2n} \sum_{i=1}^n y_i^2 \right)^{\frac{1}{2}} \quad (3.14)$$

$$= \left(\frac{1}{2n} \sum_{i=1}^n x_i^2 \right)^{\frac{1}{2}}, \quad (3.15)$$

which is identical to the MLE for the Rayleigh pdf.

The procedure for finding the MoM estimate of α is identical to the Rayleigh MoM procedure, however the variables in Equation 24 are $n = 5$, $a = \frac{1}{2\alpha^2}$, $p = 2$, and $k = 3$.

Thus,

$$\mu_2 = \left(\frac{1}{\alpha^2} \right) \frac{\Gamma(3)}{2 \left(\frac{1}{2\alpha^2} \right)^3} \quad (3.16)$$

$$= 8\alpha^4. \quad (3.17)$$

Setting μ_2 equal to the sampled second moment and solving for α gives:

$$\hat{\alpha}_{MoM} = \left(\frac{1}{8n} \sum_{i=1}^n x_i^2 \right)^{\frac{1}{4}}. \quad (3.18)$$

Unlike the Rayleigh pdf, the Rayleigh Squared pdf does not have identical MLE and MoM estimates.

3.2.3 One-Dominant-Plus-Rayleigh For n IID data samples, this pdf is defined as (DiFranco and Rubin, 1968:407)

$$p(x_1, x_2, \dots, x_n | \alpha) = \prod_{i=1}^n \frac{9x_i^3}{2\alpha^4} \exp\left(\frac{-3x_i^2}{2\alpha^2}\right), \quad (3.19)$$

$$n \geq 0.$$

Taking the natural logarithm of both sides of the equation gives:

$$\ln p(x_1, x_2, \dots, x_n | \alpha) = n \ln 9 - n \ln 2 - 4n \ln \alpha + 3 \sum_{i=1}^n \ln x_i - \frac{3}{2\alpha^2} \sum_{i=1}^n x_i^2. \quad (3.20)$$

Taking the derivatives of both sides with respect to α gives:

$$\frac{\partial \ln p(x_1, x_2, \dots, x_n | \alpha)}{\partial \alpha} = \frac{-4n}{\alpha} + \frac{3}{\alpha^3} \sum_{i=1}^n x_i^2. \quad (3.21)$$

Setting the result equal to zero and solving for α gives:

$$\hat{\alpha}_{MLE} = \left(\frac{3}{4n} \sum_{i=1}^n x_i^2 \right)^{\frac{1}{2}}. \quad (3.22)$$

As with the Rayleigh pdf, $\hat{\alpha}_{MOM} = \hat{\alpha}_{MLE}$.

3.2.4 Lognormal For n IID data samples, this pdf is defined as (Law and Kelton, 1982:164)

$$p(x_1, x_2, \dots, x_n | \sigma, \mu) = \prod_{i=1}^n \frac{1}{x_i \sigma (2\pi)^{\frac{1}{2}}} \exp\left(\frac{-(\ln x_i - \mu)^2}{2\sigma^2}\right) \quad (3.23)$$

$$x > 0.$$

which is the transformation $y = \ln x$ applied to the Normal pdf. Taking the natural logarithm of both sides gives:

$$\ln p(x_1, x_2, \dots, x_n | \sigma, \mu) = -n \ln \sigma - \frac{n}{2} \ln 2 - \frac{n}{2} \ln \pi - \sum_{i=1}^n \ln x_i \quad (3.24)$$

$$- \frac{1}{2\sigma^2} \sum_{i=1}^n (\ln x_i - \mu)^2. \quad (3.25)$$

Taking the derivative with respect to μ gives:

$$\frac{\partial \ln p(x_1, x_2, \dots, x_n | \sigma, \mu)}{\partial \mu} = \frac{-1}{\sigma^2} \sum_{i=1}^n (\ln x_i - \mu). \quad (3.26)$$

Setting the derivative equal to zero and solving for μ gives:

$$\hat{\mu}_{MLE} = \frac{1}{n} \sum_{i=1}^n \ln x_i. \quad (3.27)$$

Taking the derivative with respect to σ gives:

$$\frac{\partial \ln p(x_1, x_2, \dots, x_n | \sigma, \mu)}{\partial \sigma} = \frac{-n}{\sigma} + \frac{1}{\sigma^3} \sum_{i=1}^n (\ln x_i - \mu)^2. \quad (3.28)$$

Setting the derivative equal to zero and solving for σ gives:

$$\hat{\sigma}_{MLE} = \left(\frac{1}{n} \sum_{i=1}^n (\ln x_i - \hat{\mu})^2 \right)^{\frac{1}{2}}. \quad (3.29)$$

The MoM estimates are found by transforming the lognormal pdf to the normal pdf. If

$$y_1, y_2, \dots, y_n = \ln x_1, \ln x_2, \dots, \ln x_n \quad (3.30)$$

and x_1, x_2, \dots, x_n are lognormally distributed random variables, then y_1, y_2, \dots, y_n have a normal distribution. By definition,

$$\hat{\mu}_{MoM} = \frac{1}{n} \sum_{i=1}^n y_i \quad (3.31)$$

$$= \frac{1}{n} \sum_{i=1}^n \ln x_i \quad (3.32)$$

$$= \hat{\mu}_{MLE}$$

$$\hat{\mu}_{2MoM} = \frac{1}{n} \sum_{i=1}^n y_i^2 \quad (3.33)$$

$$= \frac{1}{n} \sum_{i=1}^n (\ln x_i)^2 \quad (3.34)$$

$$\hat{\sigma}_{MoM} = (\hat{\mu}_{2MoM} - \hat{\mu}_{MoM}^2)^{\frac{1}{2}} \quad (3.35)$$

$$= \left(\frac{1}{n} \sum_{i=1}^n (\ln x_i)^2 - \left(\frac{1}{n} \sum_{i=1}^n \ln x_i \right)^2 \right)^{\frac{1}{2}} \quad (3.36)$$

$$= \hat{\sigma}_{MLE}.$$

3.2.5 Normal For n IID data samples, the Normal pdf is defined as (Law and Kelton, 1982:163)

$$p(x_1, x_2, \dots, x_n | \sigma, \mu) = \frac{1}{\sqrt{2\pi\sigma^2}} \exp\left(\frac{-1}{2\sigma^2} \sum_{i=1}^n (x_i - \mu)^2\right), \quad (3.37)$$

for $-\infty \leq x \leq \infty$. Since the same parameters were determined for the Lognormal pdf, the procedure to arrive at the MLE and MoM Normal parameters will be skipped and the results presented:

$$\hat{\mu}_{MLE} = \hat{\mu}_{MoM} \quad (3.38)$$

$$= \frac{1}{n} \sum_{i=1}^n x_i \quad (3.39)$$

$$\hat{\sigma}_{MLE} = \hat{\sigma}_{MoM} \quad (3.40)$$

$$= \left(\frac{1}{n} \sum_{i=1}^n (x_i - \hat{\mu})^2 \right)^{\frac{1}{2}}. \quad (3.41)$$

3.2.6 *Beta* For n IID data samples, the Beta pdf is defined as (Law and Kelton, 1982:165)

$$p(x_1, x_2, \dots, x_n | \alpha, \beta) = \frac{\Gamma^n(\alpha + \beta)}{\Gamma^n(\alpha)\Gamma^n(\beta)} \left(\prod_{i=1}^n x_i\right)^{\alpha-1} \left(\prod_{i=1}^n (1 - x_i)\right)^{\beta-1} \quad (3.42)$$

for $0 \leq x_1, x_2, \dots, x_n \leq 1$. Taking the natural logarithm of both sides gives:

$$\begin{aligned} \ln p(x_1, x_2, \dots, x_n | \alpha, \beta) &= n \ln \Gamma(\alpha + \beta) - n \ln \Gamma(\alpha) \\ &- n \ln \Gamma(\beta) + (\alpha - 1) \sum_{i=1}^n \ln x_i + (\beta - 1) \sum_{i=1}^n \ln(1 - x_i). \end{aligned} \quad (3.43)$$

Taking the derivative with respect to α and setting the result equal to zero gives:

$$\begin{aligned} \frac{\partial \ln p(x_1, x_2, \dots, x_n | \alpha, \beta)}{\partial \alpha} &= n \frac{\partial \ln \Gamma(\alpha + \beta)}{\partial \alpha} - n \frac{\partial \ln \Gamma(\alpha)}{\partial \alpha} + \sum_{i=1}^n \ln x_i \\ &= 0. \end{aligned} \quad (3.44)$$

Taking the derivative with respect to β and setting the result equal to zero gives:

$$\begin{aligned} \frac{\partial \ln p(x_1, x_2, \dots, x_n | \alpha, \beta)}{\partial \beta} &= n \frac{\partial \ln(\alpha + \beta)}{\partial \beta} - n \frac{\partial \ln(\beta)}{\partial \beta} + \sum_{i=1}^n \ln(1 - x_i) \\ &= 0. \end{aligned} \quad (3.45)$$

Beckman and Tietjen show that equations 3.45 and 3.46 can be rearranged to

$$\Psi(\hat{\alpha}) - \Psi(\hat{\alpha} + \hat{\beta}) = \ln G_1 \quad (3.46)$$

$$\Psi(\hat{\beta}) - \Psi(\hat{\alpha} + \hat{\beta}) = \ln G_2, \quad (3.47)$$

where Ψ is the digamma function and

$$G_1 = \prod_{i=1}^n (x_i)^{\frac{1}{n}} \quad (3.48)$$

$$G_2 = \prod_{i=1}^n (1 - x_i)^{\frac{1}{n}}. \quad (3.50)$$

(Beckman and Tietjen, 1978:253-258). They proceed to show that equations 3.47 and 3.48 can be solved simultaneously, resulting in one equation with one variable:

$$\Psi(\hat{\beta}) - \Psi\{(\Psi^{-1}(\ln G_1 - \ln G_2 + \Psi(\hat{\beta}))) + \hat{\beta}\} - \ln G_2 = 0. \quad (3.51)$$

They give a Fortran root-solving program which, for the assumptions they make, gives six decimal place accuracy. They also give a table of selected G_1 and G_2 values and corresponding $\hat{\alpha}_{MLE}$ and $\hat{\beta}_{MLE}$ values. Law and Kelton expand the table to cover the full range of G_1 and G_2 values (Law and Kelton, 1982:213-214). Values not listed in the tables can be arrived at by interpolation. Beckman and Tietjen claim two decimal place accuracy for this method.

The MoM estimates for α and β can be found without resorting to numerical methods. The mean and variance of the Beta pdf are given as (Law and Kelton, 1982:165):

$$\mu = \frac{\alpha}{\alpha + \beta} \quad (3.52)$$

$$= \frac{1}{n} \sum_{i=1}^n x_i \quad (3.53)$$

$$\sigma^2 = \frac{\alpha\beta}{(\alpha + \beta + 1)(\alpha + \beta)^2} \quad (3.54)$$

$$= \mu_2 - \mu^2. \quad (3.55)$$

Solving for μ_2 gives:

$$\mu_2 = \frac{\alpha\beta}{(\alpha + \beta + 1)(\alpha + \beta)^2} + \frac{\alpha}{\alpha + \beta} \quad (3.56)$$

$$= \frac{\alpha(\alpha + 1)}{(\alpha + \beta)(\alpha + \beta + 1)} \quad (3.57)$$

$$= \frac{1}{n} \sum_{i=1}^n x_i^2. \quad (3.58)$$

Solving equations 3.52 and 3.56 simultaneously for α and β gives:

$$\hat{\alpha}_{MOM} = \frac{\frac{1}{n} \sum_{i=1}^n x_i (\frac{1}{n} \sum_{i=1}^n x_i - \frac{1}{n} \sum_{i=1}^n x_i^2)}{\frac{1}{n} \sum_{i=1}^n x_i^2 - (\frac{1}{n} \sum_{i=1}^n x_i)^2} \quad (3.59)$$

$$\hat{\beta}_{MOM} = \frac{(1 - \frac{1}{n} \sum_{i=1}^n x_i) (\frac{1}{n} \sum_{i=1}^n x_i - \frac{1}{n} \sum_{i=1}^n x_i^2)}{\frac{1}{n} \sum_{i=1}^n x_i^2 - (\frac{1}{n} \sum_{i=1}^n x_i)^2}. \quad (3.60)$$

3.2.7 Weibull For n IID data samples, the Weibull pdf is defined as (Law and Kelton, 1982:163):

$$p(x_1, x_2, \dots, x_n | \alpha, \beta) = \prod_{i=1}^n \alpha \beta^{-\alpha} x_i^{\alpha-1} \exp(-(\frac{x_i}{\beta})^\alpha), \quad (3.61)$$

$$x_i \geq 0. \quad (3.62)$$

Taking the natural logarithm of both sides gives:

$$\ln p(x_1, x_2, \dots, x_n | \alpha, \beta) = n \ln \alpha - n \alpha \ln \beta + (\alpha - 1) \sum_{i=1}^n \ln x_i - \beta^{-\alpha} \sum_{i=1}^n x_i^\alpha. \quad (3.63)$$

Taking the derivative with respect to β gives:

$$\frac{\partial \ln p(x_1, x_2, \dots, x_n | \alpha, \beta)}{\partial \beta} = \frac{-n \alpha}{\beta} + \alpha \beta^{-(\alpha+1)} \sum_{i=1}^n x_i^\alpha. \quad (3.64)$$

Setting the result equal to zero and solving for β gives:

$$\hat{\beta}_{MLE} = (\frac{1}{n} \sum_{i=1}^n x_i^\alpha)^{\frac{1}{\alpha}}. \quad (3.65)$$

Taking the derivative with respect to α gives:

$$\frac{\partial \ln p(x_1, x_2, \dots, x_n | \alpha, \beta)}{\partial \alpha} = \frac{n}{\alpha} - n \ln \beta + \sum_{i=1}^n \ln x_i + \beta^{-\alpha} \ln \beta \sum_{i=1}^n x_i^\alpha \quad (3.66)$$

$$- \beta^{-\alpha} \sum_{i=1}^n x_i^\alpha \ln x_i. \quad (3.67)$$

Setting the result equal to zero, substituting the expression for β in equation 3.65 into β in equation 3.66 and solving for α gives:

$$\hat{\alpha}_{MLE} = \left(\frac{\sum_{i=1}^n x_i^{\hat{\alpha}} \ln x_i}{\sum_{i=1}^n x_i^{\hat{\alpha}}} - \frac{1}{n} \sum_{i=1}^n \ln x_i \right)^{-1}. \quad (3.68)$$

$\hat{\alpha}$ can be solved for numerically, using Newton's Method:

$$x_{n+1} = x_n - \frac{f(x_n)}{f'(x_n)}. \quad (3.69)$$

The resulting equation to find $\hat{\alpha}$ using Newton's Method is

$$\hat{\alpha}_{k+1} = \hat{\alpha}_k + \frac{\frac{1}{n} \sum_{i=1}^n \ln x_i + \frac{1}{\hat{\alpha}_k} - \frac{\sum_{i=1}^n x_i^{\hat{\alpha}_k} \ln x_i}{\sum_{i=1}^n x_i^{\hat{\alpha}_k}}}{\frac{1}{\hat{\alpha}_k^2} + \frac{\frac{\sum_{i=1}^n x_i^{\hat{\alpha}_k}}{\sum_{i=1}^n x_i^{\hat{\alpha}_k} (\ln x_i)^2} - (\sum_{i=1}^n x_i^{\hat{\alpha}_k} \ln x_i)^2}{(\sum_{i=1}^n x_i^{\hat{\alpha}_k})^2}} \quad (3.70)$$

The initial value chosen for $\hat{\alpha}$ can be the MoM value which will be determined next.

The first two moments of the Weibull pdf are (Derman, 1973:386)

$$\mu = \beta \Gamma(1 + \frac{1}{\alpha}) \quad (3.71)$$

$$\mu_2 = \beta^2 \Gamma(1 + \frac{2}{\alpha}). \quad (3.72)$$

Thus,

$$\frac{\mu^2}{\mu_2} = \frac{(\Gamma(1 + \frac{1}{\hat{\alpha}_{MoM}}))^2}{\Gamma(1 + \frac{2}{\hat{\alpha}_{MoM}})} \quad (3.73)$$

$$= \frac{(\frac{1}{n} \sum_{i=1}^n x_i)^2}{\frac{1}{n} \sum_{i=1}^n x_i^2} \quad (3.74)$$

Derman gives a table for determining values of $\frac{1}{\alpha}$ given $\frac{(\Gamma(1+\frac{1}{\alpha}))^2}{\Gamma(1+\frac{2}{\alpha})}$ (Derman, 1973:386). Once $\hat{\alpha}$ is found, $\hat{\beta}$ is given by

$$\hat{\beta}_{MoM} = \frac{\frac{1}{n} \sum_{i=1}^n x_i}{\Gamma(1 + \frac{1}{\hat{\alpha}_{MoM}})}. \quad (3.75)$$

3.3 Data Inputs

The program ASPECT accepts data inputs in $n \times m$ matrix form. This is meant to allow windows of data to be studied. Because the RCS surface map is 3-dimensional, care should be taken when determining window size to prevent data distortion at the window edges. A θ_1 by ϕ_1 size data set can be compared with any θ_2 by ϕ_2 data set, but both data sets must result in rectangular matrices. Every sample interval increment along the θ -axis should be a new row and every increment along the ϕ -axis should be a new column.

ASPECT is designed to build pdf models from static data which are assumed to be Independent Identically Distributed (IID) random variables. Dynamic data may be used if no significant correlation exists between the time samples. If significant correlation exists, the time spacing can be lengthened to a point where there is a maximum acceptable correlation between the time samples. The resulting data should be checked to insure enough samples have been used to represent a statistically significant data base (Dowdy, 1991:165).

Past efforts toward computerized RCS modeling have focused on building models assuming all aspect angles have an equal probability of being presented to a radar. In these cases, data from a narrow range of aspect angles were compared with the whole range of values from the aircraft. The values from the windows tended to be concentrated in one narrow range of the spectrum of the entire data set. This concentration would result in small sample variances at most aspect angles. The mean of the window would vary relative to the full range of values; its size depended on what part of the aircraft was being modeled. In contrast, the mean of the window relative to itself would stay fairly close to the median of the window and the variance would be much larger than the variance of the window compared to full-range data. Henceforth in this study, when parameters are estimated by comparing a localized window of data against the full-range of aircraft data, the comparison will be referred to as Window vs. Full-Range. When the parameters are estimated by comparing a localized window of data with itself, the comparison will be referred to as Window vs. Window. The stability of the mean and large size of the variance for the Window vs. Window data are caused by the fact that the normalization of the data causes the windowed data to cover as many values as the full-range data. A

consequence of the different statistical natures of the Window vs. Full-Range and the Window vs. Window comparisons is that there are differences in the level of effectiveness pdfs have with the two comparisons.

3.4 ASPECT Program Operation

This section gives a step by step explanation of the operation of the ASPECT program.

3.4.1 Step 1: Input Prompts The user is prompted to input the name of the data file to be used, the number of separate windows the full-range of data is to be taken from, and the length and width of each of the full-range windows. The program then linearizes the data, turning it into a single row of values. The data is linearized one row at a time so the position of the modeled window sampled within the full range doesn't shift. The user must determine before hand the beginning and ending linearized sample numbers of the modeled window. This is easily done for a Window vs. Window comparison, since the total one-dimensional length of the full-range is output as the variable 'data'. 'data' would be the ending sample in this case.

The data is normalized as it is input. Because ASPECT performs pdf selection by analyzing the statistical characteristics of a single set of input data, the relative amplitudes of the samples within the set are the only data needed to generate the pdfs. For this reason, normalization can be performed without fear of distorting the empirical distribution of the data. ASPECT normalizes the data because all pdfs except the Normal require minimum sample values of 0, and the Beta pdf requires a maximum sample value of at most 1.

After normalization, the user is prompted for the beginning and ending samples of the modeled window. It is from this sample set that all the statistics used in the pdfs are determined.

3.4.2 Step 2: Generation of Statistics The mean and second moment are the only statistics necessary to determine the parameters of the pdfs.

3.4.3 Step 3: Parameter Determination In this section, the Beta and Weibull parameters are determined. $\hat{\alpha}_{MoM}$ and $\hat{\beta}_{MoM}$ are determined automatically. The subroutine 'interp' is called to determine the Weibull parameters. 'interp' contains Table 3.1 from Derman, which gives values for $\frac{1}{\hat{\alpha}_{MoM}}$ from values of $\frac{m^2}{m_2}$. 'interp' uses linear interpolation to find $\frac{1}{\hat{\alpha}_{MoM}}$, then finds $\hat{\beta}_{MoM}$.

Once the Beta and Weibull MoM parameters are determined, ASPECT asks the user if the MLE parameters are desired for the Beta or Weibull pdfs (MLE parameters equal MoM parameters for all other pdfs). If Weibull MLE is desired, the subroutine 'newton' is called. 'newton' prompts the user for an initial value for $\hat{\alpha}_{MLE}$ ($\hat{\alpha}_{MoM}$ is recommended) and performs a Newton's Method iteration process on equation 3.70 until equation 3.68 is true. If an initial value for $\hat{\alpha}_{MLE}$ is chosen too far from the actual $\hat{\alpha}_{MLE}$, the iterations could run away to infinity, in which case the ASPECT program operation will pause and inform the user that ∞ has been encountered and that 'c' must be entered to break out of the program. If another attempt is made, a good starting point usually turns out to be a value closer to zero than $\hat{\alpha}_{MoM}$.

If the Beta MLE parameters are desired, the 'bmle' subroutine is called. This subroutine performs a double linear interpolation to find $\hat{\alpha}_{MLE}$ and $\hat{\beta}_{MLE}$ from Table 5.12 in Law and Kelton, given G_1 and G_2 as described earlier in this chapter.

If the MLE parameters are produced, they will be the parameters used in the cdf and pdf plots and the goodness-of-fit tests.

3.4.4 Step 4: PDF and CDF Plots After all pdf parameters are determined, the pdfs are plotted individually, as is a histogram of the windowed data. The program can be manipulated to allow multiple graph plots for visual comparisons, but since there are many occasions when one pdf or histogram will dwarf all the other functions, multiple graph plots are not done automatically. The points on the plots are found by finding values for the pdfs for every $\frac{1}{200}$ increment from 0 to 1.

The empirical cdf (ecdf) is found by first comparing the windowed data with the same set of incremented values used to find the pdfs. If a windowed sample is within $\pm \frac{1}{400}$ of the incremented value, a counter that is initialized at 0 is increased by 1. Each

windowed data sample is compared with each incremented value. The counter is zeroed for each new incremented value. The number the counter assigns to each incremented value is the magnitude of the increase of the ecdf at the incremented value.

The other cdfs are found by increasing the value of the cdf by the magnitude of the pdf at each of the incremented values used in the pdf formation. The ecdf and the cdfs are then all normalized by dividing each cdf by its largest (final) value.

Each cdf is then individually plotted against the ecdf for a visual goodness-of-fit assessment. As with the pdf plots, the program can be manipulated to compare more than one cdf at a time.

3.4.5 Step 5: Goodness-of-Fit Kolmogorov and Chi-Square test statistics are produced for each cdf. The Kolmogorov test statistics are found as explained in Chapter 2. To determine the Chi-Square test statistics, equal probability bin intervals must be found. Determining the interval points requires finding the inverse values of the distribution functions for the required bin probabilities. For many distributions, the inverse values cannot be found in closed form. However, the approximate interval points can be found relatively easily using numerical methods as demonstrated in the following example:

Suppose the number of histogram bins chosen was three. Then, for equal probability, every bin would have a 33% chance of a sample occurring in its interval. For a sample set of normalized data, the first bin would have a low interval of 0. The high interval point of the first bin and the low interval point of the second bin would be the input value that produced the cdf value closest to $\frac{1}{3}$. The high interval point of the second bin and the low interval point of the third bin would be the input value that produced the cdf value closest to $\frac{2}{3}$. The high end interval of the third bin would be 1. Values from the window would then be placed in the bin whose intervals they fell between. This method results in two decimal place accuracy.

The test statistics for each cdf are printed out for the Kolmogorov and the Chi-Square tests.

3.4.6 Step 6: Optimum Model Determination The optimum pdf is declared to be the pdf with the smallest Kolmogorov test statistic. The name of the pdf as well as the estimated parameters are printed out. The Kolmogorov test statistic is used because, on occasions when the Kolmogorov test and the Chi-Square test disagree, visual assessment usually agrees with Kolmogorov.

The user must refer to tables to determine the level of significance the pdf produces.

3.5 Summary

This chapter explained the computations required to impliment the 'ASPECT' RCS model optimization program. The MLE and MoM parameters for all pdfs used were determined. The required inputs and format were explained.

IV. Determination of Optimum RCS Models for Window vs. Full-Range Sample Sets

4.1 Introduction

This chapter will begin with an overview of the types of parameters of several pdfs and the effects changes in those parameters will have on the shape of the pdfs. The rest of the chapter will analyze how the pdfs handled the empirical distribution of the data from each aspect window when compared with the full-range of data. Window vs. Full-Range comparisons are the standard method for forming RCS models.

Three different types of data will be tested at each of the three modeled aspect windows. The first type will be fighter data with samples taken in the $\theta = 90^\circ$ plane. The second type will be fighter data with samples taken in a wider θ window: $\theta = 90^\circ \pm 5^\circ$. The third type of data will be missile data in the $\theta = 90^\circ$ plane.

4.2 Parameter Types

The pdfs considered in this investigation will be characterized by three parameters, namely location, scale, and shape.

Location parameters determine where the centroid of the probability densities is located in the range of the pdf values. Location parameters are used in the Normal and Lognormal pdfs.

Scale parameters compress or expand the probability density a pdf will have over its range. For the pdfs used here, a decreasing scale parameter value will compress pdfs, an increasing scale parameter value will expand pdfs. A compressed pdf will exhibit very small probability densities over most of its range and very large probability densities over a small portion of its range. An expanded pdf will exhibit increased probability densities over the majority of its range, but the peak probability densities will be much lower than those of a compressed pdf. Scale parameters are used in the Normal, Lognormal, and Weibull pdfs.

Shape parameters determine both the shape and location of the pdf. They can cause the pdf to behave like a negative or positive exponential function, a lognormal function, or a normal function. Shape parameters are used in Beta, Weibull, and Rayleigh-class pdfs.

All parameters used in this study are linear combinations of the mean (m) and second moment (m_2). The mean and second moment are two of the three components that can determine a pdf's effectiveness. The third component is the skew of the pdf. Skew is the difference in the slopes on either side of the peak values of a pdf. If the right slope is steeper than the left slope, the pdf is skewed to the right. If the left slope is steeper than the right slope, the pdf is skewed to the left.

The following subsections discuss each pdf's response to changes in its parameters.

4.2.1 Normal The location parameter μ will center the pdf at the mean of the sample set. The scale parameter σ will expand the pdf for increasing values of variance and compress the pdf for decreasing values of variance. The Normal pdf is never skewed. Figure 4.1 shows the Normal pdf's response to changes in μ and σ .

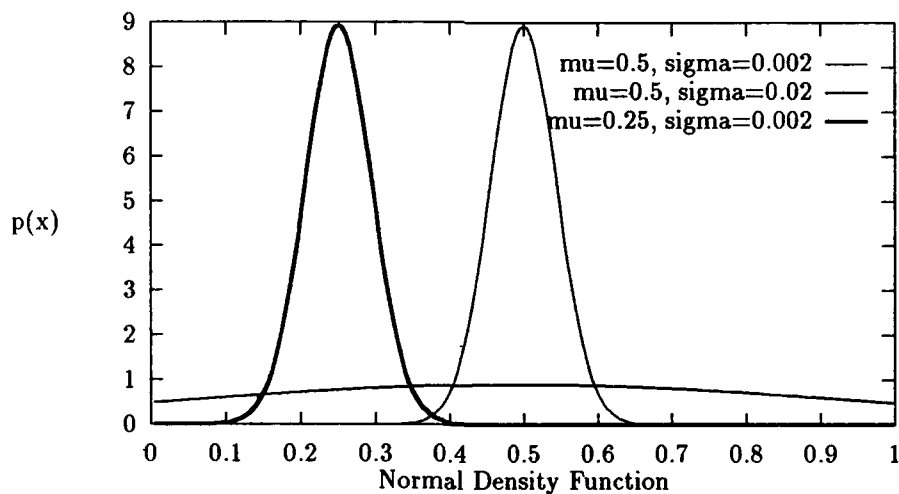


Figure 4.1. Normal pdf's response to changes in μ and σ

4.2.2 Lognormal Since the lognormal pdf acts as a normal pdf applied to the natural logarithm of the sample set, the location parameter μ centers the pdf around the mean of the natural logarithm of the sample set. This will cause the pdf to be skewed to the left of the true mean of the sample set. The skewing will be further enhanced by the sample variable in the denominator of the non-exponential portion of the pdf which is the result of the Jacobian of the transformation $y = \ln x$. This variable will result in enhanced probability densities for lower-range sample values. The scale parameter σ compresses the pdf for decreasing sample variances and expands the pdf for increasing sample variances. Figure 4.2 shows the Lognormal pdf's response to changes in μ and σ .

4.2.3 Weibull The shape parameter α will cause the pdf to approximate an exponential pdf at low values ($\alpha < 3$) and is the exponential pdf for $\alpha = 1$. At higher values of α , the pdf will become more normal in appearance and center on the sample mean. The scale parameter β compresses the pdf for small values of β and expands the pdf for large values of β . The Weibull pdf is always skewed to the right for values of $\alpha \geq 4$. Figure 4.3 shows the Weibull pdf's response to changes in α and β .

4.2.4 Beta The Beta pdf has two shape parameters, α and β . The ratio and magnitudes of α and β determine the shape of the pdf. If $\alpha > \beta$, the pdf will be skewed to the right against the high boundary of the data range. If $\alpha < \beta$, the pdf will be skewed to the left against the low boundary of the data range. If $\alpha = \beta$, the pdf will be normal shaped and will be centered in the data range. If $\alpha = \beta = 1$, the pdf is uniform, with a magnitude of 1. If α or β is less than 1, the pdf approximates an exponential function, increasing toward the high range boundary if $\alpha > \beta$ or the low range boundary if $\alpha < \beta$. If α and β are both less than one, then the pdf will approximate two exponential functions. One exponential will increase toward the high range boundary, the other will increase toward the low range boundary. Figure 4.4 shows the Beta pdf's response to changes in α and β .

The Beta pdf is the most flexible pdf used in this study, making it useful for sample sets that do not exhibit a Normal-type distribution. However, it is much less responsive to changes in variance than the Lognormal, Normal, or Weibull pdfs and cannot attain the highly compressed forms required to model sample sets with small variances.

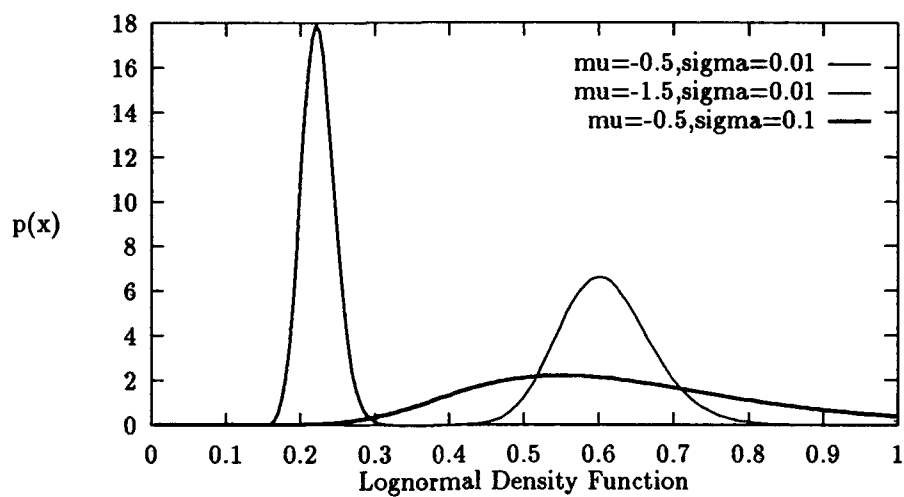


Figure 4.2. Lognormal pdf's response to changes in μ and σ

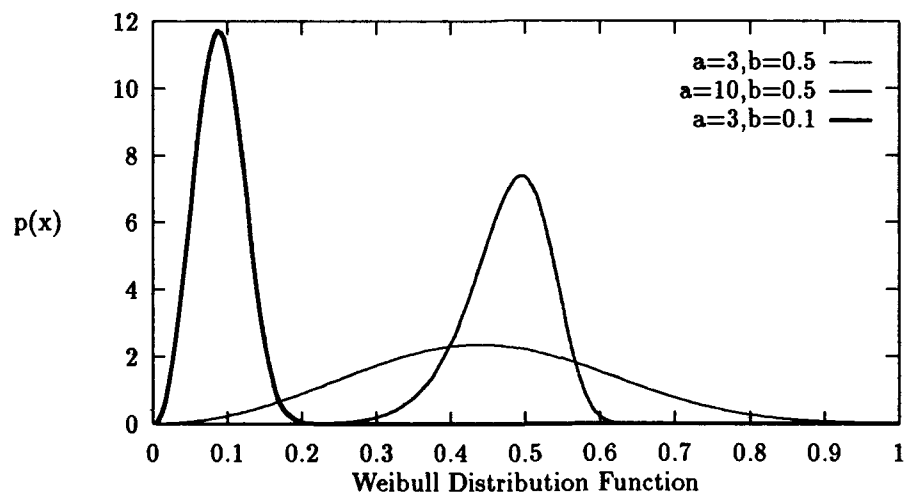


Figure 4.3. Weibull pdf's response to changes in α and β

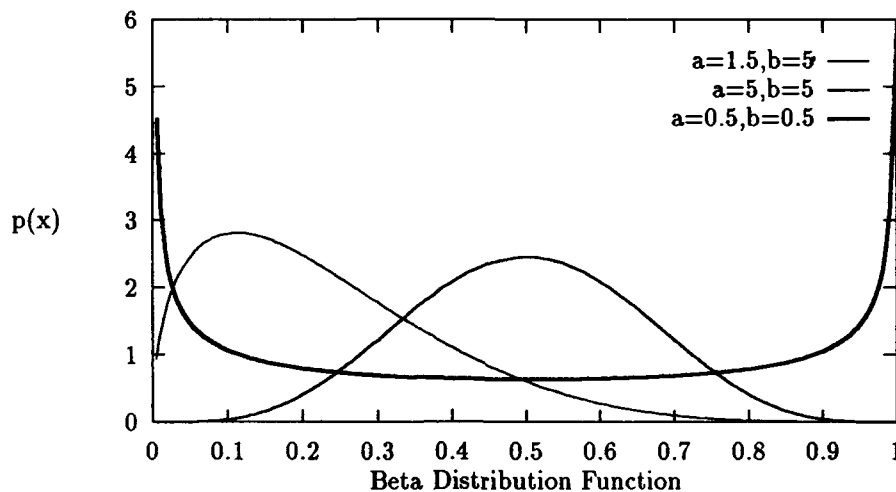


Figure 4.4. Beta pdf's response to changes in α and β

4.2.5 Rayleigh Class The Rayleigh class shape parameter α is a linear transformation of the second moment of the sample set. The maximum values of the Rayleigh class pdfs are always skewed to the left of the sample mean. Small values of α will compress the pdfs and force the maximum probability density closer to the sample mean. Large values of α will expand the pdfs and force the maximum probability density farther away from the sample mean. The Rayleigh ($y = x^2$) pdf is actually a negative exponential function, whose highest probability density is always at zero. Because the Rayleigh class pdfs are dependent only on the sample second moment, they are less responsive to changes in variance than any of the other pdfs used in this study. Figure 4.5 shows the Rayleigh pdf's responses to changes in α .

4.3 Test Results for Window vs. Full-Range RCS Models

This section will present an analysis of the behaviour of the pdfs to different aspect windows studied. The Kolmogorov Level of Significance, and the Chi-Square Level of Significance for Window vs. Full-Range RCS Models are presented in Appendix A.

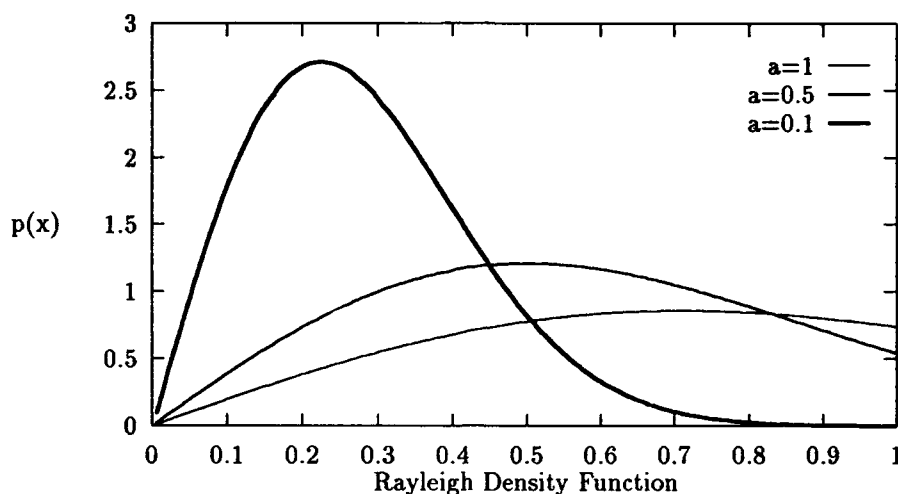


Figure 4.5. Rayleigh pdf's response to changes in α

Due to the Rayleigh-class pdfs' inability to compress for low variances, the Rayleigh-class pdfs (Rayleigh, One-Dominant-Plus-Rayleigh, and Rayleigh Squared made poor Window vs. Full-Range models for all sample sets. For this reason, the performance of the Rayleigh-class pdfs will not be discussed in the following sections, but the results are listed in the tables of Appendix A along with the other pdfs.

In the following sections, the pdfs with the lowest Kolmogorov and Chi-Square test statistics are presented. If more than one pdf has the lowest Chi-Square test statistic, the low Chi-Square pdf with the lowest Kolmogorov test statistic is presented as the best Chi-Square pdf. If that pdf happens to be the pdf with the lowest Kolmogorov test statistic of all pdfs, two Chi-Square pdfs are presented for comparison.

4.3.1 Nose-On Fighter: $\theta = 90^\circ$ The sample set is characterized by a medium range mean ($m=0.52$), a relatively small variance ($\text{var}=7.06 \times 10^{-4}$), a small number of samples ($n=11$), and is skewed to the right. The cdfs and pdfs with the lowest Kolmogorov and Chi-Square test statistics are compared with the sample set and presented in Figures 4.6-4.9.

The Kolmogorov Goodness-of-Fit Test (KGFT) declares the Weibull MLE and MoM, Lognormal, and Normal pdfs to have a Level of Significance (LoS) greater than 20% (the highest LoS given by Conover (Conover, 1980: Table 14). However, the Weibull MLE has the smallest test statistic and is chosen as the optimum pdf. The Weibull MLE is the most compressed pdf (highest probability density over narrowest range). As can be seen by the CDF figures, the Empirical Cumulative Distribution Function (ECDF) is skewed to the right. The Weibull pdfs are the only pdfs able to match this skewing to any degree.

Because of the small number of samples, the Chi-Square Goodness-of-Fit Test (CGFT) is limited to one degree of freedom by the restrictions listed in section 2.5. For this reason, the minimum test statistic is shared by the Weibull MLE and MoM, Lognormal, and Normal pdfs. The CGFT is more conservative than the KGFT, declaring the LoS to be between 10% and 25%. This range of LoS is the second highest range listed by Conover (Conover, 1980: Table 2).

4.3.2 Nose-On Fighter: $\theta = 90^\circ \pm 5^\circ$ This sample set is characterized by a medium range mean ($m=0.45$), a small variance ($\text{var}=2.21 \times 10^{-4}$), a large number of samples ($n=121$), and a rightward skew. The pdfs and cdfs with the lowest Kolmogorov and Chi-Square test statistics are presented in Figures 4.10-4.13. The KGFT declares the Weibull MLE and MoM pdfs to have a LoS greater than 20%, with the Weibull MoM having a slightly lower test statistic than the Weibull MLE. The Weibull MoM matches the test statistic with the highest compression. The Weibull pdfs are the only ones able to match the rightward skew of the sample set.

The CGFT declares the Normal pdf to have the highest LoS ($10\% \geq \alpha \geq 5\%$). The CGFT declares all the other pdfs to have a LoS less than 0.1%. This is a poor showing for all pdfs and is probably due to the few degrees of freedom (2) used in the test. Time limitations prevented building a CGFT with the many degrees of freedom which can be used with large sample sets. Visual assessments of Figures 4.10-4.13 show the Weibull MoM pdf to be virtually indistinguishable from the sample set, while the Normal pdf cannot match the rightward skew of the sample set.

4.3.3 Nose-On Missile: $\theta = 90^\circ$ This sample set is characterized by a medium range mean ($m=0.47$), a small variance ($\text{var}=2.23 \times 10^{-4}$), a medium number of samples ($n=21$), and no visible skew. The best Kolmogorov and ChiSquare pdfs and cdfs are presented in Figures 4.14-4.17.

The KGFT declares the Weibull MLE and MoM, Lognormal, and Normal pdfs to have a LoS greater than 20%. The Normal pdf has the smallest test statistic, the Lognormal's test statistic is slightly larger. Unlike the other Nose-On sample sets, the optimum pdf does not have the highest probability distribution. In fact, the Weibull MLE and MoM and Lognormal pdfs all have higher probability densities than the Normal. However, the Weibull pdfs are skewed to the right and the Lognormal pdf is skewed to the left. The Normal pdf is optimum because of the lack of a skewed sample set and the closeness of the values of the peak probability densities.

The CGFT declares the Weibull MLE and MoM, Lognormal, and Normal pdfs all to have a LoS between 2.5% and 5%. Though a visual assessment of Figures 4.14 and 4.16 shows the Lognormal and Normal pdfs to be a very close match to the sample set, the CDFT declares all the pdfs to be a poor fit.

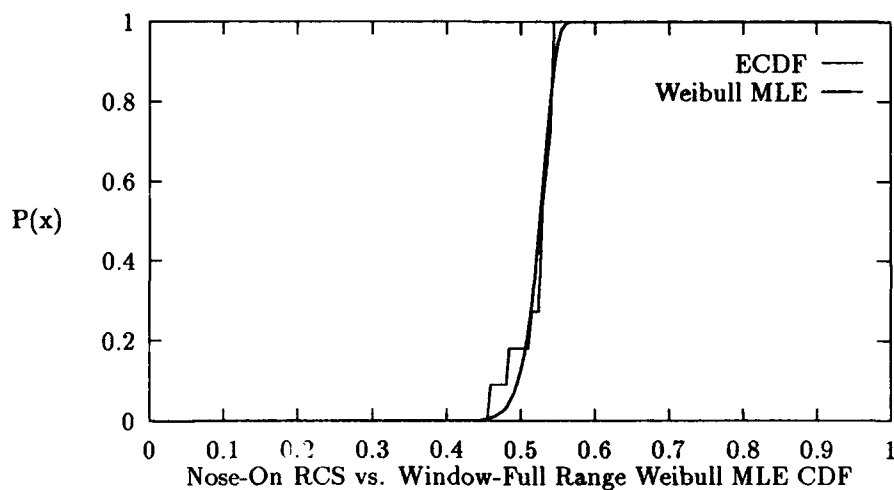


Figure 4.6. Top KGFT and CGFT CDF of Fighter Data at Nose-On $\pm 5^\circ$, 0.5° sample interval, $\theta = 90^\circ$, $\theta - \theta$ polarization, 1 GHz Full-Scale

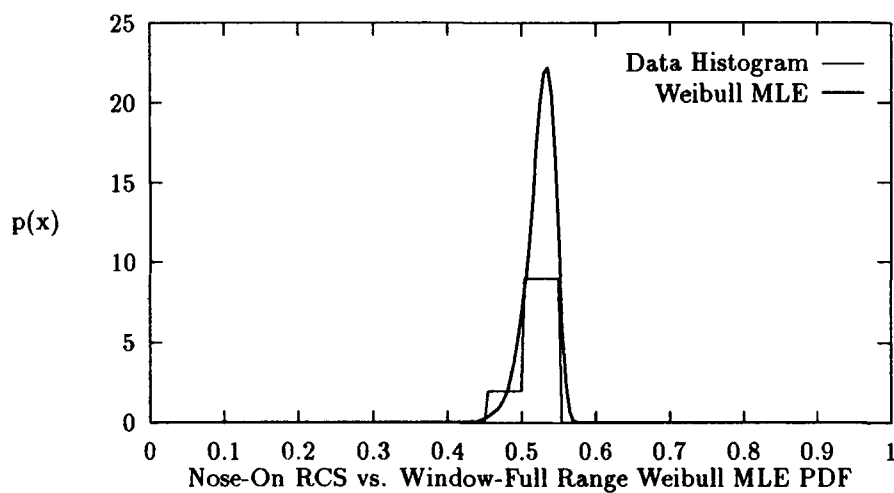


Figure 4.7. Top KGFT and CGFT PDF of Fighter Data at Nose-On $\pm 5^\circ$, 0.5° sample interval, $\theta = 90^\circ$, $\theta - \theta$ polarization, 1 GHz Full-Scale

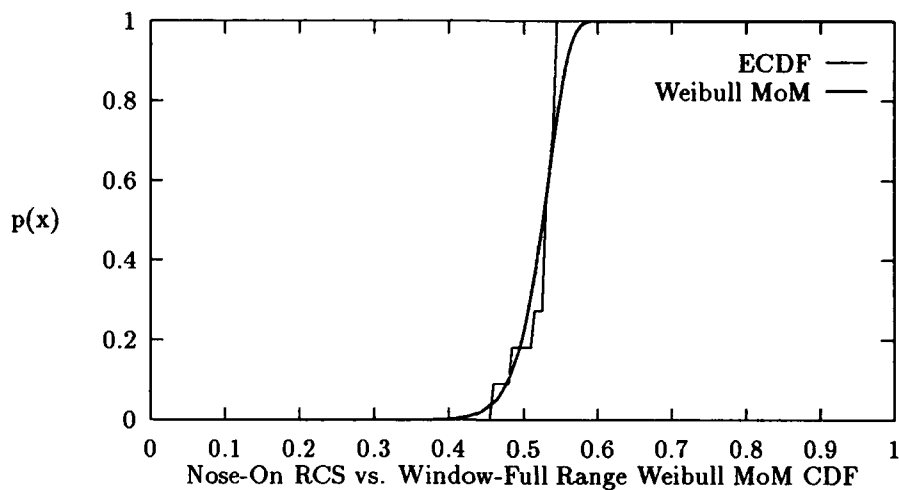


Figure 4.8. Top CGFT CDF of Fighter Data at Nose-On $\pm 5^\circ$, 0.5° sample interval, $\theta = 90^\circ$, $\theta - \theta$ polarization, 1 GHz Full-Scale

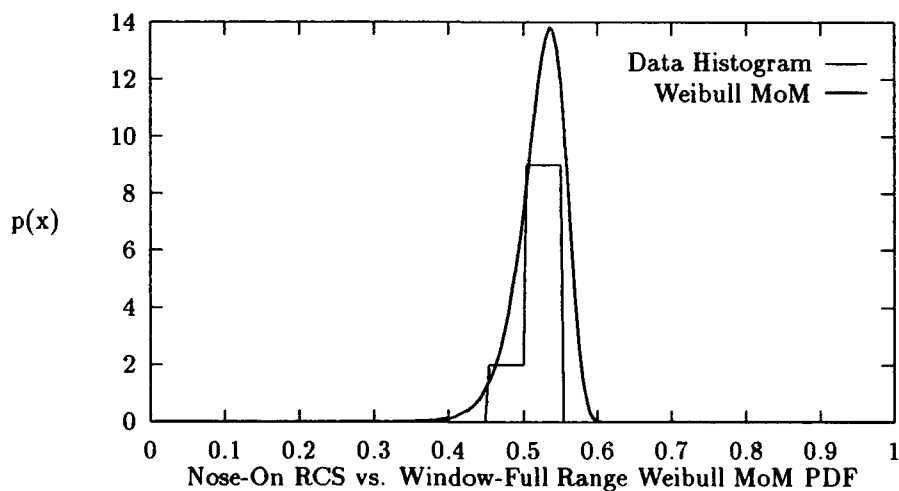


Figure 4.9. Top CGFT PDF of Fighter Data at Nose-On $\pm 5^\circ$, 0.5° sample interval, $\theta = 90^\circ$, $\theta - \theta$ polarization, 1 GHz Full-Scale

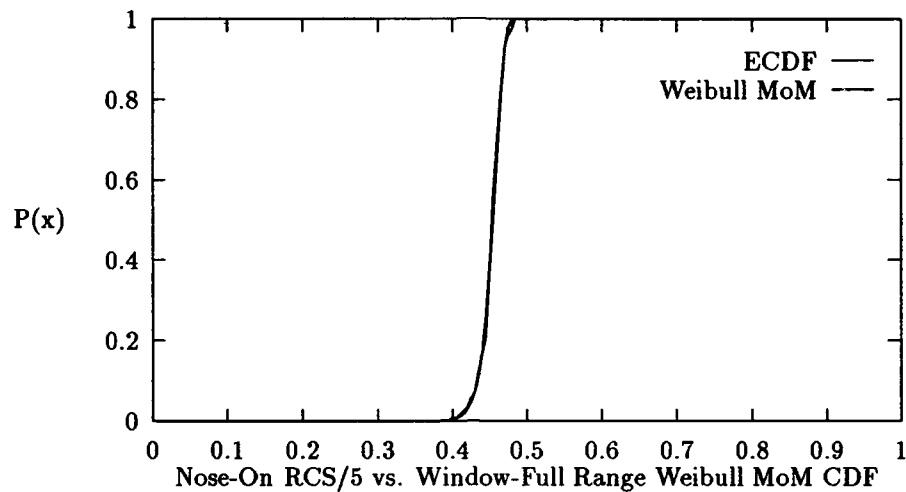


Figure 4.10. Top KGFT CDF of Fighter Data at Nose-On $\pm 5^\circ$, 0.5° sample interval, $\theta = 90^\circ \pm 5^\circ$, $\theta - \theta$ polarization, 1 GHz Full-Scale

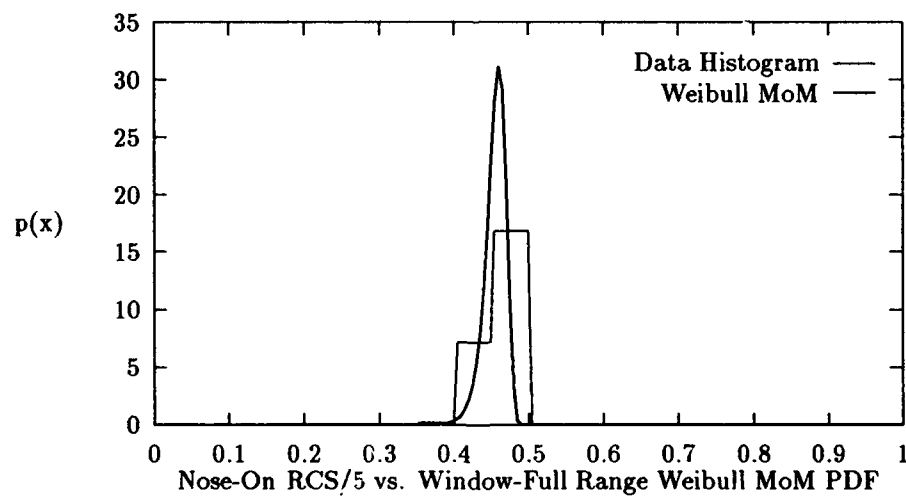


Figure 4.11. Top KGFT PDF of Fighter Data at Nose-On $\pm 5^\circ$, 0.5° sample interval, $\theta = 90^\circ \pm 5^\circ$, $\theta - \theta$ polarization, 1 GHz Full-Scale

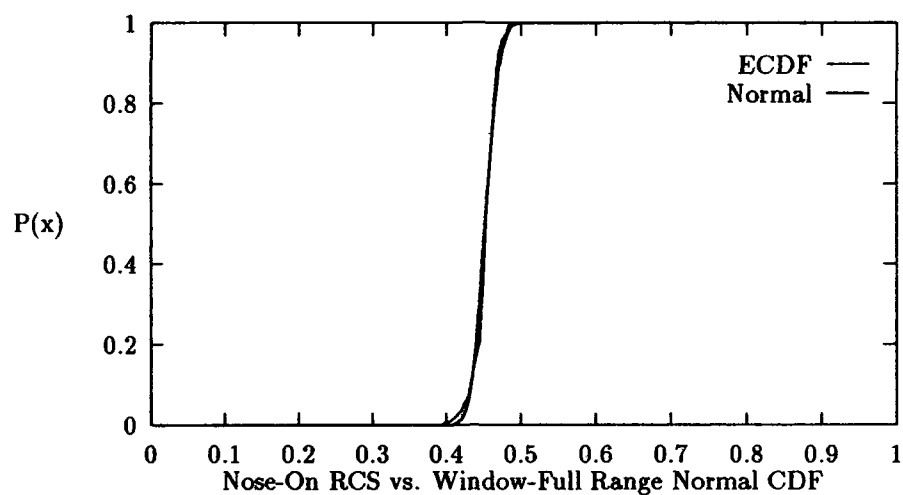


Figure 4.12. Top CGFT CDF of Fighter Data at Nose-On $\pm 5^\circ$, 0.5° sample interval, $\theta = 90^\circ \pm 5^\circ$, $\theta - \theta$ polarization, 1 GHz Full-Scale

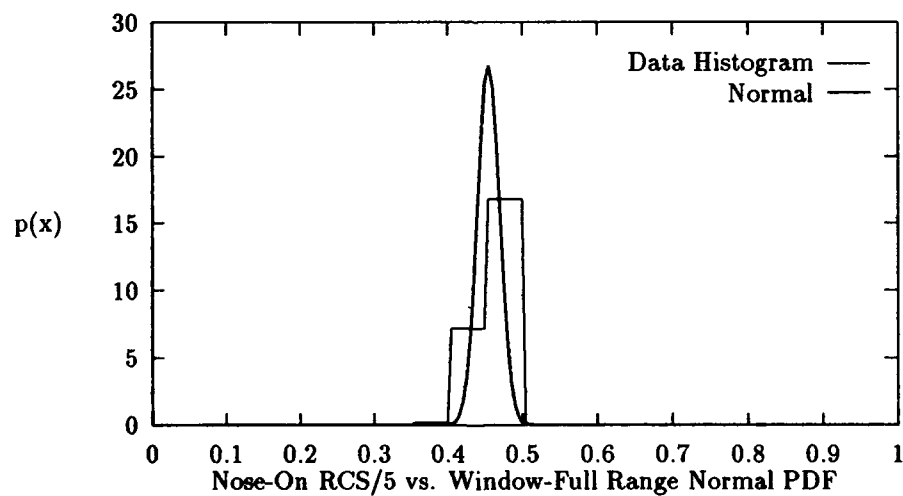


Figure 4.13. Top CGFT PDF of Fighter Data at Nose-On $\pm 5^\circ$, 0.5° sample interval, $\theta = 90^\circ \pm 5^\circ$, $\theta - \theta$ polarization, 1 GHz Full-Scale

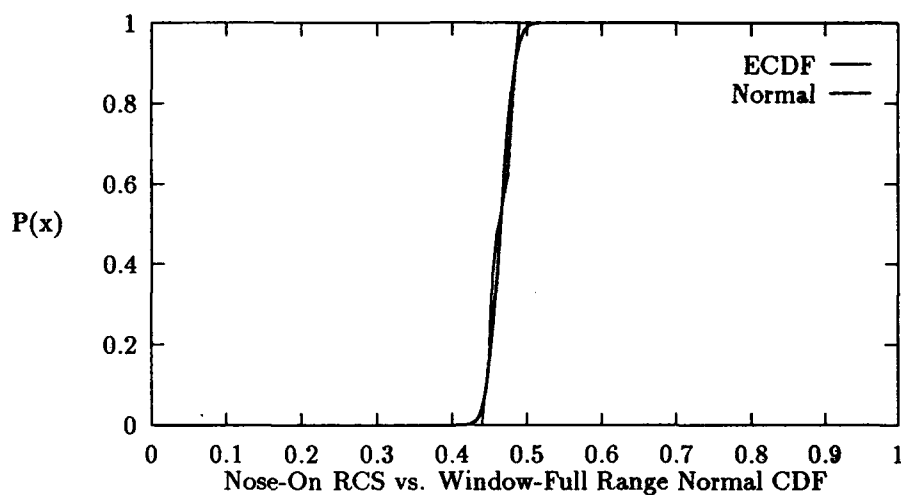


Figure 4.14. Top KGFT and CGFT CDF of Missile Data at Nose-On $\pm 5^\circ$, 0.5° sample interval, $\theta = 90^\circ$, $\theta - \theta$ polarization, 18 GHz Full-Scale

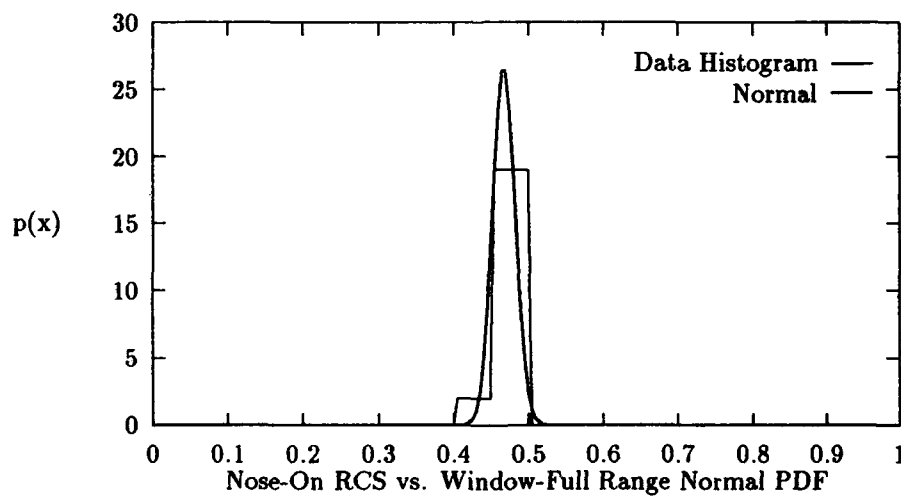


Figure 4.15. Top KGFT and CGFT PDF of Missile Data at Nose-On $\pm 5^\circ$, 0.5° sample interval, $\theta = 90^\circ$, $\theta - \theta$ polarization, 18 GHz Full-Scale

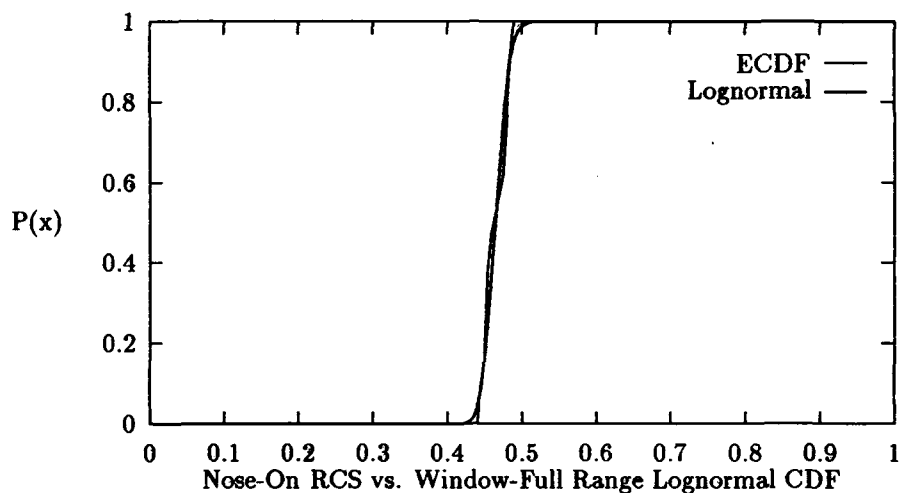


Figure 4.16. Top CGFT CDF of Missile Data at Nose-On $\pm 5^\circ$, 0.5° sample interval, $\theta = 90^\circ$, $\theta - \theta$ polarization, 18 GHz Full-Scale

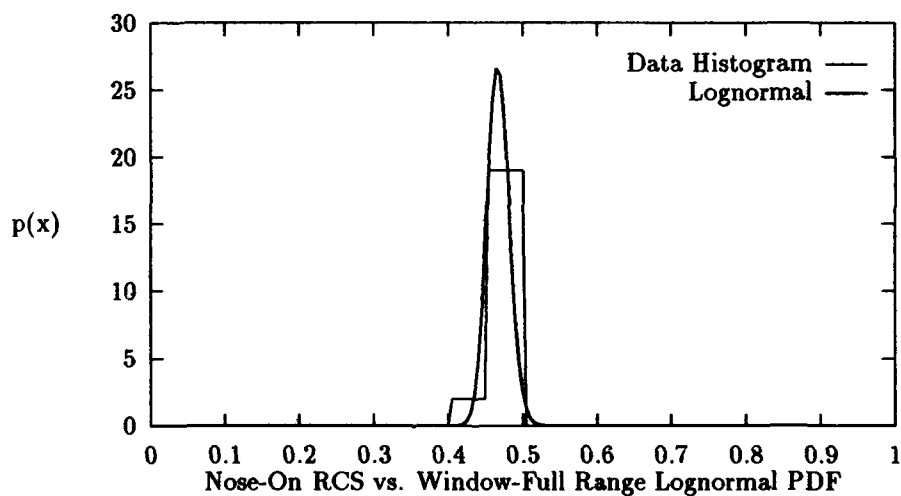


Figure 4.17. Top CGFT PDF of Missile Data at Nose-On $\pm 5^\circ$, 0.5° sample interval, $\theta = 90^\circ$, $\theta - \theta$ polarization, 18 GHz Full-Scale

4.3.4 Broadside Fighter: $\theta = 90^\circ$ This sample set is characterized by a high range mean ($m=0.67$), a large variance ($\text{var}=1.44 \times 10^{-2}$), a medium number of samples ($n=21$), and a slight rightward skew. The best Kolmogorov and Chi-Square pdfs and cdfs are presented in Figures 4.18-4.21.

The KGFT declares the Beta MLE and MoM, Weibull MLE and MoM, and Normal pdfs to have a LoS greater than 20%. The Beta MLE has the lowest test statistic. Since the sample mean is greater than 0.5, the Beta pdf is skewed rightward, along with the Weibull pdf. The large variance greatly expands the variance sensitive pdfs (Lognormal, Normal, and Weibull), leaving the Beta MLE pdf with the highest probability density.

The CGFT agrees with the KGFT, declaring the Beta MLE and Weibull MLE pdfs to have a LoS greater than 25%. However, the CGFT rates the Beta MoM, Weibull MoM, Lognormal, and Normal pdfs relatively poorly ($10\% > \text{LoS} > 2.5\%$).

4.3.5 Broadside Fighter: $\theta = 90^\circ \pm 5^\circ$ This sample set is characterized by a medium range mean ($m=0.55$), a medium sized variance ($\text{var}=4.3 \times 10^{-3}$), a large number of samples ($n=231$), and a slight rightward skew. The resulting pdfs and cdfs are presented in Figures 4.22 and 4.23.

The large percentage of off-broadside samples in this sample set compared with the Broadside Fighter: $\theta = 90^\circ$ sample set has lowered the sample mean. The medium range sample mean prevents the Beta pdf from skewing. The medium size variance expands the Normal and Lognormal pdfs more severely than the Weibull pdfs. The KGFT declares the Weibull MLE and MoM pdfs to have a LoS greater than 20%. The Weibull MoM has the lowest test statistic and the highest probability density.

The CGFT gives the Weibull MoM the lowest test statistic, which results in the highest LoS ($10\% > \alpha > 5\%$), a relatively poor result.

4.3.6 Broadside Missile: $\theta = 90^\circ$ This sample set is characterized by a high range mean ($m=0.81$), a large variance ($\text{var}=1.96 \times 10^{-2}$), a small number of samples ($n=41$), and a strong rightward skewing. The resulting pdfs and cdfs are presented in Figures 4.24-4.27.

The KGFT declares the Beta MLE and MoM, the Weibull MLE and MoM, and the Normal pdfs to have a LoS greater than 20%. However, the combination of a wide variance, a high mean, and a strong rightward skew gives the Beta pdfs much lower test statistics than the other pdfs. The Beta MLE has the highest probability density, but this level of compression forces the peak probability density far to the right of the sample mean. With the β parameter approaching 1.00, the Beta MLE pdf approximates a positive exponential function. the Beta MoM does not compress as severely as the Beta MoM with the large sample mean and therefore attains the lowest test statistic. Although the Weibull pdfs are skewed to the right as well, the wide variance expands the pdfs too severely for them to be as effective as the Beta pdfs.

The CGFT declares the Beta MLE and MoM pdfs to have a LoS greater than 25%. The CGFT rated the Weibull MLE and MoM relatively highly as well, giving them a LoS between 10% and 25%.

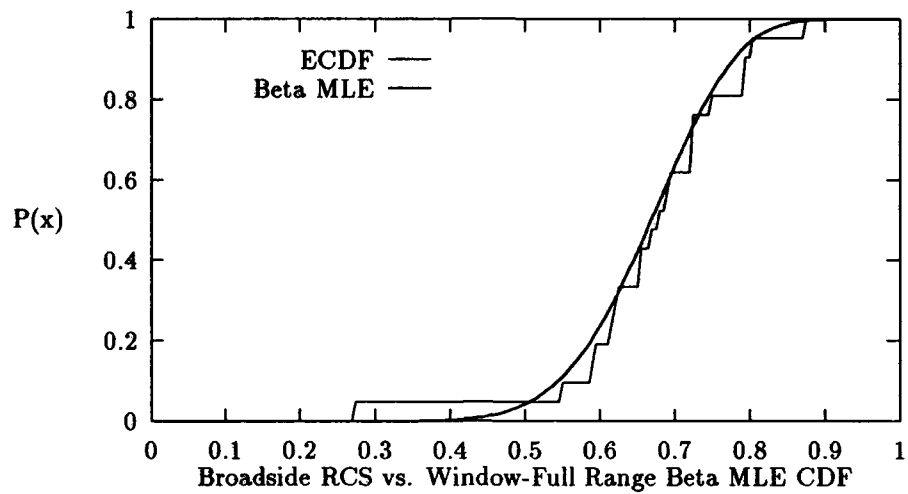


Figure 4.18. Top KGFT and CGFT CDF of Fighter Data at Broadside $\pm 5^\circ$, 0.5° sample interval, $\theta = 90^\circ$, $\theta - \theta$ polarization, 1 GHz Full-Scale

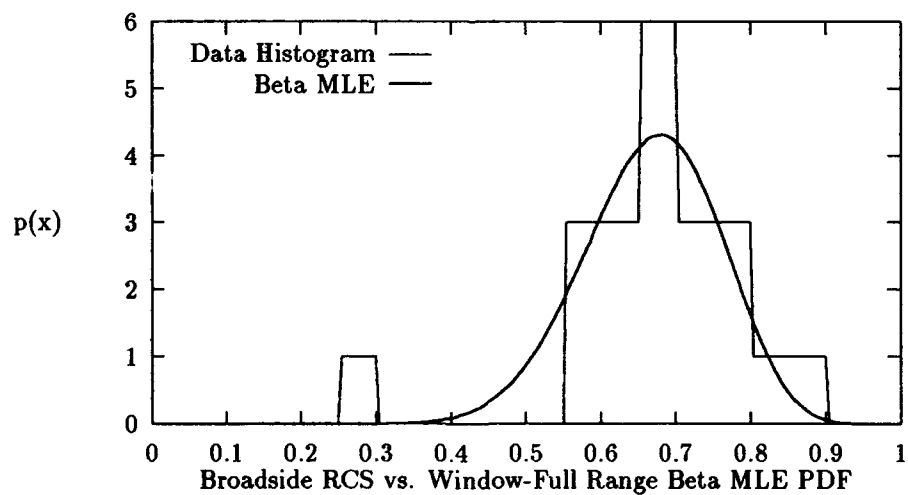


Figure 4.19. Top KGFT and CGFT PDF of Fighter Data at Broadside $\pm 5^\circ$, 0.5° sample interval, $\theta = 90^\circ$, $\theta - \theta$ polarization, 1 GHz Full-Scale

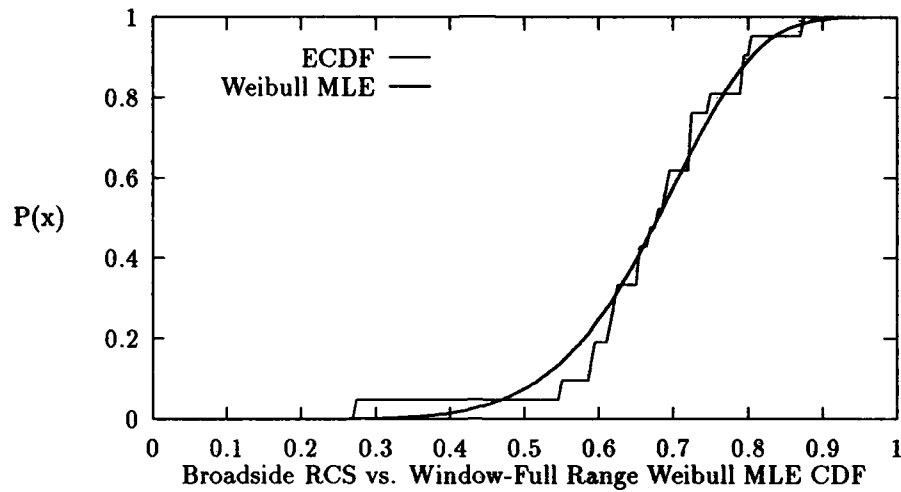


Figure 4.20. Top CGFT CDF of Fighter Data at Broadside $\pm 5^\circ$, 0.5° sample interval, $\theta = 90^\circ$, $\theta - \theta$ polarization, 1 GHz Full-Scale

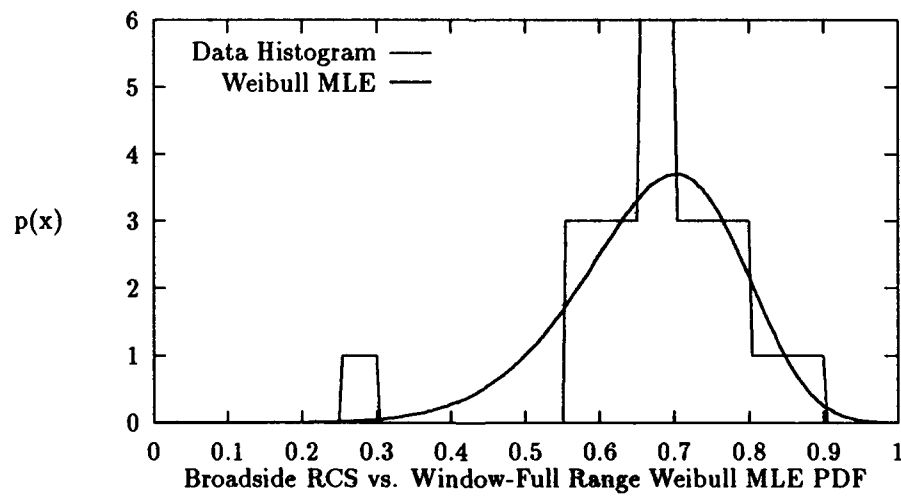


Figure 4.21. Top CGFT PDF of Fighter Data at Broadside $\pm 5^\circ$, 0.5° sample interval, $\theta = 90^\circ$, $\theta - \theta$ polarization, 1 GHz Full-Scale

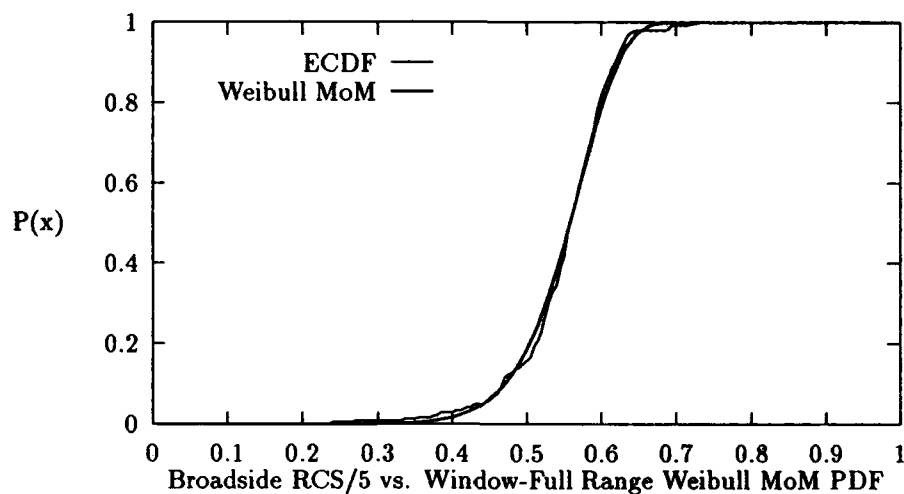


Figure 4.22. Top KGFT and CGFT CDF of Fighter Data at Nose-On $\pm 5^\circ$, 0.5° sample interval, $\theta = 90^\circ \pm 5^\circ$, $\theta - \theta$ polarization, 1 GHz Full-Scale

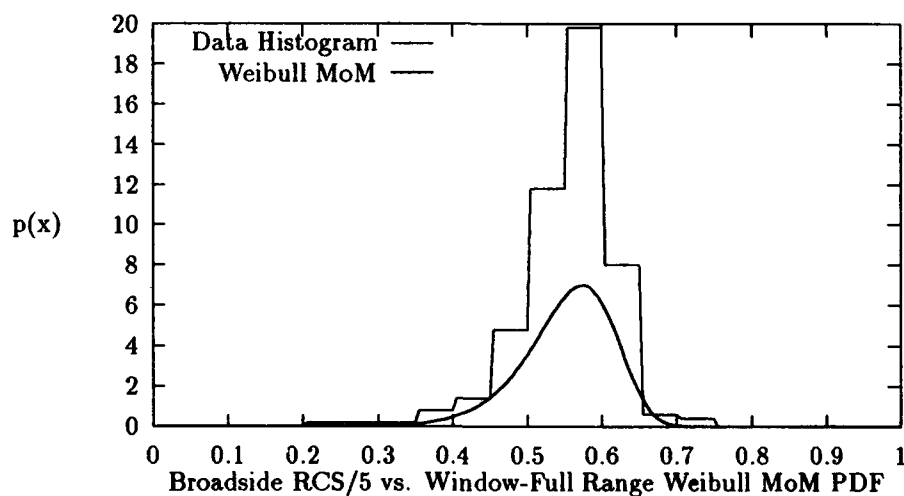


Figure 4.23. Top KGFT and CGFT PDF of Fighter Data at Nose-On $\pm 5^\circ$, 0.5° sample interval, $\theta = 90^\circ \pm 5^\circ$, $\theta - \theta$ polarization, 1 GHz Full-Scale

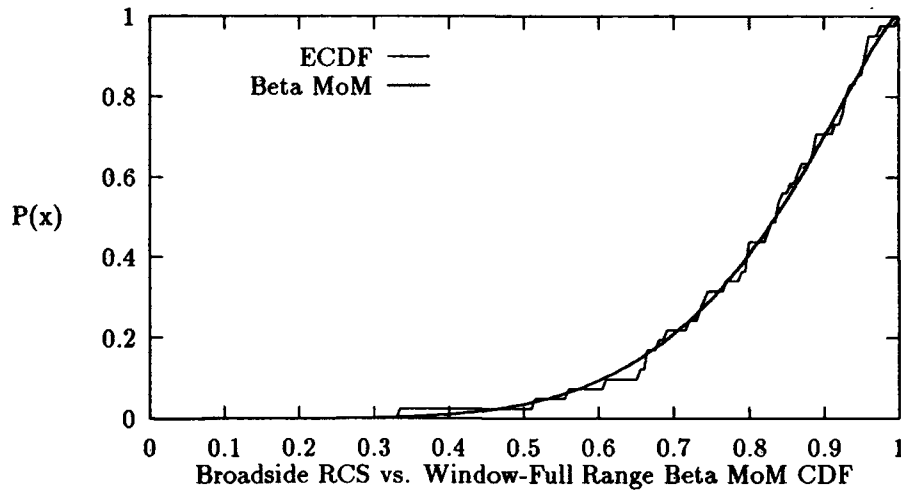


Figure 4.24. Top KGFT and CGFT CDF of Missile Data at Broadside $\pm 5^\circ$, 0.5° sample interval, $\theta = 90^\circ$, $\theta - \theta$ polarization, 18 GHz Full-Scale

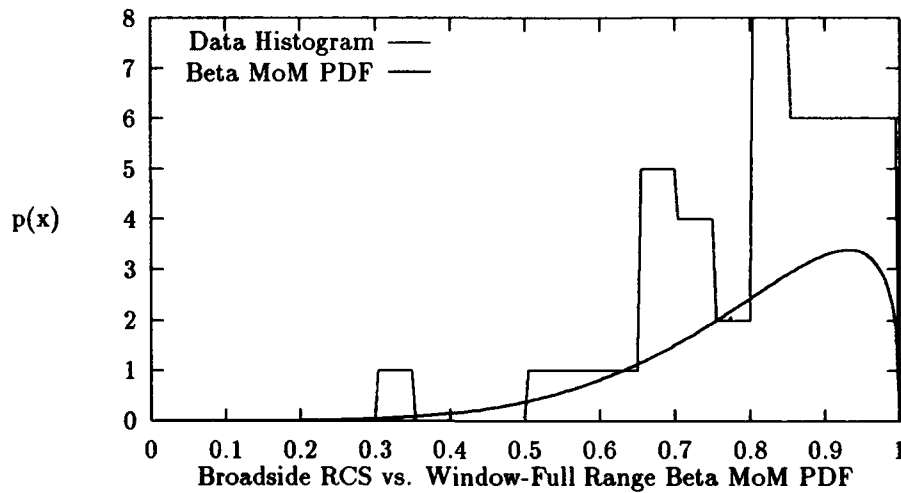


Figure 4.25. Top KGFT and CGFT PDF of Missile Data at Broadside $\pm 5^\circ$, 0.5° sample interval, $\theta = 90^\circ$, $\theta - \theta$ polarization, 18 GHz Full-Scale

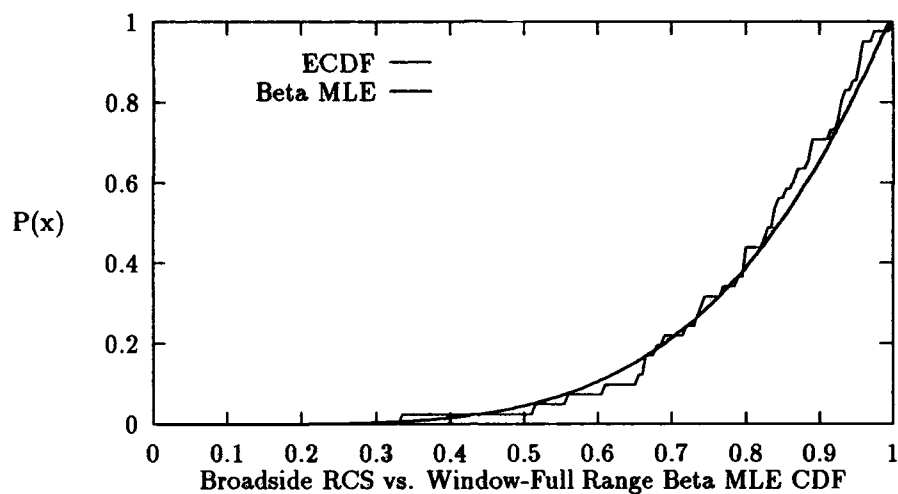


Figure 4.26. Top CGFT CDF of Missile Data at Broadside $\pm 5^\circ$, 0.5° sample interval, $\theta = 90^\circ$, $\theta - \theta$ polarization, 18 GHz Full-Scale

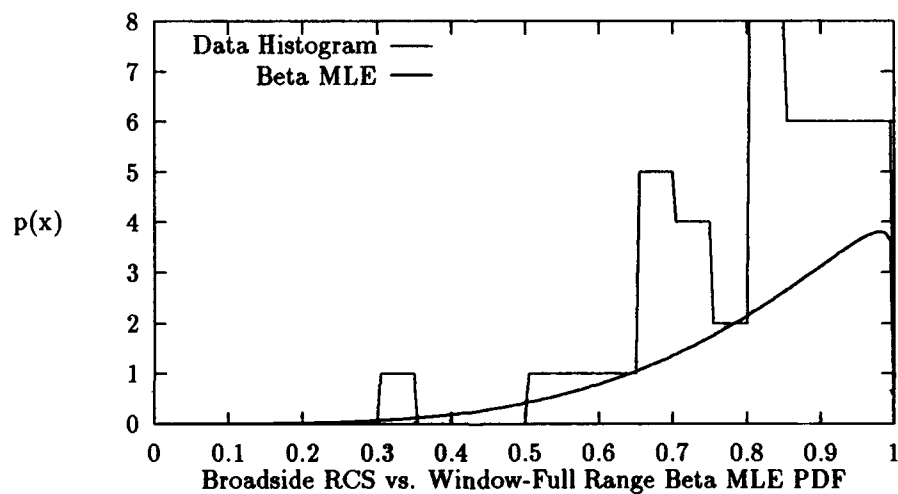


Figure 4.27. Top CGFT PDF of Missile Data at Broadside $\pm 5^\circ$, 0.5° sample interval, $\theta = 90^\circ$, $\theta - \theta$ polarization, 18 GHz Full-Scale

4.3.7 Tail-On Fighter: $\theta = 90^\circ$ This sample set is characterized by a low range mean ($m=0.23$), a medium sized variance ($\text{var}=2.8 \times 10^{-3}$), a small number of samples ($n=11$), and a slight skew to the right. The resulting pdfs and cdfs are presented in Figures 4.28-4.31. The low-range mean skews the Beta pdfs to the left, approaching the Lognormal function in shape. The medium size variance expands the Lognormal and Normal pdfs to a greater extent than the Weibull pdfs. The KGFT declares the Beta MLE and MoM, Weibull MLE and MoM, Lognormal, and Normal pdfs to have a LoS greater than 20%. The Weibull MLE pdf matches the rightward skew with the highest compression and attains the highest probability density and lowest test statistic.

The CGFT declares the Beta MLE and MoM, Weibull MLE and MoM, and Normal pdfs to have a LoS greater than 25%. The one degree of freedom prevents picking a winner from these pdfs.

4.3.8 Tail-On Fighter: $\theta = 90^\circ \pm 5^\circ$ This sample set is nearly identical to the Tail-On Fighter: $\theta = 90^\circ$ sample set. It is characterized by a low-range mean ($m=0.25$), a medium size variance ($\text{var}=2.5 \times 10^{-3}$), a large number of samples ($n=121$), and a rightward skew. The resulting pdfs and cdfs are presented in Figures 4.32-4.35.

As in the last section, the Beta pdfs are skewed to the left along with the Lognormal pdf, and the Lognormal and Normal pdfs are expanded to a greater extent than the Weibull pdfs. The Weibull pdfs match the rightward skew of the sample set. The KGFT declares the Weibull MLE and MoM and the Normal pdfs to have a LoS greater than 20%. The Weibull MLE attains the lowest test statistic and highest probability density.

The CGFT declares the Beta MoM, Weibull MoM, and Normal pdfs to have a LoS between 5% and 2.5%. This is another poor performance for a large sample set. The Beta MoM and Normal pdfs have the lowest test statistic.

4.3.9 Tail-On Missile: $\theta = 90^\circ$ This sample set is characterized by a medium range mean ($m=0.58$), a small variance ($\text{var}=2.82 \times 10^{-4}$), a small number of samples ($n=21$), and a slight leftward skew. The pdfs and cdfs are presented in Figures 4.36-4.39.

This is the only sample set that is skewed to the left. With the middle range mean forcing the Beta pdf into a Normal-type distribution, the Lognormal pdf is the only pdf that can match the leftward skew. In addition, the small variance gives the Lognormal and Normal pdfs the compression to match that of the Weibull pdfs. The KGFT declares the Weibull MLE and MoM, Lognormal, and Normal pdfs to have a LoS greater than 20%. The Lognormal pdf matches the highest probability density with the lowest test statistic.

The CGFT declares the Weibull MLE and MoM, Lognormal, and Normal pdfs to have a LoS between 10% and 25%. These pdfs have identical test statistics.

4.4 Summary of Window vs. Full-Range RCS Models

Statistical analysis of the fighter and missile data reveals that even at the largest Window vs. Full-Range variances, high compression is required to effectively model the sample sets. The most compressed pdf attains the lowest Kolmogorov test statistic in seven of the nine sample sets modeled. Because of the importance of maximum compression, the pdfs' response to changes in variance is the most important factor in determining best goodness-of-fit. The Beta pdfs' limited response to variance changes make the pdfs ineffective for small variance sample sets but most effective for large variance sample sets. The reverse is true for the Lognormal and Normal pdfs. The Weibull pdfs compress at small variances at the same rate as the Lognormal and Normal pdfs but do not expand at the same rate as the Lognormal and Normal pdfs for large variances. Therefore, the Weibull pdfs are able to perform effectively at both high and low variance sample sets. The Weibull's response to variance changes enables the pdf to be the only function that attains a Kolmogorov LoS greater than 20% for every sample set.

The skew of the sample sets is also important in determining goodness-of-fit. In seven of the nine sample sets modeled, the sample set is skewed to the right. This enhances the Weibull pdfs' effectiveness and hurt the Lognormal and Normal pdfs' effectiveness. It helps the Beta pdfs' effectiveness for high-mean sample sets, but hurt the Beta pdfs' effectiveness elsewhere. The consistent skewing of the data indicates that sample variances will not get much lower than the low values of the sample sets observed. At the lowest variance levels, skewing is insignificant. At this level the Normal pdf becomes the most effective model.

The mean only effects the Beta pdfs' performance, skewing the pdf as described in section 4.2.4.

The mean and variance of the fighter and missile sample sets are similar in two of the three aspect windows modeled. Both nose-on sample sets are characterized by a mid-range mean and a small variance. Both broadside sample sets possess high-range means and large variances. The sample sets possess different characteristics at the tail-on aspect. The fighter sample set possesses a low range mean and medium variance, while the missile sample set possesses a mid-range mean and small variance.

The variances of the sample sets are indicators of the number of scattering surfaces at each aspect angle, with a small variance indicating few scatterers and a large variance indicating many scatterers. This being the case, the magnitude of the variance at each aspect window of the missile and fighter sample sets is typical of what would be expected for each class of object.

The mean of each sample set reflects the degree of perpendicular reflection of the scattering surfaces at each aspect window. Again, the experimental data matches what would be expected for both classes of objects.

The relatively consistent rightward skewing of the data was not expected. Every sample set of fighter data is rightward skewed. However, each missile aspect angle is skewed differently: the broadside is skewed rightward, the tail-on is skewed leftward and the nose-on is not skewed. If the rightward skewing is a consistent trait in aircraft data, the Weibull would be the most effective pdf for Window vs. Full-Range models.

The MLE performs better for small sample sets, while the MoM performs better for large sample sets. There is no apparent correlation between mean or variance and parameter estimator performance.

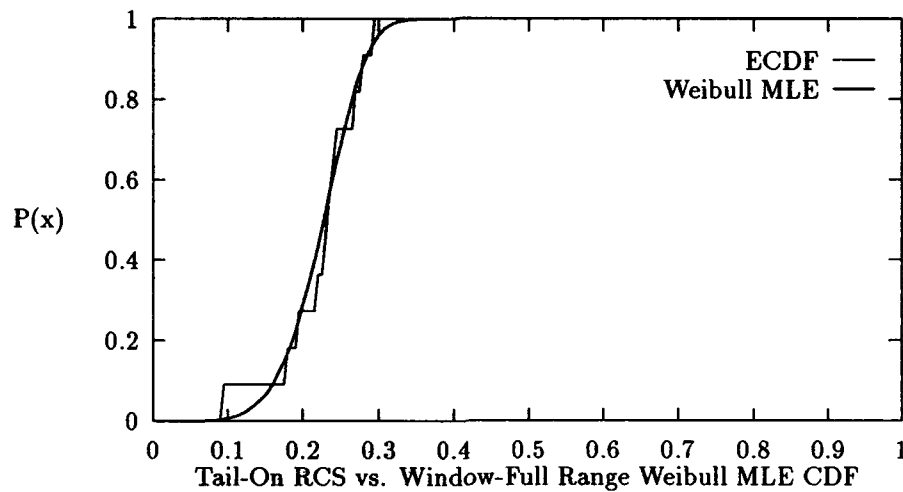


Figure 4.28. Top KGFT and CGFT CDF of Fighter Data at Tail-On $\pm 5^\circ$, 0.5° sample interval, $\theta = 90^\circ$, $\theta - \theta$ polarization, 1 GHz Full-Scale

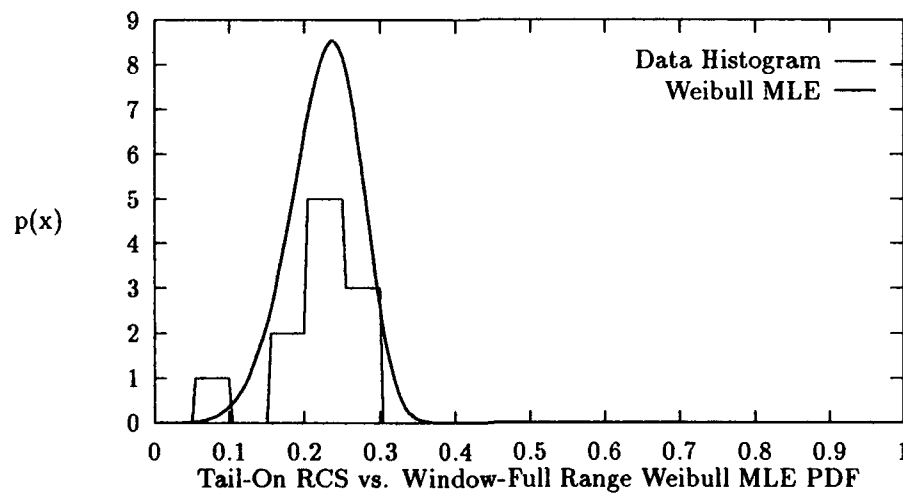


Figure 4.29. Top KGFT and CGFT PDF of Fighter Data at Tail-On $\pm 5^\circ$, 0.5° sample interval, $\theta = 90^\circ$, $\theta - \theta$ polarization, 1 GHz Full-Scale

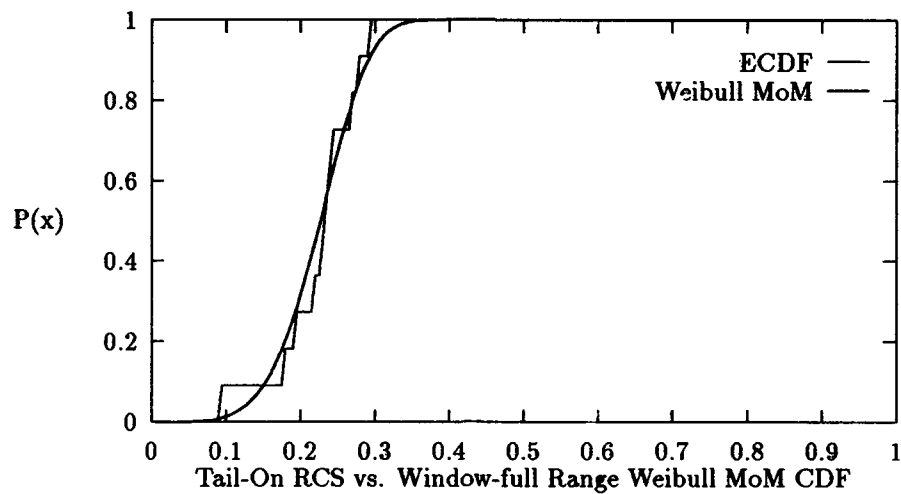


Figure 4.30. Top CGFT CDF of Fighter Data at Tail-On $\pm 5^\circ$, 0.5° sample interval, $\theta = 90^\circ$, $\theta - \theta$ polarization, 1 GHz Full-Scale

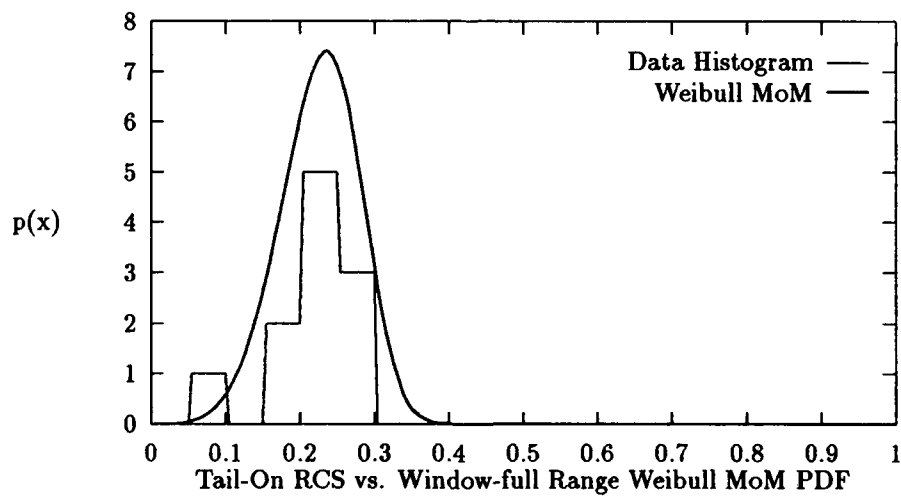


Figure 4.31. Top CGFT PDF of Fighter Data at Tail-On $\pm 5^\circ$, 0.5° sample interval, $\theta = 90^\circ$, $\theta - \theta$ polarization, 1 GHz Full-Scale

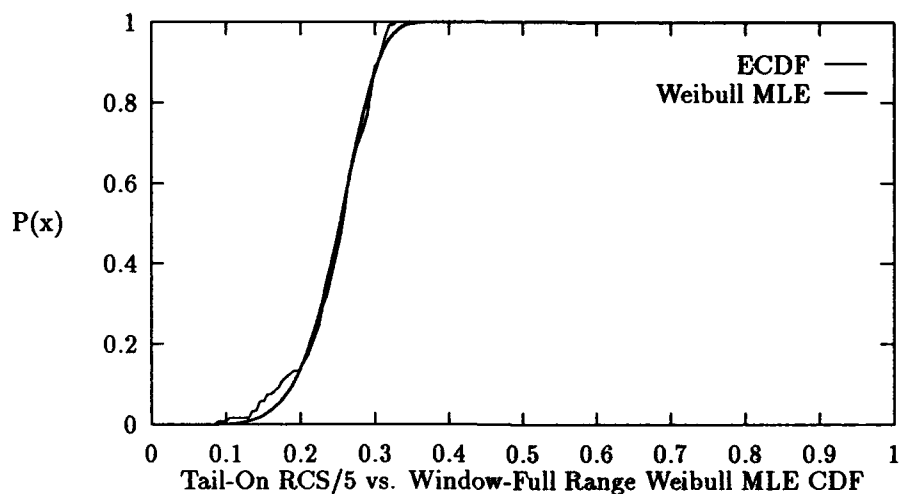


Figure 4.32. Top KGFT CDF of Fighter Data at Tail-On $\pm 5^\circ$, 0.5° sample interval, $\theta = 90^\circ \pm 5^\circ$, $\theta - \theta$ polarization, 1 GHz Full-Scale

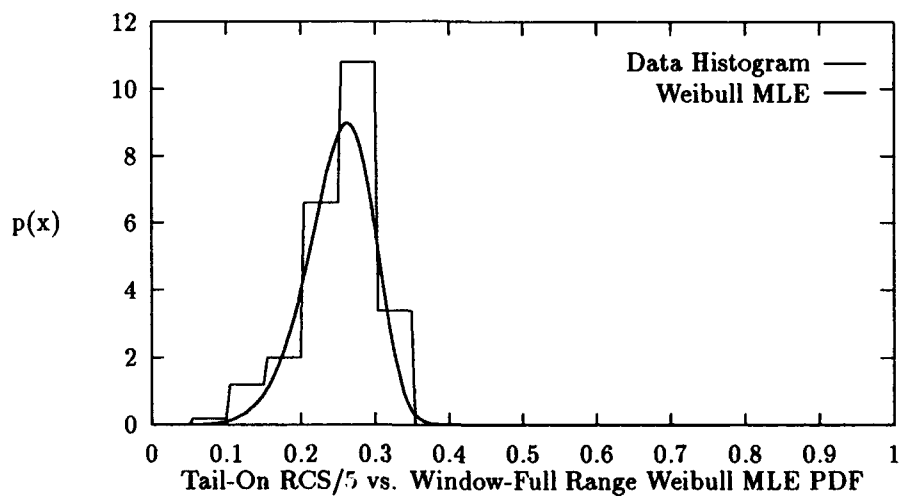


Figure 4.33. Top KGFT PDF of Fighter Data at Tail-On $\pm 5^\circ$, 0.5° sample interval, $\theta = 90^\circ \pm 5^\circ$, $\theta - \theta$ polarization, 1 GHz Full-Scale

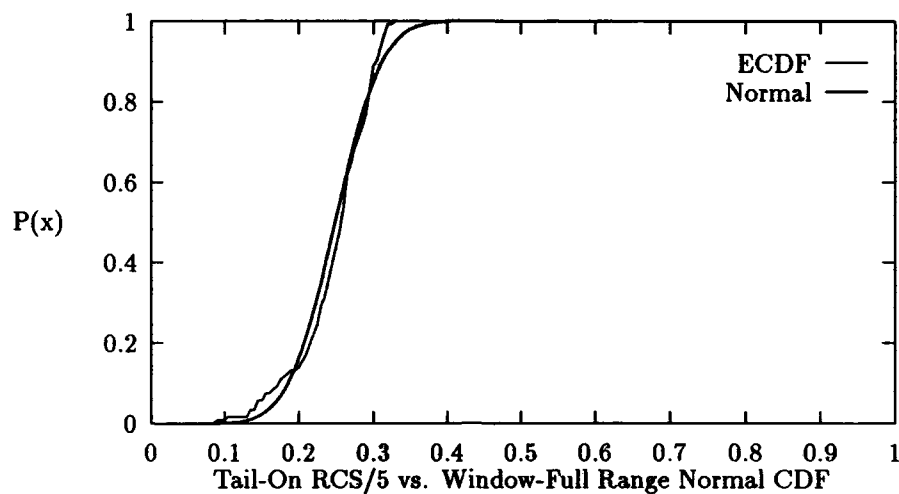


Figure 4.34. Top CGFT CDF of Fighter Data at Tail-On $\pm 5^\circ$, 0.5° sample interval, $\theta = 90^\circ \pm 5^\circ$, $\theta - \theta$ polarization, 1 GHz Full-Scale

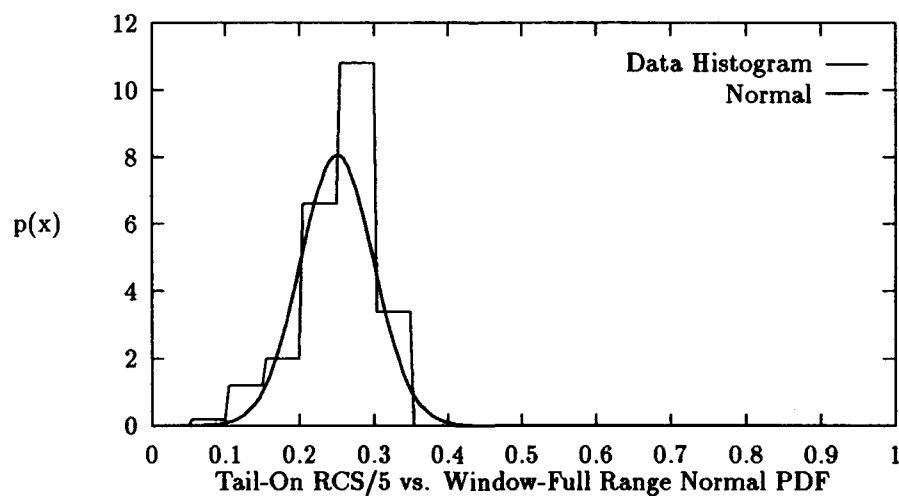


Figure 4.35. Top CGFT PDF of Fighter Data at Tail-On $\pm 5^\circ$, 0.5° sample interval, $\theta = 90^\circ \pm 5^\circ$, $\theta - \theta$ polarization, 1 GHz Full-Scale

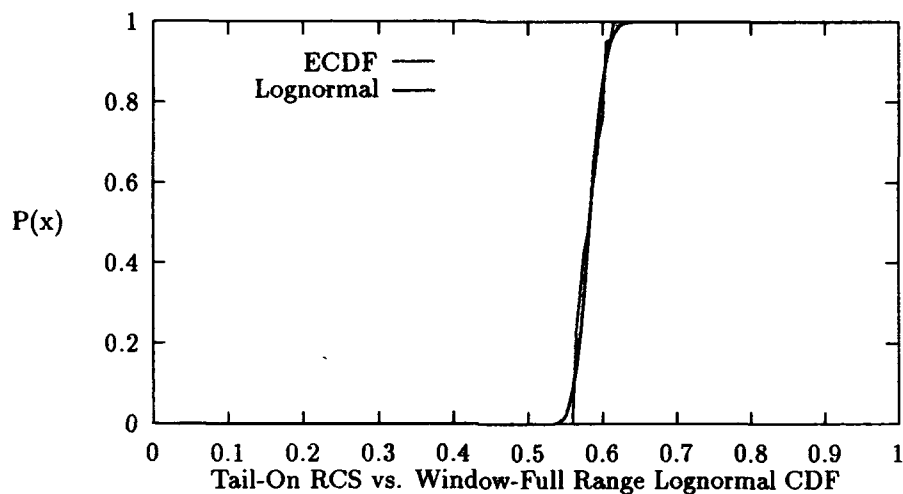


Figure 4.36. Top KGFT and CGFT CDF of Missile Data at Tail-On $\pm 5^\circ$, 0.5° sample interval, $\theta = 90^\circ$, $\theta - \theta$ polarization, 18 GHz Full-Scale

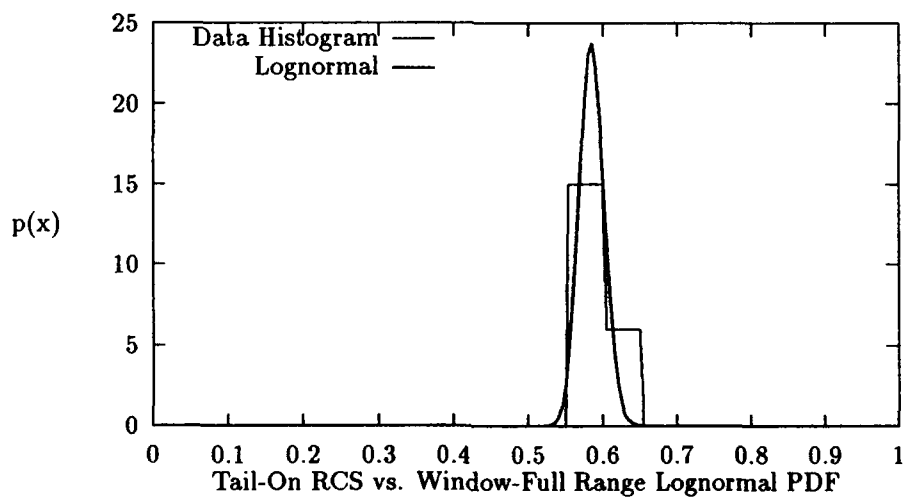


Figure 4.37. Top KGFT and CGFT PDF of Missile Data at Tail-On $\pm 5^\circ$, 0.5° sample interval, $\theta = 90^\circ$, $\theta - \theta$ polarization, 18 GHz Full-Scale

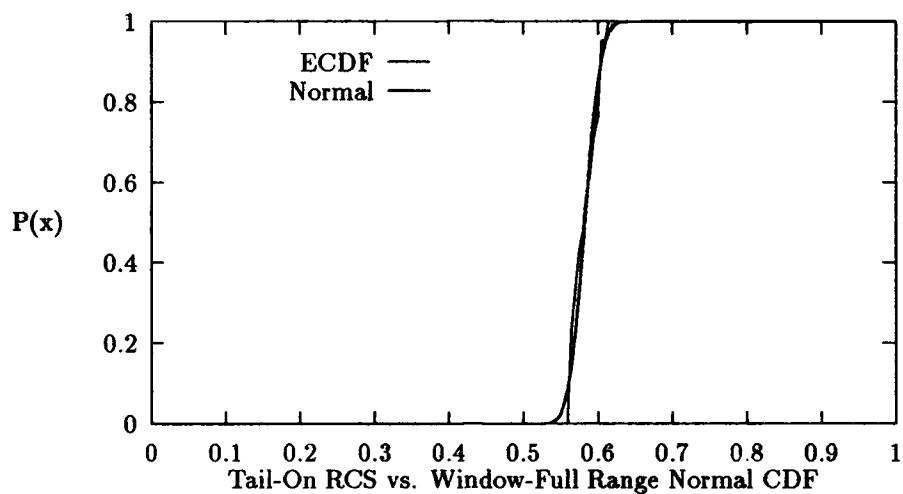


Figure 4.38. Top CGFT CDF of Missile Data at Tail-On $\pm 5^\circ$, 0.5° sample interval, $\theta = 90^\circ$, $\theta - \theta$ polarization, 18 GHz Full-Scale

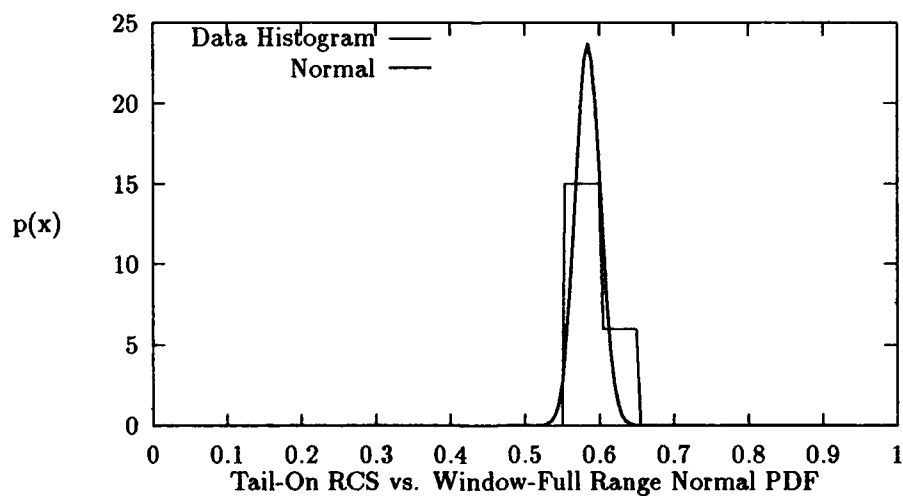


Figure 4.39. Top CGFT PDF of Missile Data at Tail-On $\pm 5^\circ$, 0.5° sample interval, $\theta = 90^\circ$, $\theta - \theta$ polarization, 18 GHz Full-Scale

V. Determination of Optimum Model for Window vs. Window Comparisons

5.1 Introduction

This chapter will analyze how each pdf handles the empirical distribution of the data from each aspect window when the statistical characteristics are derived from the aspect window solely. The aspect windows and types of aircraft studied will be identical to that of Chapter IV.

Because the statistical characteristics are derived solely from the aspect windows, the normalized range of each sample set will stretch from zero to one. This is in contrast to the Window vs. Full-Range comparisons where the sample set could be restricted to a small section of the full range and usually was.

The expanded range of the sample sets should result in a consistently larger sample variance.

The Kolmogorov Level of Significance, and the Chi-Square Level of Significance for Window vs. Full-Range RCS Models are presented in Appendix A.

5.2 Test Results for Window vs. Window RCS Models

5.2.1 Nose-On Fighter: $\theta = 90^\circ$ This data set is characterized by a mean of 0.74, a variance of 9.07×10^{-2} , a small number of samples ($n = 11$), and a strong rightward skew. The best fit KGFT and CGFT models are presented in Figures 5.1-5.4.

This variance is four times larger than the largest Window vs. Full-Range variance. The mean is also larger than most of the Window vs. Full-Range means. The wide variance expands the pdfs so they can cover a sample set than is beginning to appear uniform. The KGFT declares the Beta MLE and MoM pdfs to have a LoS greater than 20%. The Beta MLE has the lowest Kolmogorov test statistic. However, for this sample set, visual assessment agrees with the CGFT, which declares the Beta MoM to be the only pdf with a LoS greater than 25%. The average separation between the Beta MoM and the sample set (0.0544) is much smaller than the difference between the Beta MLE and

the sample set (0.1275). However, the $n = 10$ sample climbs at a much higher rate than the Beta MoM. For this data sample, the Beta MoM is less expanded than the MLE. The parameters for the Beta function are less than one for the MoM and the MLE. This causes the pdf to approximate a negative exponential function against the low-range boundary and a positive exponential function against the high-range boundary. The MoM pdf has unequal parameters which skew the emphasis of the two exponential functions toward the positive exponential function against the high-range boundary. This closely matches the data histogram. The MLE has small, equal parameters, which press the two exponential functions against their respective boundaries. This is the result of an extreme form of expansion.

No other pdf could approximate the sample set because of the high variance.

5.2.2 Nose-On Fighter: $\theta = 90^\circ \pm 5^\circ$ This data set is characterized by a mean of 0.64, a variance of 2.9×10^{-2} , a large number of samples ($n = 121$), and no discernable skew. The best fit KGFT and CGFT models are presented in Figures 5.5-5.8.

Though a non-skewed sample set with a mean above 0.5 can mean trouble for the Beta pdfs, the wide variance expands all other pdfs to a greater extent. The KGFT declares the Beta MoM to have the highest LoS, though it is only between 10% and 20%. There are no other pdfs with that range of LoS. The lack of skew with a mean shifted off mid-range hurts the Beta pdfs, but the large variance prevents the Normal, Lognormal, or Weibull pdfs from compressing enough to match or improve the performance of the Beta pdfs. A visual assessment shows the Weibull MoM and Normal pdfs matching the Beta MoM in tracking the ECDF. The CGFT declares the Normal and Weibull pdfs to have the lowest test statistic. The CGFT gives the pdfs a LoS between 5% and 2.5%.

5.2.3 Nose-On Missile: $\theta = 90^\circ$ This data set is characterized by a mean of 0.50, the widest variance of any sample set ($\text{var}=0.1083$), a small number of samples ($n = 21$), and no discernable skew. The best fit KGFT and CGFT models are presented in Figures 5.9-5.10.

The sample set appears to have a fairly uniform distribution. The Beta pdfs will present a uniform distribution if $\alpha = \beta = 1$. If α and β are equal but less than one, the pdf is expanded toward the boundaries of the range. The Beta MoM is the least expanded of the Beta pdfs and attains the lowest Kolmogorov test statistic. The Beta MLE and MoM, Normal, and Rayleigh pdfs attain a Kolmogorov LoS greater than 20%. Because the mean of the sample set is mid-range, the Beta pdfs do not skew and therefore are able to maintain a fairly constant probability density throughout the range.

The CGFT agrees with the KGFT, giving the Beta MoM a LoS greater than 20%.

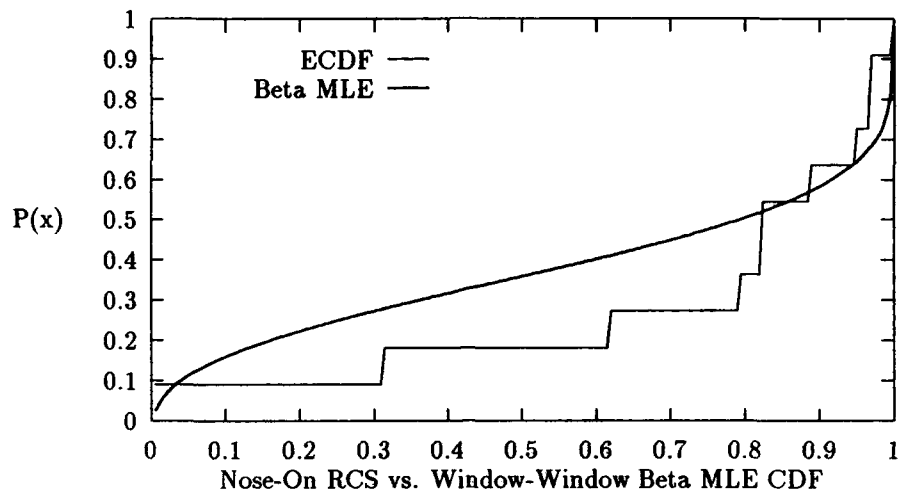


Figure 5.1. Top KGFT CDF of Fighter Data at Nose-On $\pm 5^\circ$, 0.5° sample interval, $\theta = 90^\circ$, $\theta - \theta$ polarization, 1 GHz Full-Scale

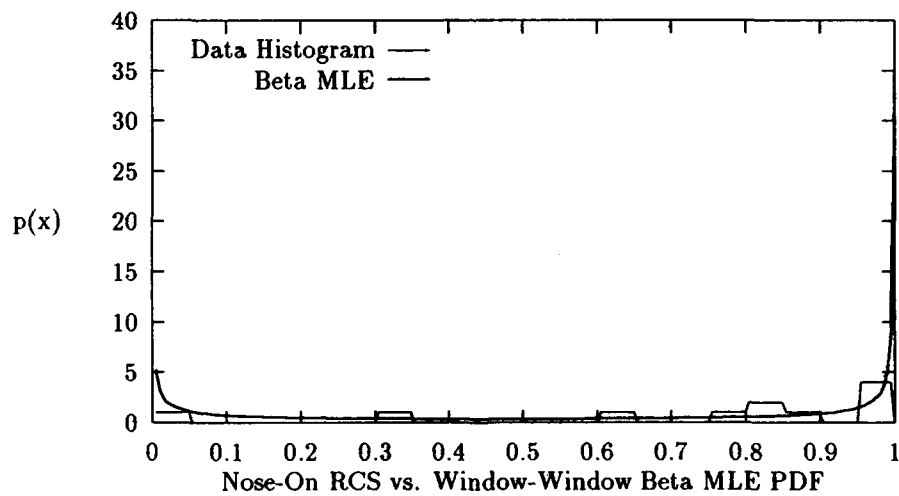


Figure 5.2. Top KGFT PDF of Fighter Data at Nose-On $\pm 5^\circ$, 0.5° sample interval, $\theta = 90^\circ$, $\theta - \theta$ polarization, 1 GHz Full-Scale

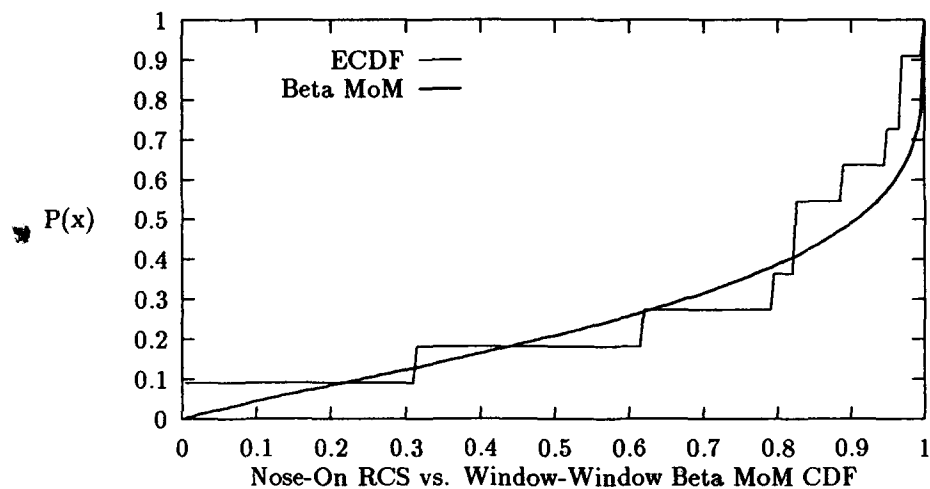


Figure 5.3. Top CGFT CDF of Fighter Data at Nose-On $\pm 5^\circ$, 0.5° sample interval, $\theta = 90^\circ$, $\theta - \theta$ polarization, 1 GHz Full-Scale

[

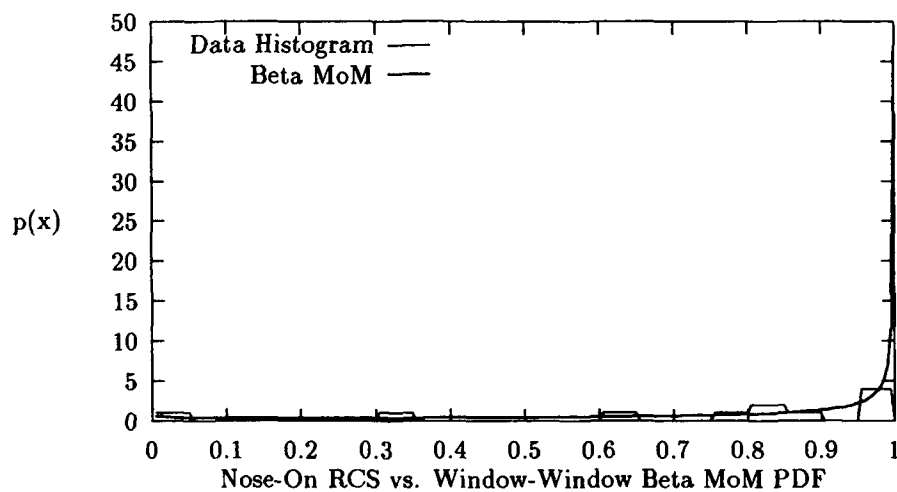


Figure 5.4. Top CGFT PDF of Fighter Data at Nose-On $\pm 5^\circ$, 0.5° sample interval, $\theta = 90^\circ$, $\theta - \theta$ polarization, 1 GHz Full-Scale

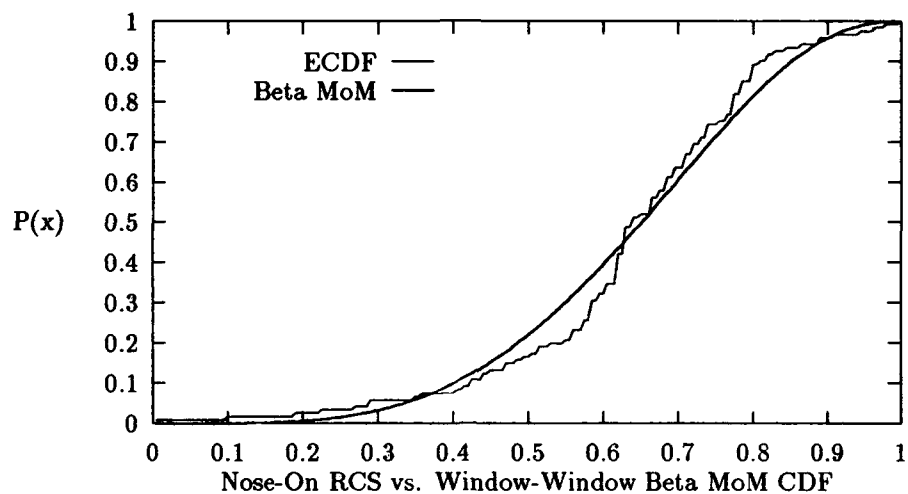


Figure 5.5. Top KGFT CDF of Fighter Data at Nose-On $\pm 5^\circ$, 0.5° sample interval, $\theta = 90^\circ \pm 5^\circ$, $\theta - \theta$ polarization, 1 GHz Full-Scale

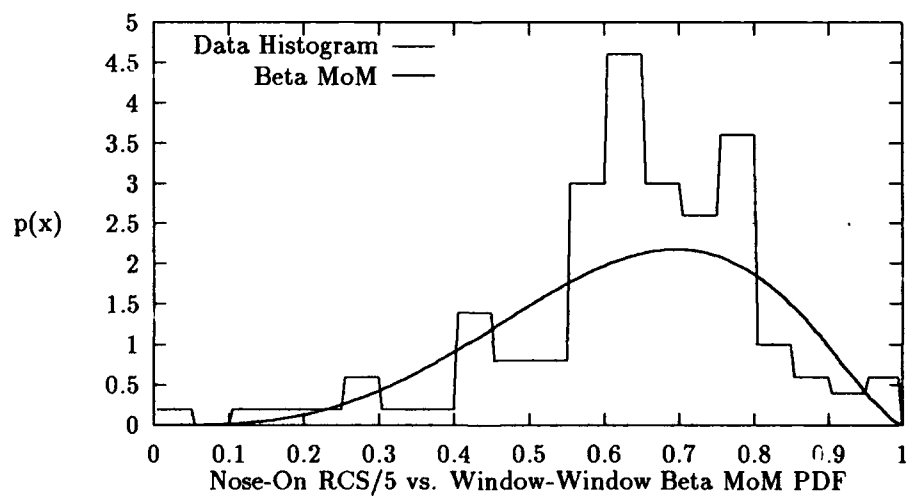


Figure 5.6. Top KGFT PDF of Fighter Data at Nose-On $\pm 5^\circ$, 0.5° sample interval, $\theta = 90^\circ \pm 5^\circ$, $\theta - \theta$ polarization, 1 GHz Full-Scale

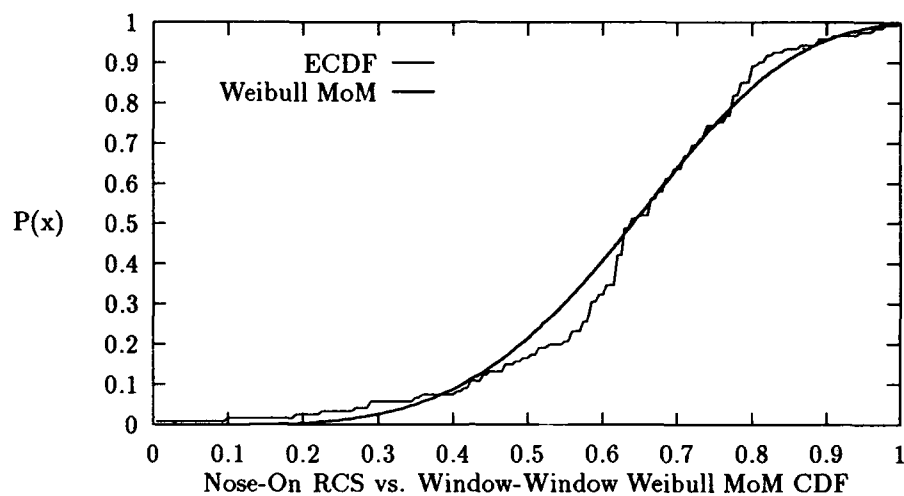


Figure 5.7. Top CGFT CDF of Fighter Data at Nose-On $\pm 5^\circ$, 0.5° sample interval, $\theta = 90^\circ \pm 5^\circ$, $\theta - \theta$ polarization, 1 GHz Full-Scale

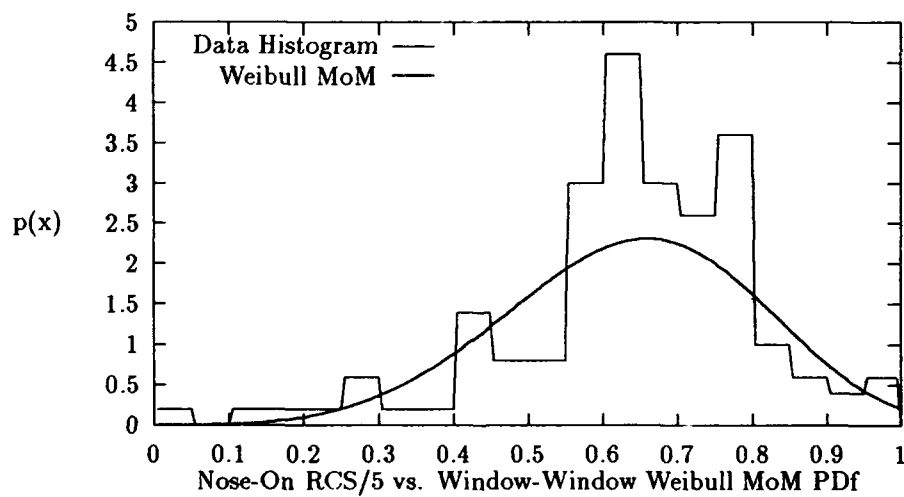


Figure 5.8. Top CGFT PDF of Fighter Data at Nose-On $\pm 5^\circ$, 0.5° sample interval, $\theta = 90^\circ \pm 5^\circ$, $\theta - \theta$ polarization, 1 GHz Full-Scale

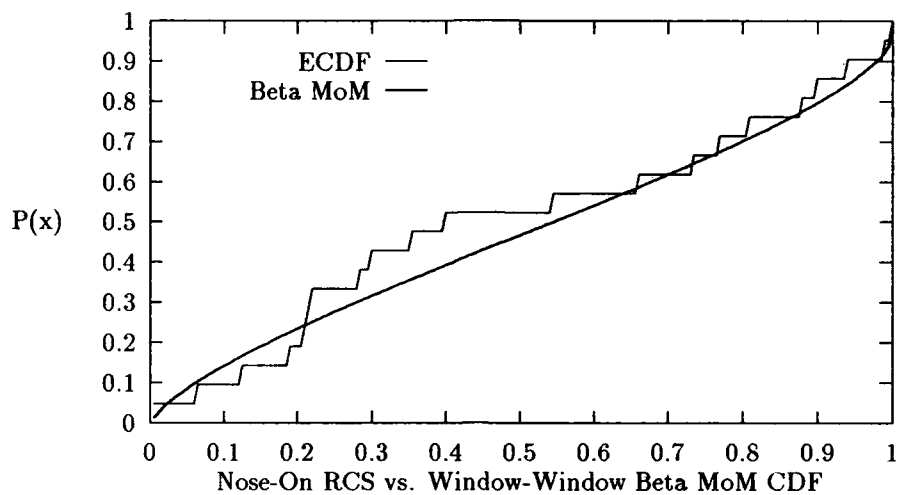


Figure 5.9. Top KGFT and CDFT CDF of Missile Data at Nose-On $\pm 5^\circ$, 0.5° sample interval, $\theta = 90^\circ$, $\theta - \theta$ polarization, 18 GHz Full-Scale

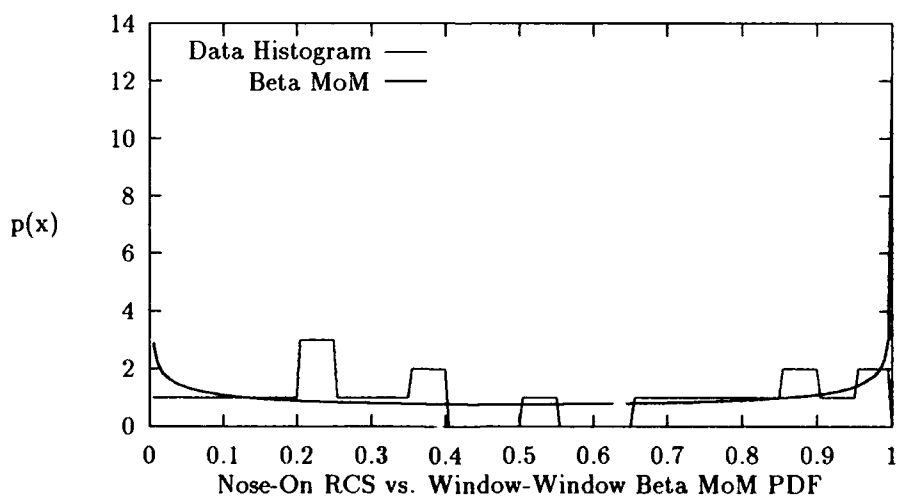


Figure 5.10. Top KGFT and CGFT PDF of Missile Data at Nose-On $\pm 5^\circ$, 0.5° sample interval, $\theta = 90^\circ$, $\theta - \theta$ polarization, 18 GHz Full-Scale

5.2.4 Broadside Fighter: $\theta = 90^\circ$ This data set is characterized by a mean of 0.66, a variance of 3.9×10^{-2} , a small number of samples ($n = 21$), and no discernable skew. The best fit KGFT and CGFT models are presented in Figures 5.11-5.14.

The KGFT declares the Beta MoM, Weibull MoM, and Normal pdfs to have a LoS greater than 20%. The Weibull MLE's α parameter is expanded below a value of three, so the pdf shifts far to the left, where it begins to approximate the negative exponential function. Both Beta MLE parameters are expanded below one, so the pdf is pressed against both range boundaries. However, the small variance (for Window vs. Window comparisons) requires a pdf that can approximate a normal function. The Weibull MoM and Normal pdfs have normal shaped functions. Because the mean is above 0.5, the Beta MoM is skewed right, but the Beta MoM is able to maintain a higher compression than the Weibull MoM and Normal pdfs, and attains the lowest Kolmogorov test statistic.

Because their densities are centered correctly, the CGFT declares the Weibull MoM and Normal pdfs to have the highest LoS ($25\% > \alpha > 10\%$). Visual assessment tends to agree with the CGFT again.

5.2.5 Broadside Fighter: $\theta = 90^\circ \pm 5^\circ$ This data set is characterized by a mean of 0.64, a variance of 1.8×10^{-2} , a large number of samples ($n = 231$), and a rightward skew. The best fit KGFT and CGFT models are presented in Figures 5.15-5.16.

The sample variance is the smallest of the Window vs. Window comparisons. This allows the Weibull MoM to compress and become rightward skewed to the extent that the Weibull MoM attains the lowest Kolmogorov test statistic, although none of the pdfs match the compression of the sample set. The Beta MoM and Weibull MoM pdfs attain the highest LoS ($20\% > \alpha > 10\%$).

The CGFT declares the Weibull MoM to have the lowest test statistic, though, as with all other large sample sets, the test statistic results in a poor LoS.

5.2.6 Broadside Missile: $\theta = 90^\circ$ This data set is characterized by a mean of 0.71, a variance of 4.46×10^{-2} , a small number of samples ($n = 41$), and a rightward skew. The best fit KGFT and CGFT models are presented in Figures 5.17-5.20.

The Beta MLE is expanded into a postive exponential function by the very high mean. The Beta MoM does not skew to the extent of the Beta MLE and approximates a ramp function. The Weibull pdfs approach a normal function and, along with the Normal pdf, reach their maximum probability density too early. The KGFT declares the Beta MoM, Weibull MoM, and Normal pdfs to have a LoS greater than 20%. The Beta MoM has the smallest test statistic, with a value less than half that of the Weibull MoM or Normal pdfs.

The CGFT agrees with the KGFT, giving the Beta MoM a LoS greater than 25%. Visual assessment clearly shows the Beta MoM to be the best-fit pdf.

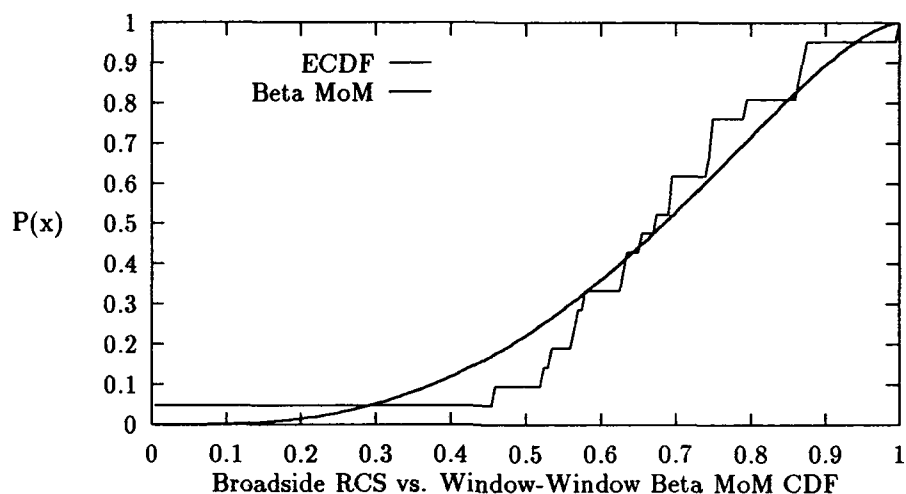


Figure 5.11. Top KGFT CDF of Fighter Data at Broadside $\pm 5^\circ$, 0.5° sample interval, $\theta = 90^\circ$, $\theta - \theta$ polarization, 1 GHz Full-Scale

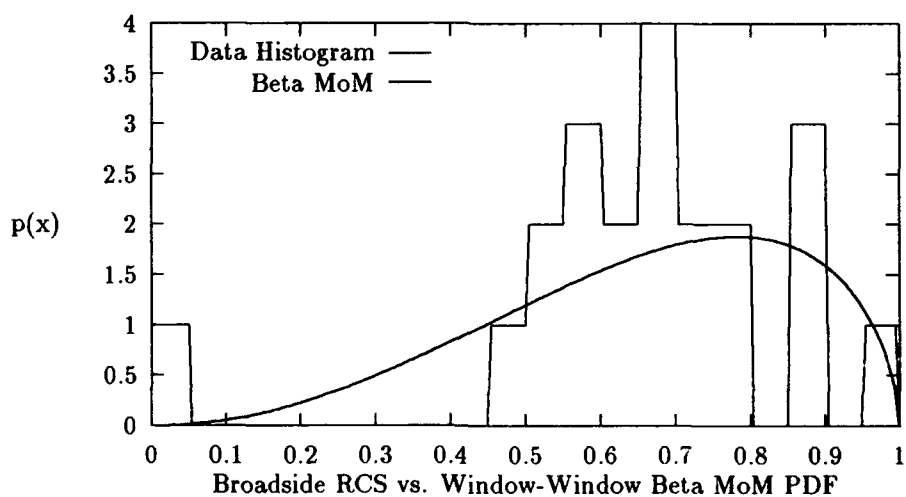


Figure 5.12. Top KGFT PDF of Fighter Data at Broadside $\pm 5^\circ$, 0.5° sample interval, $\theta = 90^\circ$, $\theta - \theta$ polarization, 1 GHz Full-Scale

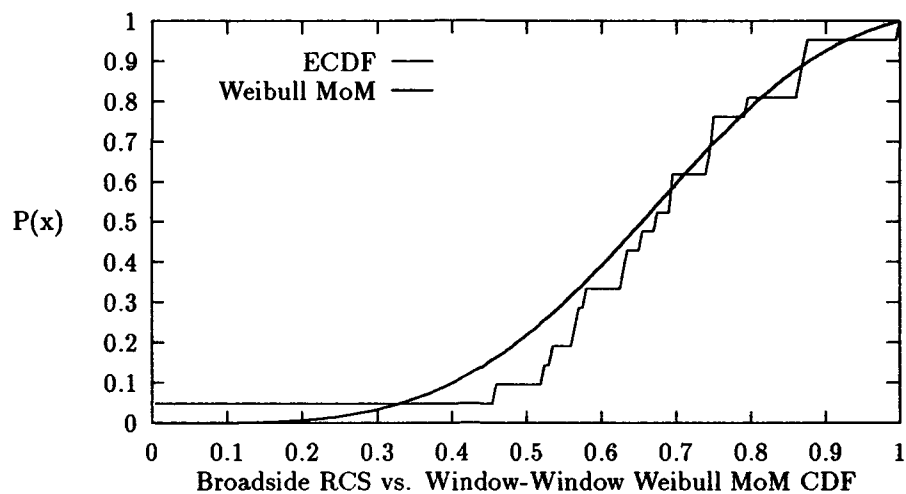


Figure 5.13. Top CGFT CDF of Fighter Data at Broadside $\pm 5^\circ$, 0.5° sample interval, $\theta = 90^\circ$, $\theta - \theta$ polarization, 1 GHz Full-Scale

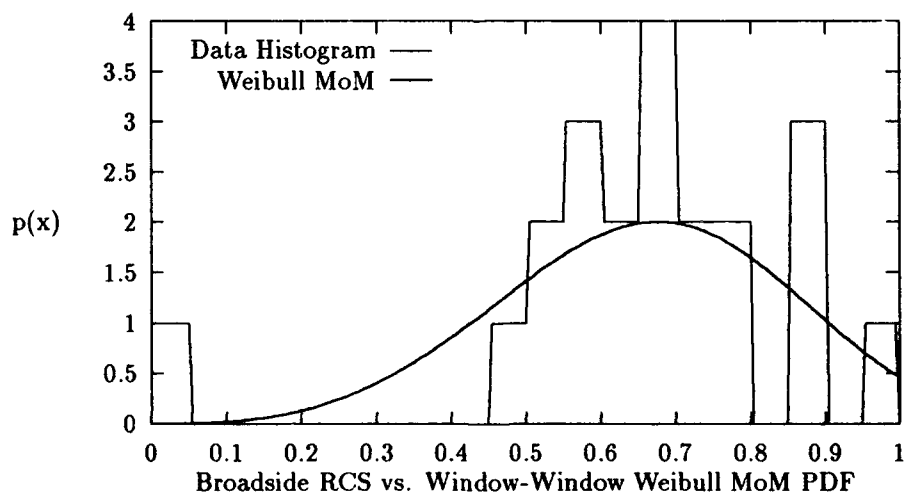


Figure 5.14. Top CGFT PDF of Fighter Data at Broadside $\pm 5^\circ$, 0.5° sample interval, $\theta = 90^\circ$, $\theta - \theta$ polarization, 1 GHz Full-Scale

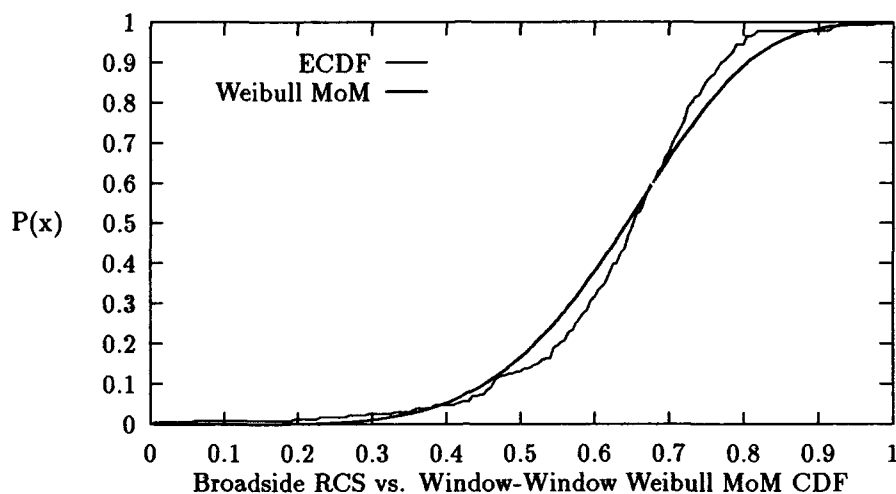


Figure 5.15. Top KGFT and CGFT CDF of Fighter Data at Broadside $\pm 5^\circ$, 0.5° sample interval, $\theta = 90^\circ \pm 5^\circ$, $\theta - \theta$ polarization, 1 GHz Full-Scale

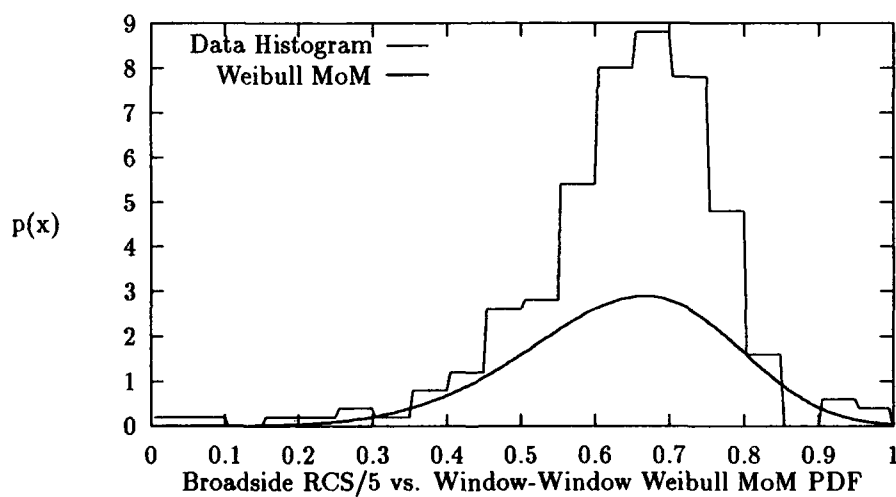


Figure 5.16. Top KGFT and CGFT PDF of Fighter Data at Broadside $\pm 5^\circ$, 0.5° sample interval, $\theta = 90^\circ \pm 5^\circ$, $\theta - \theta$ polarization, 1 GHz Full-Scale

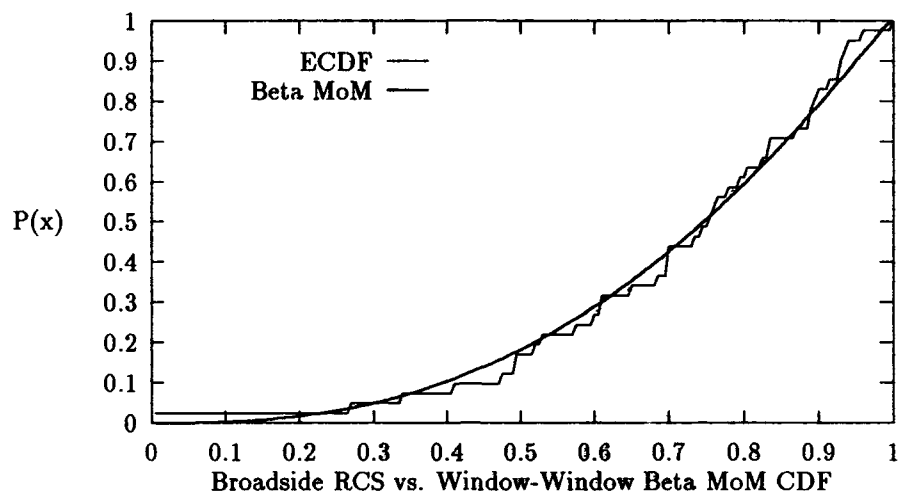


Figure 5.17. Top KGFT and CGFT CDF of Missile Data at Broadside $\pm 5^\circ$, 0.5° sample interval, $\theta = 90^\circ$, $\theta - \theta$ polarization, 18 GHz Full-Scale

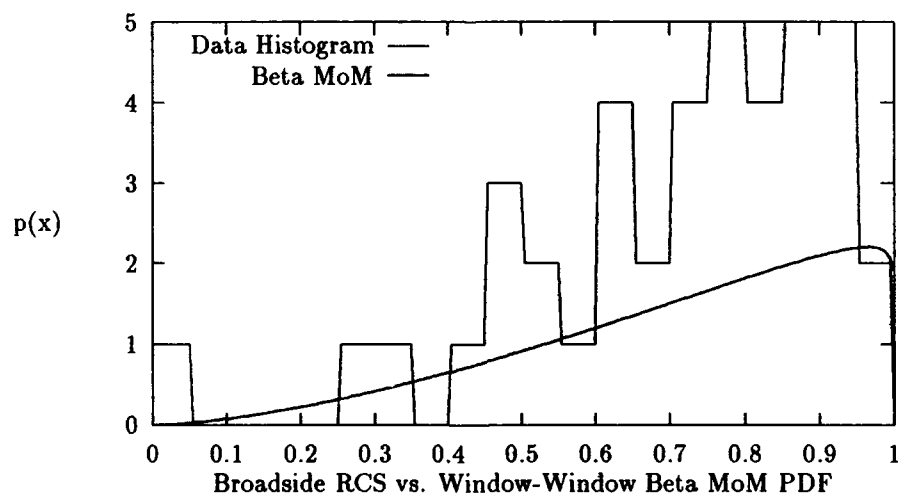


Figure 5.18. Top KGFT and CGFT PDF of Missile Data at Broadside $\pm 5^\circ$, 0.5° sample interval, $\theta = 90^\circ$, $\theta - \theta$ polarization, 18 GHz Full-Scale

5.2.7 Tail-On Fighter: $\theta = 90^\circ$ This data set is characterized by a mean of 0.66, a variance of 6.92×10^{-2} , a small number of samples ($n = 11$), and no discernible skew. The best-fit KGFT and CGFT models are presented in Figures 5.21-5.24.

Though the variance is not the largest of the sample sets, the samples appear almost uniformly distributed. There are many pdfs to which the KGFT gives an LoS greater than 20%: Beta MLE and MoM, Weibull MoM, Normal, and One-Dominant-Plus-Rayleigh. The Beta MLE is expanded to the extent that the exponential functions are pressed tight against the range boundaries. The Beta MoM is a positive exponential function with a very shallow slope until very close to the high-range boundary. The pdf approximates a uniform distribution to a certain extent. The Weibull MoM, Normal, and One-Dominant-Plus-Rayleigh pdfs are all normal functions centered near the sample mean. The KGFT gives the Beta MoM the lowest test statistic.

The CGFT declares the Beta MLE and MoM pdfs to have the highest LoS ($\alpha > 25\%$). Though the Beta MLE may be evenly distributed about the mean, a visual assessment indicates that the Beta MLE does not come close to approximating the sample set.

5.2.8 Tail-On Fighter: $\theta = 90^\circ \pm 5^\circ$ This data set is characterized by a mean of 0.68, a variance of 4.25×10^{-2} , a large number of samples ($n = 121$), and no discernible skew. The best-fit KGFT and CGFT models are presented in Figures 5.25-5.28.

The variance is tighter for this sample set than the Tail-On Fighter: $\theta = 90^\circ$ sample set. The KGFT declares the Beta MoM pdf to have a LoS greater than 20%, along with the lowest test statistic. As has been seen in many other sample sets, the Beta MoM is the only pdf able to maintain high compression at wide variances and a rightward skew. The Weibull MoM and Normal pdfs produce normal functions centered on the sample mean. As variance increases, the Weibull pdf becomes normal shaped, then begins to skew left.

The CGFT declares the Weibull MoM and Beta MoM pdfs to have the highest LoS, though, as with all the large sample sets, the LoS is poor ($5\% > \alpha > 2.5\%$). The Weibull MoM has the lowest test statistic. A visual assessment shows the Beta MoM to have the best fit.

5.2.9 Tail-On Missile: $\theta = 90^\circ$ This data set is characterized by a mean of 0.43, a variance of 0.103, a small number of samples ($n = 21$), and slight leftward skew. The best-fit KGFT and CGFT models are presented in Figures 5.29-5.30.

With the second highest variance, this sample set is nearly uniform. All parameters for the Beta pdfs are less than one, so they are expanded to opposing exponential functions. As usual, the Beta MoM is less expanded than the Beta MLE, so the Beta MoM has a fairly high probability density across the sample range. The Weibull MoM skews leftward, but skews too far. The high-range probability densities are not large enough. The Normal pdf puts too much emphasis on the middle range of the sample set. The KGFT declares the Beta MoM and Weibull MoM to have a LoS greater than 20%. The Beta MoM has the lowest test statistic.

The CGFT agrees with the KGFT, declaring the Beta MoM to be the only pdf with a LoS greater than 25%. Visual assessment agrees with the two tests.

5.3 Analysis of Window vs. Window RCS Models

5.3.1 PDF Performance The Window vs. Window sample sets have a consistently high mean: Avg. mean = 0.68, standard deviation = 9.4×10^{-2} . The variance ranges from 1.8×10^{-2} to 1.02×10^{-1} . This range's low end is the high end of the Window vs. Full-Range variance range, and the range's high end is a level of magnitude above the top of the Window vs. Full-Range variance range. Consequently, the variance sensitive pdfs (Weibull, Lognormal, Normal) are expanded much more than the Beta pdfs. The Weibull MLE shape parameter has a value less than one four times, at these values, the Weibull pdf approximates the negative exponential function. Because only one of the sample sets is skewed left, the extreme expansion of the Weibull MLE makes the pdf ineffective for Window vs. Window modeling. The Weibull MoM is not as variance sensitive, but is still skewed left when the sample sets are not.

The scale parameter of the Lognormal pdf causes the pdf to approximate a negative exponential function when the parameter is greater than one. This is the case in eight of the nine sample sets. In the ninth case, the sample set has the smallest variance. The

pdf is still centered far to the left of the sample set values. The lognormal pdf is more sensitive to variance changes than any other pdf. The wide variance skews the pdf to the left consistently, making the pdf ineffective.

The Normal pdf does not expand as fast as the Lognormal. When the Beta pdf is skewed too far to the right for the sample mean, the Normal is able to outperform the Beta in the CGFT. This only happens at the lower sample variances.

The Weibull MoM performs well at the same low variances that the Normal performs well on. At these variances, the Weibull MoM outperforms the Beta MoM on the CGFT. At the lowest Window vs. Window sample set, the Weibull MoM outperforms the Beta MoM on the KGFT. For the three lowest sample variances, a visual assessment indicates the Weibull MoM to be as good or better a model than the Beta MoM.

The Rayleigh and One-Dominant-Plus-Rayleigh pdfs perform slightly better than they do for Window vs. Full-Range models. The high variances expand the sample sets to the extent that the permanently expanded Rayleigh class pdfs can occasionally model the sample sets well. This permanent expansion is due to consistent sample second moments which are not significantly different in value from the Window vs. Full-Range sample sets.

The Rayleigh ($y = x^2$) pdf is consistently ineffective, as it is for the Window vs. Full-Range models.

The Beta pdf is made for the Window vs. Window sample sets. The pdf remains expansion resistant to high variances. The high variances result in a multitude of sample distributions which also favor the Beta over other pdfs. The expansion resistance and versatility of the pdf give it as high a Kolmogorov LoS as any pdf in every sample set. The Beta pdf has the lowest Kolmogorov test statistic in eight of the nine sample sets. The ninth sample set possesses the smallest variance of the group.

Perhaps because the pdf skews at the routinely high means of the Window vs. Window sample sets, the Beta pdf does not perform as well on the Chi-Square tests. This would be caused by the uneven distribution about the sample set mean that the Beta pdf exhibits. The Weibull and Normal pdfs outperform the Beta on the sample sets with the

four lowest variances when the CGFT is used. Visual assessment agrees with the CGFT once out of the three cases where there is a difference between the KGFT and the CGFT.

5.3.2 Parameter Estimation The MoM outperforms the MLE in every sample set. In the one sample set where the Beta MLE is rated better than the MoM by the KGFT, a visual assessment clearly indicates the Beta MoM to have the better fit. Though the consistently wide variances may be the cause of the MoM's success in Window vs. Window models, variance plays no apparent role in determining the optimum parameter estimator in Window vs. Full-Range models. The determiner in those models appears to be the number of samples in the sample set. In the Window vs. Window models, sample size makes no contribution toward parameter estimator effectiveness.

5.3.3 Sample Set Behaviour The wide sample variance experienced matches expectations for this type of model. The high mean of the Window vs. Window models matches the rightward skew of Window vs. Full-Range models. The high mean of the Window vs. Window sample sets could be a result of the relatively high RCS magnitudes encountered at the modeled windows. The relatively high magnitudes would cause the majority of the samples to be large along with a few small samples. This hypothesis is backed up by the fact that the two sample sets that do not have large means occur in the Tail-On and Nose-On windows, which do not have as large RCS magnitudes as the Broadside windows.

5.4 Summary

This chapter studies the results of the Window vs. Window RCS modeling procedure. It shows that the variance of the sample sets is much larger than the variance of the Window vs. Full-Range sample sets. The mean is found to be consistently high in the sample range.

It is shown that, for the large variances exhibited, the Beta pdf is the only pdf able to handle the resulting large variety of sample distributions.

The best parameter estimator is clearly the Method of Moments. The reason for this could be the large sample variances, but this is uncertain.

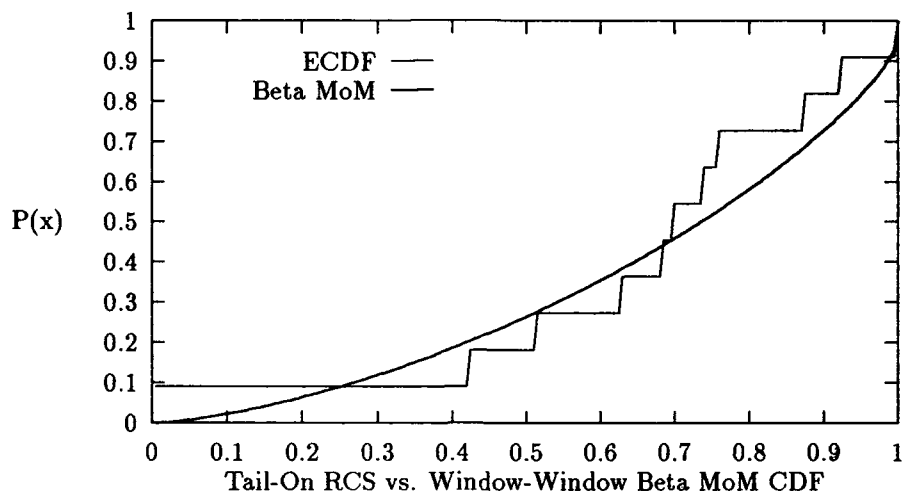


Figure 5.19. Top KGFT and CGFT CDF of Fighter Data at Tail-On $\pm 5^\circ$, 0.5° sample interval, $\theta = 90^\circ$, $\theta - \theta$ polarization, 1 GHz Full-Scale

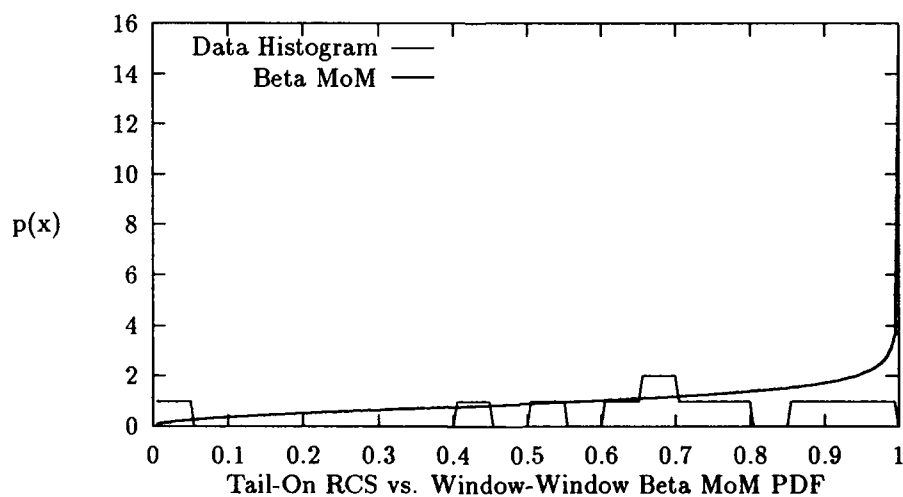


Figure 5.20. Top KGFT and CGFT PDF of Fighter Data at Tail-On $\pm 5^\circ$, 0.5° sample interval, $\theta = 90^\circ$, $\theta - \theta$ polarization, 1 GHz Full-Scale

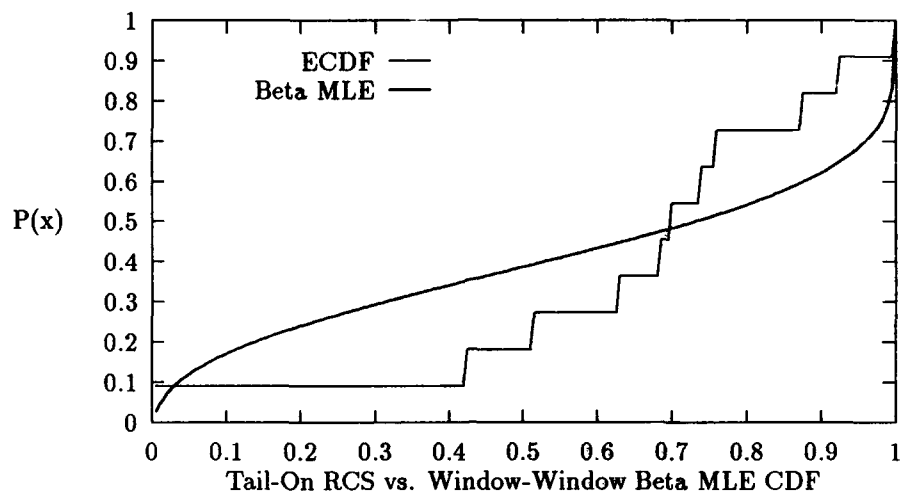


Figure 5.21. Top CGFT CDF of Fighter Data at Tail-On $\pm 5^\circ$, 0.5° sample interval, $\theta = 90^\circ$, $\theta - \theta$ polarization, 1 GHz Full-Scale

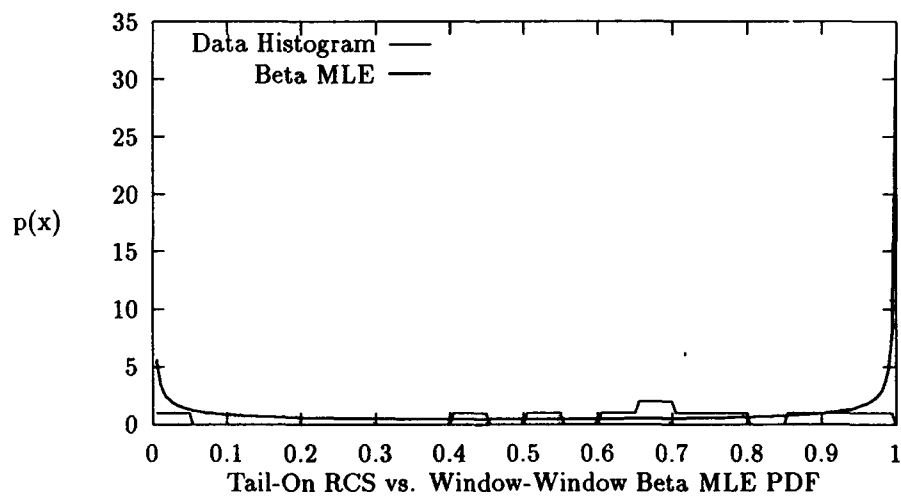


Figure 5.22. Top CGFT PDF of Fighter Data at Tail-On $\pm 5^\circ$, 0.5° sample interval, $\theta = 90^\circ$, $\theta - \theta$ polarization, 1 GHz Full-Scale

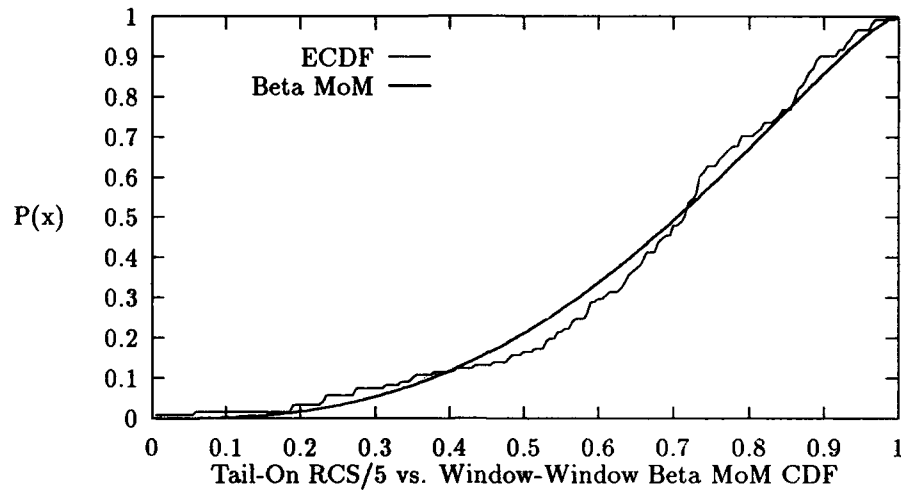


Figure 5.23. Top KGFT CDF of Fighter Data at Tail-On $\pm 5^\circ$, 0.5° sample interval, $\theta = 90^\circ \pm 5^\circ$, $\theta - \theta$ polarization, 1 GHz Full-Scale

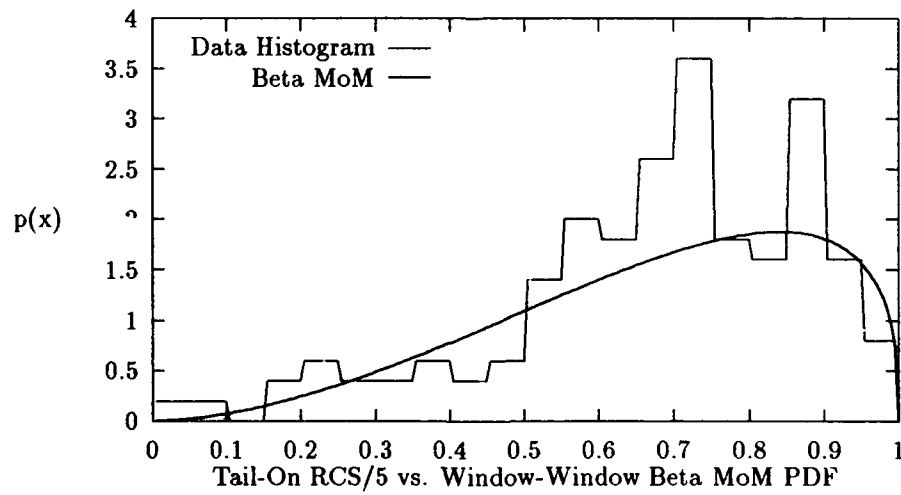


Figure 5.24. Top KGFT PDF of Fighter Data at Tail-On $\pm 5^\circ$, 0.5° sample interval, $\theta = 90^\circ \pm 5^\circ$, $\theta - \theta$ polarization, 1 GHz Full-Scale

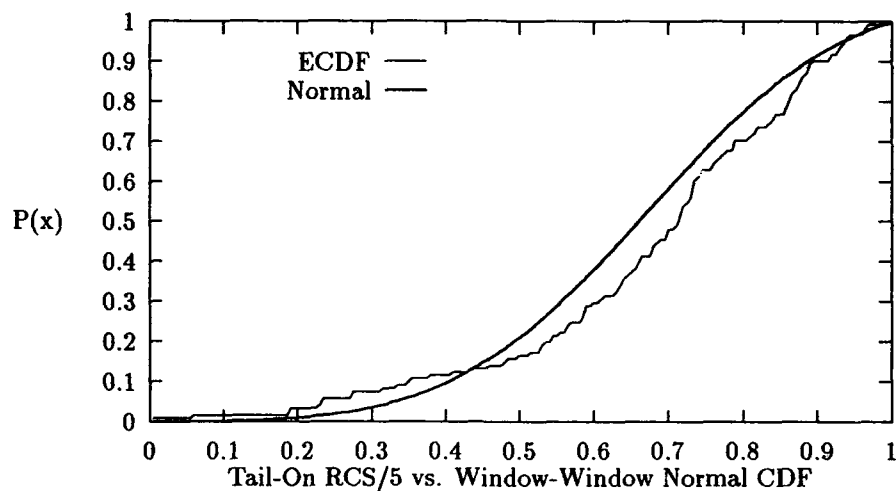


Figure 5.25. Top CGFT CDF of Fighter Data at Tail-On $\pm 5^\circ$, 0.5° sample interval, $\theta = 90^\circ \pm 5^\circ$, $\theta - \theta$ polarization, 1 GHz Full-Scale

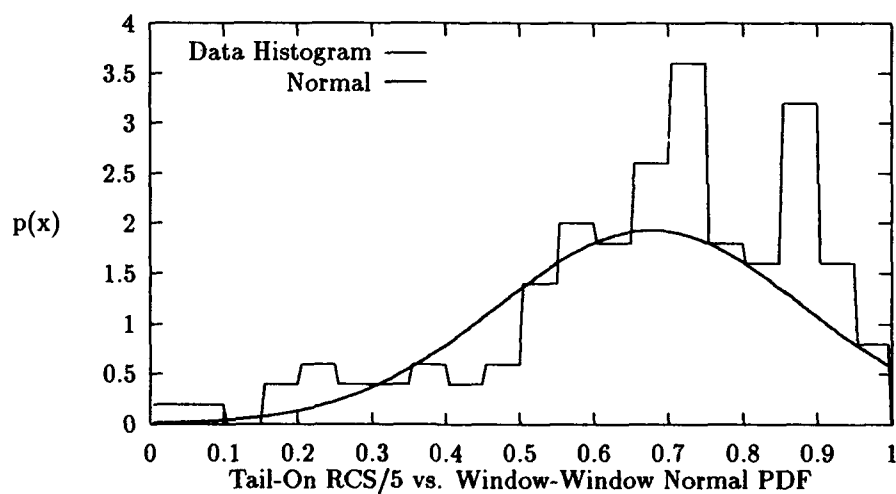


Figure 5.26. Top CGFT PDF of Fighter Data at Tail-On $\pm 5^\circ$, 0.5° sample interval, $\theta = 90^\circ \pm 5^\circ$, $\theta - \theta$ polarization, 1 GHz Full-Scale

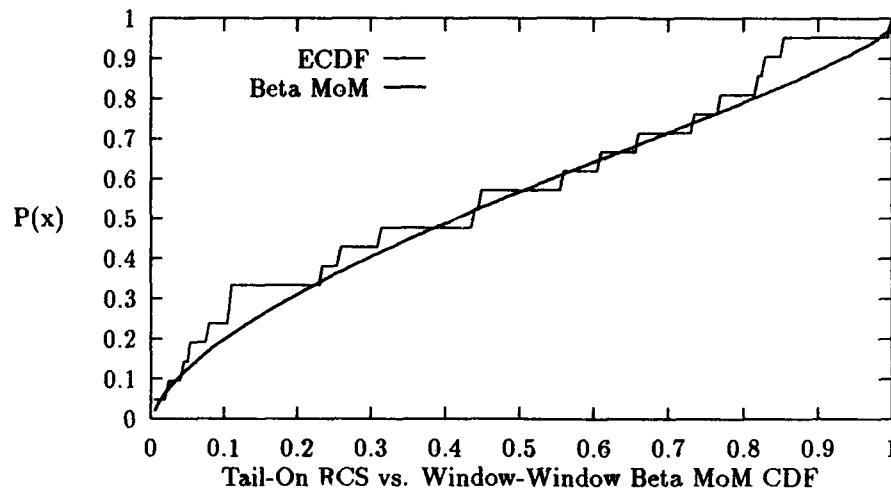


Figure 5.27. Top KGFT and CGFT CDF of Missile Data at Tail-On $\pm 5^\circ$, 0.5° sample interval, $\theta = 90^\circ$, $\theta - \theta$ polarization, 18 GHz Full-Scale

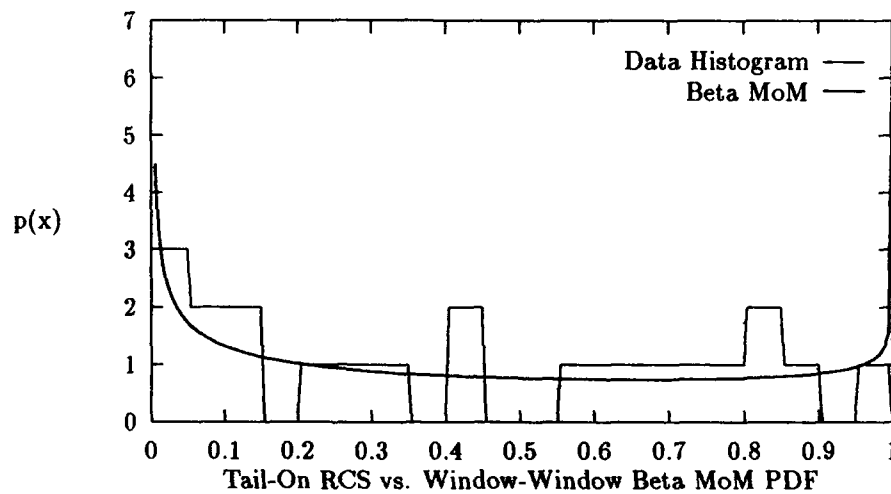


Figure 5.28. Top KGFT and CGFT PDF of Missile Data at Tail-On $\pm 5^\circ$, 0.5° sample interval, $\theta = 90^\circ$, $\theta - \theta$ polarization, 18 GHz Full-Scale

VI. Conclusions and Recommendations

6.0.1 Conclusions 1. The statistical characteristics of the three modeled aspect windows can be predicted. These characteristics will determine the optimum pdf.

2. The Weibull pdf will consistently be the optimum pdf for narrow variance sample sets. The Beta pdf will consistently be the optimum pdf for wide variance sample sets.

3. Though never quite as reliable as Window vs. Full-Range models, Window vs. Window models perform satisfactorily for the Kolmogorov Goodness-of-Fit test under the specifications of Section 2.5. The decrease in reliability is probably due to the wider variance of the Window vs. Window sample sets.

4. The Method of Moments will be the superior parameter estimator for Window vs. Window models. The Maximum Likelihood Estimator tends to be the superior parameter estimator for small-sample-set Window vs. Full-Range models, the Method of Moments tends to be the superior parameter estimator for large-sample-set Window vs. Full-Range models.

5. When determining goodness-of-fit, a visual assessment should always be performed to insure the pdf with the lowest test statistic is the closest match to the ECDF. Both the Kolmogorov and Chi-Square tests can give erroneous results under certain conditions. One bad sample can cause a close fitting pdf to fail the Kolmogorov test, while skewed sample sets can cause problems for the Chi-Square test.

6.0.2 Recommendations 1. Build signal detection and signal identification models using the optimized static RCS models as the base RCS value. Use numerical methods to determine the received detected waveform plus noise.

2. Form methods for measuring data skew. This would provide a method for better explaining why a particular pdf is optimum. Use numerical methods to determine the skew of the pdf models.

3. Evaluate more data sets to verify the statistical characteristics of the sample sets noted in this study.

4. Determine the causes of the varying performances of the MoM and MLE parameter estimators.

Appendix A. *Test Statistics and Levels of Significance*

The Kolmogorov and Chi-Square results are presented for every aspect angle and both aircraft types.

Table A.1. Fighter: $\theta = 90^\circ$ Kolmogorov Levels of Significance for Window vs. Full-Range, n =number of samples, T_1 =Test Statistic, $W_p=1-\alpha$ Quantile

| <i>pdf</i> | <i>Window Center</i> | <i>n</i> | <i>T₁</i> | <i>W_p</i> | <i>Level of Significance</i> |
|----------------|----------------------|----------|----------------------|----------------------|------------------------------|
| Beta MLE | 0° | 11 | 0.3325 | 0.352 | 20% > α > 10% |
| Beta MoM | | | | | |
| Weibull MLE | | | 0.2144 | 0.308 | α > 20% |
| Weibull MoM | | | 0.2346 | 0.308 | α > 20% |
| Lognormal | | | 0.2958 | 0.308 | α > 20% |
| Normal | | | 0.2883 | 0.308 | α > 20% |
| Rayleigh | | | 0.5474 | 0.468 | 1% > α |
| Rayleigh-y MLE | | | 0.7872 | 0.468 | 1% > α |
| Rayleigh-y MLE | | | 0.7253 | 0.468 | 1% > α |
| Rayleigh+1 | | | 0.4527 | 0.468 | 2% > α > 1% |
| Beta MLE | 90° | 21 | 0.1156 | 0.226 | α > 20% |
| Beta MoM | | | 0.1427 | 0.226 | α > 20% |
| Weibull MLE | | | 0.1192 | 0.226 | α > 20% |
| Weibull MoM | | | 0.1420 | 0.226 | α > 20% |
| Lognormal | | | 0.2247 | 0.259 | 20% > α > 10% |
| Normal | | | 0.1455 | 0.226 | α > 20% |
| Rayleigh | | | 0.4964 | 0.344 | 1% > α |
| Rayleigh-y MLE | | | 0.7239 | 0.344 | 1% > α |
| Rayleigh-y MoM | | | 0.7180 | 0.344 | 1% > α |
| Rayleigh+1 | | | 0.3740 | 0.344 | 1% > α |
| Beta MLE | 180° | 11 | 0.1555 | 0.308 | α > 20% |
| Beta MoM | | | 0.1854 | 0.308 | α > 20% |
| Weibull MLE | | | 0.1285 | 0.308 | α > 20% |
| Weibull MoM | | | 0.1468 | 0.308 | α > 20% |
| Lognormal | | | 0.2262 | 0.308 | α > 20% |
| Normal | | | 0.1632 | 0.308 | α > 20% |
| Rayleigh | | | 0.3520 | 0.391 | 10% > α > 5% |
| Rayleigh-y MLE | | | 0.6263 | 0.308 | 1% > α |
| Rayleigh-y MoM | | | 0.3701 | 0.391 | 10% > α > 5% |
| Rayleigh+1 | | | 0.2515 | 0.308 | α > 20% |

Table A.2. Fighter: $\theta = 90^\circ$ Chi-Square Levels of Significance for Window vs. Full-Range, n =number of samples, DoF= Degrees of Freedom, T_1 =Test Statistic, $W_p=1-\alpha$ Quantile

| <i>pdf</i> | <i>Window Center</i> | <i>n</i> | <i>DoF</i> | T_1 | W_p | <i>Level of Significance</i> |
|----------------|----------------------|----------|------------|---------|-------|------------------------------|
| Beta MLE | 0° | 11 | 1 | 4.4545 | 5.024 | 5% > α > 2.5% |
| Beta MoM | | | | | | |
| Weibull MLE | | | 1 | 2.2727 | 2.706 | 25% > α > 10% |
| Weibull MoM | | | 1 | 2.2727 | 2.706 | 25% > α > 10% |
| Lognormal | | | 1 | 2.2727 | 2.706 | 25% > α > 10% |
| Normal | | | 1 | 2.2727 | 2.706 | 25% > α > 10% |
| Rayleigh | | | 1 | 11 | 10.83 | 0.1% > α |
| Rayleigh-y MLE | | | 1 | 11 | 10.83 | 0.1% > α |
| Rayleigh-y MoM | | | 1 | 11 | 10.83 | 0.1% > α |
| Rayleigh+1 | | | 1 | 7.3636 | 7.879 | 1% > α > 0.5% |
| Beta MLE | 90° | 21 | 1 | 0.5238 | 1.323 | α > 25% |
| Beta MoM | | | 1 | 4.3333 | 5.024 | 5% > α > 2.5% |
| Weibull MLE | | | 1 | 0.5238 | 1.323 | α > 25% |
| Weibull MoM | | | 1 | 4.3333 | 5.024 | 5% > α > 2.5% |
| Lognormal | | | 1 | 4.7143 | 5.024 | 5% > α > 2.5% |
| Normal | | | 1 | 3.5714 | 3.841 | 10% > α > 5% |
| Rayleigh | | | 2 | 18.8095 | 13.82 | 0.1% > α |
| Rayleigh-y MLE | | | 2 | 55.3810 | 13.82 | 0.1% > α |
| Rayleigh-y MoM | | | 2 | 55.3810 | 13.82 | 0.1% > α |
| Rayleigh+1 | | | 2 | 13.0952 | 13.82 | 0.5% > α > 0.1% |
| Beta MLE | 180° | 11 | 1 | 0.8182 | 1.323 | α > 25% |
| Beta MoM | | | 1 | 0.8182 | 1.323 | α > 25% |
| Weibull MLE | | | 1 | 0.8182 | 1.323 | α > 25% |
| Weibull MoM | | | 1 | 0.8182 | 1.323 | α > 25% |
| Lognormal | | | 1 | 2.2727 | 2.706 | 25% > α > 10% |
| Normal | | | 1 | 0.8182 | 1.323 | α > 25% |
| Rayleigh | | | 1 | 4.4545 | 5.024 | 5% > α > 2.5% |
| Rayleigh-y MLE | | | 1 | 7.3636 | 7.879 | 1% > α > 0.5% |
| Rayleigh-y MoM | | | 1 | 4.4545 | 5.024 | 5% > α > 2.5% |
| Rayleigh+1 | | | 1 | 2.2727 | 2.706 | 25% > α > 10% |

Table A.3. Missile: $\theta = 90^\circ$ Kolmogorov Levels of Significance for Window vs. Full-Range, n =number of samples, T_1 =Test Statistic, $W_p=1-\alpha$ Quantile

| <i>pdf</i> | <i>Window Center</i> | <i>n</i> | <i>T₁</i> | <i>W_p</i> | <i>Level of Significance</i> |
|----------------|----------------------|----------|----------------------|----------------------|------------------------------|
| Beta MLE | 0° | 21 | 0.4186 | 0.344 | 1% > α |
| Beta MoM | | | | | |
| Weibull MLE | | | 0.1435 | 0.226 | $\alpha > 20\%$ |
| Weibull MoM | | | 0.1586 | 0.226 | $\alpha > 20\%$ |
| Lognormal | | | 0.1368 | 0.226 | $\alpha > 20\%$ |
| Normal | | | 0.1337 | 0.226 | $\alpha > 20\%$ |
| Rayleigh | | | 0.5976 | 0.344 | 1% > α |
| Rayleigh-y MLE | | | 0.8201 | 0.344 | 1% > α |
| Rayleigh-y MoM | | | 0.7322 | 0.344 | 1% > α |
| Rayleigh+1 | | | 0.5351 | 0.344 | 1% > α |
| Beta MLE | 90° | 41 | 0.0840 | 0.167 | $\alpha > 20\%$ |
| Beta MoM | | | 0.0476 | 0.167 | $\alpha > 20\%$ |
| Weibull MLE | | | 0.1189 | 0.167 | $\alpha > 20\%$ |
| Weibull MoM | | | 0.1147 | 0.167 | $\alpha > 20\%$ |
| Lognormal | | | 0.2216 | 0.237 | 5% $\alpha > 2\%$ |
| Normal | | | 0.1532 | 0.167 | $\alpha > 20\%$ |
| Rayleigh | | | 0.5076 | 0.255 | 1% > α |
| Rayleigh-y MLE | | | 0.7092 | 0.255 | 1% > α |
| Rayleigh-y MoM | | | 0.7281 | 0.255 | 1% > α |
| Rayleigh+1 | | | 0.3551 | 0.255 | 1% > α |
| Beta MLE | 180° | 21 | 0.4392 | 0.344 | 1% > α |
| Beta MoM | | | | | |
| Weibull MLE | | | 0.1248 | 0.226 | $\alpha > 20\%$ |
| Weibull MoM | | | 0.1355 | 0.226 | $\alpha > 20\%$ |
| Lognormal | | | 0.1018 | 0.226 | $\alpha > 20\%$ |
| Normal | | | 0.1033 | 0.226 | $\alpha > 20\%$ |
| Rayleigh | | | 0.6373 | 0.344 | 1% > α |
| Rayleigh-y MLE | | | 0.8382 | 0.344 | 1% > α |
| Rayleigh-y MoM | | | 0.8051 | 0.344 | 1% > α |
| Rayleigh+1 | | | 0.5624 | 0.344 | 1% > α |

Table A.4. Missile: $\theta = 90^\circ$ Chi-Square Levels of Significance for Window vs. Full-Range, n =number of samples, DoF= Degrees of Freedom, T_1 =Test Statistic, $W_p=1-\alpha$ Quantile

| <i>pdf</i> | <i>Window Center</i> | <i>n</i> | <i>DoF</i> | T_1 | W_p | <i>Level of Significance</i> |
|----------------|----------------------|----------|------------|----------|-------|------------------------------|
| Beta MLE | 0° | 21 | 1 | 28.7143 | 10.83 | 0.1% > α |
| Beta MoM | | | | | | |
| Weibull MLE | | | 1 | 4.3333 | 5.024 | 5% > α > 2.5% |
| Weibull MoM | | | 1 | 4.3333 | 5.024 | 5% > α > 2.5% |
| Lognormal | | | 1 | 4.3333 | 5.024 | 5% > α > 2.5% |
| Normal | | | 1 | 4.3333 | 5.024 | 5% > α > 2.5% |
| Rayleigh | | | 2 | 63 | 13.82 | 0.1% > α |
| Rayleigh-y MLE | | | 2 | 63 | 13.82 | 0.1% > α |
| Rayleigh-y MoM | | | 2 | 25.6667 | 13.82 | 0.1% > α |
| Rayleigh+1 | | | 2 | 63 | 13.82 | 0.1% > α |
| Beta MLE | 90° | 41 | 2 | 0.3415 | 2.773 | α > 25% |
| Beta MoM | | | 2 | 1.3171 | 2.773 | α > 25% |
| Weibull MLE | | | 2 | 3.2683 | 4.605 | α > 25% |
| Weibull MoM | | | 2 | 3.26830 | 2.773 | 25% > α > 10% |
| Lognormal | | | 2 | 17.5366 | 13.82 | 0.1% > α |
| Normal | | | 2 | 5.4634 | 5.991 | 10% > α > 5% |
| Rayleigh | | | 3 | 38.6829 | 16.27 | 0.1% > α |
| Rayleigh-y | | | 3 | 127.1207 | 16.27 | 0.1% > α |
| Rayleigh-y | | | 3 | 127.1207 | 16.27 | 0.1% > α |
| Rayleigh+1 | | | 3 | 21.8537 | 16.27 | 0.1% > α |
| Beta MLE | 180° | 21 | 1 | 25.6667 | 10.83 | 0.1% > α |
| Beta MoM | | | | | | |
| Weibull MLE | | | 1 | 2.4286 | 2.706 | 25% > α > 10% |
| Weibull MoM | | | 1 | 2.4286 | 2.706 | 25% > α > 10% |
| Lognormal | | | 1 | 2.4286 | 2.706 | 25% > α > 10% |
| Normal | | | 1 | 2.5286 | 2.706 | 25% > α > 10% |
| Rayleigh | | | 2 | 63 | 13.82 | 0.1% > α |
| Rayleigh-y | | | 2 | 63 | 13.82 | 0.1% > α |
| Rayleigh-y | | | 2 | 63 | 13.82 | 0.1% > α |
| Rayleigh+1 | | | 2 | 63 | 13.82 | 0.1% > α |

Table A.5. Fighter: $\theta = 90^\circ \pm 5^\circ$ Kolmogorov Levels of Significance for Window vs. Full-Range, n =number of samples, T_1 =Test Statistic, $W_p=1-\alpha$ Quantile

| <i>pdf</i> | <i>Window Center</i> | <i>n</i> | <i>T₁</i> | <i>W_p</i> | <i>Level of Significance</i> |
|----------------|----------------------|----------|----------------------|----------------------|------------------------------|
| Beta MLE | 0° | 121 | 0.3745 | 0.148 | 1% > α |
| Beta MoM | | | | | |
| Weibull MLE | | | 0.0733 | 0.097 | $\alpha > 20\%$ |
| Weibull MoM | | | 0.0553 | 0.097 | $\alpha > 20\%$ |
| Lognormal | | | 0.1134 | 0.124 | 10% > $\alpha > 5\%$ |
| Normal | | | 0.1059 | 0.111 | 20% > $\alpha > 10\%$ |
| Rayleigh | | | 0.5493 | 0.148 | 1% > α |
| Rayleigh-y MLE | | | 0.7867 | 0.148 | 1% > α |
| Rayleigh-y MoM | | | 0.6893 | 0.148 | 1% > α |
| Rayleigh+1 | | | 0.4817 | 0.148 | 1% > α |
| Beta MLE | 90° | 231 | 0.1274 | 0.107 | 1% > α |
| Beta MoM | | | 0.0877 | 0.0895 | 10% > $\alpha > 5\%$ |
| Weibull MLE | | | 0.0655 | 0.070 | $\alpha > 20\%$ |
| Weibull MoM | | | 0.0432 | 0.070 | $\alpha > 20\%$ |
| Lognormal | | | 0.1248 | 0.107 | 1% > α |
| Normal | | | 0.0906 | 0.100 | 5% > $\alpha > 2\%$ |
| Rayleigh | | | 0.4475 | 0.107 | 1% > α |
| Rayleigh-y MLE | | | 0.7008 | 0.107 | 1% > α |
| Rayleigh-y MoM | | | 0.6517 | 0.107 | 1% > α |
| Rayleigh+1 | | | 0.3334 | 0.107 | 1% > α |
| Beta MLE | 180° | 121 | 0.1276 | 0.138 | 5% > $\alpha > 2\%$ |
| Beta MoM | | | 0.0986 | 0.111 | 20% > $\alpha > 10\%$ |
| Weibull MLE | | | 0.0490 | 0.097 | $\alpha > 20\%$ |
| Weibull MoM | | | 0.0655 | 0.097 | $\alpha > 20\%$ |
| Lognormal | | | 0.1364 | 0.138 | 5% > $\alpha > 2\%$ |
| Normal | | | 0.0816 | 0.097 | $\alpha > 20\%$ |
| Rayleigh | | | 0.3261 | 0.148 | 1% > α |
| Rayleigh-y MLE | | | 0.5944 | 0.148 | 1% > α |
| Rayleigh-y MoM | | | 0.3356 | 0.148 | 1% > α |
| Rayleigh+1 | | | 0.2291 | 0.148 | 1% > α |

Table A.6. Fighter: $\theta = 90^\circ \pm 5^\circ$ Chi-Square Levels of Significance for Window vs. Full-Range, n =number of samples, DoF= Degrees of Freedom, T_1 =Test Statistic, $W_p=1-\alpha$ Quantile

| <i>pdf</i> | <i>Window Center</i> | <i>n</i> | <i>DoF</i> | T_1 | W_p | <i>Level of Significance</i> |
|----------------|----------------------|----------|------------|----------|-------|------------------------------|
| Beta MLE | 0° | 121 | 2 | 263.1736 | 13.82 | 0.1% > α |
| Beta MoM | | | | | | |
| Weibull MLE | | | 2 | 19.2066 | 13.82 | 0.1% > α |
| Weibull MoM | | | 2 | 19.2066 | 13.82 | 0.1% > α |
| Lognormal | | | 2 | 29.7438 | 13.82 | 0.1% > α |
| Normal | | | 2 | 5.5702 | 5.991 | 10% > α > 5% |
| Rayleigh | | | 3 | 409.2893 | 16.27 | 0.1% > α |
| Rayleigh-y MLE | | | 3 | 464.3306 | 16.27 | 0.1% > α |
| Rayleigh-y MoM | | | 3 | 484.0000 | 16.27 | 0.1% > α |
| Rayleigh+1 | | | 3 | 181.6860 | 16.27 | 0.1% > α |
| Beta MLE | 90° | 231 | 2 | 30.5368 | 13.82 | 0.1% > α |
| Beta MoM | | | | 20.6667 | 13.82 | 0.1% > α |
| Weibull MLE | | | 2 | 11.8355 | 13.82 | 0.5% > α > 0.1% |
| Weibull MoM | | | 2 | 5.9502 | 5.991 | 10% > α > 5% |
| Lognormal | | | 2 | 81.1039 | 13.82 | 0.1% > α |
| Normal | | | 2 | 20.6667 | 13.82 | 0.1% > α |
| Rayleigh | | | 3 | 489.9307 | 16.27 | 0.1% > α |
| Rayleigh-y MLE | | | 3 | 638.4589 | 16.27 | 0.1% > α |
| Rayleigh-y MoM | | | 3 | 369.9740 | 16.27 | 0.1% > α |
| Rayleigh+1 | | | 3 | 262.7879 | 16.27 | 0.1% > α |
| Beta MLE | 180° | 121 | 2 | 21.9339 | 13.82 | 0.1% > α |
| Beta MoM | | | 2 | 6.1488 | 7.378 | 5% > α > 2.5% |
| Weibull MLE | | | 2 | 9.8678 | 10.6 | 1% > α > 0.5% |
| Weibull MoM | | | 2 | 7.1405 | 7.378 | 5% > α > 2.5% |
| Lognormal | | | 2 | 36.9504 | 13.82 | 0.1% > α |
| Normal | | | 2 | 6.1488 | 7.378 | 5% > α > 2.5% |
| Rayleigh | | | 3 | 175.5702 | 16.27 | 0.1% > α |
| Rayleigh-y MLE | | | 3 | 223.4215 | 16.27 | 0.1% > α |
| Rayleigh-y MoM | | | 3 | 160.1157 | 16.27 | 0.1% > α |
| Rayleigh+1 | | | 3 | 71.6860 | 16.27 | 0.1% > α |

Table A.7. Fighter: $\theta = 90^\circ$ Kolmogorov Levels of Significance for Window vs. Window, n =number of samples, T_1 =Test Statistic, $W_p=1-\alpha$ Quantile

| <i>pdf</i> | <i>Window Center</i> | <i>n</i> | T_1 | W_p | <i>Level of Significance</i> |
|----------------|----------------------|----------|--------|-------|------------------------------|
| Beta MLE | 0° | 11 | 0.2283 | 0.308 | $\alpha > 20\%$ |
| Beta MoM | | | 0.2792 | 0.308 | $\alpha > 20\%$ |
| Weibull MLE | | | 0.6355 | 0.468 | $1\% > \alpha$ |
| Weibull MoM | | | 0.4495 | 0.468 | $2\% > \alpha > 1\%$ |
| Lognormal | | | 0.7276 | 0.468 | $1\% > \alpha$ |
| Normal | | | 0.4274 | 0.437 | $5\% > \alpha > 2.5\%$ |
| Rayleigh | | | 0.5165 | 0.468 | $1\% > \alpha$ |
| Rayleigh-y MLE | | | 0.6349 | 0.468 | $1\% > \alpha$ |
| Rayleigh-y MLE | | | 0.6453 | 0.468 | $1\% > \alpha$ |
| Rayleigh+1 | | | 0.4381 | 0.468 | $2\% > \alpha > 1\%$ |
| Beta MLE | 90° | 21 | 0.3018 | 0.321 | $5\% > \alpha > 2\%$ |
| Beta MoM | | | 0.1527 | 0.226 | $\alpha > 20\%$ |
| Weibull MLE | | | 0.5058 | 0.344 | $1\% > \alpha$ |
| Weibull MoM | | | 0.1546 | 0.226 | $\alpha > 20\%$ |
| Lognormal | | | 0.7743 | 0.344 | $1\% > \alpha$ |
| Normal | | | 0.1578 | 0.226 | $\alpha > 20\%$ |
| Rayleigh | | | 0.4013 | 0.344 | $1\% > \alpha$ |
| Rayleigh-y MLE | | | 0.6492 | 0.344 | $1\% > \alpha$ |
| Rayleigh-y MoM | | | 0.6450 | 0.344 | $1\% > \alpha$ |
| Rayleigh+1 | | | 0.2492 | 0.259 | $20\% > \alpha > 10\%$ |
| Beta MLE | 180° | 11 | 0.2606 | 0.308 | $\alpha > 20\%$ |
| Beta MoM | | | 0.1964 | 0.308 | $\alpha > 20\%$ |
| Weibull MLE | | | 0.5803 | 0.468 | $1\% > \alpha$ |
| Weibull MoM | | | 0.2460 | 0.308 | $\alpha > 20\%$ |
| Lognormal | | | 0.7475 | 0.468 | $1\% > \alpha$ |
| Normal | | | 0.2248 | 0.308 | $\alpha > 20\%$ |
| Rayleigh | | | 0.3546 | 0.391 | $10\% > \alpha > 5\%$ |
| Rayleigh-y MLE | | | 0.5529 | 0.468 | $1\% > \alpha$ |
| Rayleigh-y MoM | | | 0.5536 | 0.468 | $1\% > \alpha$ |
| Rayleigh+1 | | | 0.2434 | 0.308 | $\alpha > 20\%$ |

Table A.8. Fighter: $\theta = 90^\circ$ Chi-Square Levels of Significance for Window vs. Window, n =number of samples, DoF= Degrees of Freedom, T_1 =Test Statistic, $W_p=1-\alpha$ Quantile

| <i>pdf</i> | <i>Window Center</i> | <i>n</i> | <i>DoF</i> | T_1 | W_p | <i>Level of Significance</i> |
|----------------|----------------------|----------|------------|---------|-------|------------------------------|
| Beta MLE | 0° | 11 | 1 | 2.2727 | 2.706 | 25% > α > 10% |
| Beta MoM | | | 1 | 0.8182 | 1.323 | α > 25% |
| Weibull MLE | | | 1 | 4.8182 | 5.024 | 5% > α > 2.5% |
| Weibull MoM | | | 1 | 1.5455 | 2.706 | 25% > α > 10% |
| Lognormal | | | 1 | 7.3636 | 7.879 | 1% > α > 0.5% |
| Normal | | | 1 | 2.2727 | 2.706 | 25% > α > 10% |
| Rayleigh | | | 1 | 4.4545 | 5.024 | 5% > α > 2.5% |
| Rayleigh-y MLE | | | 1 | 4.4545 | 5.024 | 5% > α > 2.5% |
| Rayleigh-y MoM | | | 1 | 4.4545 | 5.024 | 5% > α > 2.5% |
| Rayleigh+1 | | | 1 | 2.2727 | 2.706 | 25% > α > 10% |
| Beta MLE | 90° | 21 | 1 | 13.8571 | 10.83 | 0.1% > α |
| Beta MoM | | | 1 | 5.0952 | 6.635 | 2.5% > α > 1% |
| Weibull MLE | | | 1 | 17.6667 | 10.83 | 0.1% > α |
| Weibull MoM | | | 1 | 3.1905 | 3.841 | 10% > α > 5% |
| Lognormal | | | 1 | 55.3810 | 10.83 | 0.1% > α |
| Normal | | | 1 | 3.1905 | 3.841 | 10% > α > 5% |
| Rayleigh | | | 2 | 14.6190 | 13.82 | 0.1% > α |
| Rayleigh-y MLE | | | 2 | 48.1429 | 13.82 | 0.1% > α |
| Rayleigh-y MoM | | | 2 | 41.6667 | 13.82 | 0.1% > α |
| Rayleigh+1 | | | 2 | 4.7143 | 5.991 | 10% > α > 5% |
| Beta MLE | 180° | 11 | 1 | 0.0909 | 1.323 | α > 25% |
| Beta MoM | | | 1 | 0.0909 | 1.323 | α > 25% |
| Weibull MLE | | | 1 | 3.7273 | 3.841 | 10% > α > 5% |
| Weibull MoM | | | 1 | 1.1818 | 1.323 | α > 25% |
| Lognormal | | | 1 | 7.3636 | 7.879 | 1% > α > 0.5% |
| Normal | | | 1 | 0.8182 | 1.323 | α > 25% |
| Rayleigh | | | 1 | 2.2727 | 2.706 | 25% > α > 10% |
| Rayleigh-y MLE | | | 1 | 7.3636 | 7.879 | 1% > α > 0.5% |
| Rayleigh-y MoM | | | 1 | 7.3636 | 7.879 | 1% > α > 0.5% |
| Rayleigh+1 | | | 1 | 2.2727 | 2.706 | 25% > α > 10% |

Table A.9. Missile: $\theta = 90^\circ$ Kolmogorov Levels of Significance for Window vs. Window,
 n =number of samples, T_1 =Test Statistic, $W_p=1-\alpha$ Quantile

| <i>pdf</i> | <i>Window Center</i> | <i>n</i> | <i>T₁</i> | <i>W_p</i> | <i>Level of Significance</i> |
|----------------|--------------------------|----------|----------------------|----------------------|------------------------------|
| Beta MLE | 0° | 21 | 0.1603 | 0.226 | $\alpha > 20\%$ |
| Beta MoM | | | 0.1303 | 0.226 | $\alpha > 20\%$ |
| Weibull MLE | | | 0.2760 | 0.287 | $10\% > \alpha > 5\%$ |
| Weibull MoM | | | 0.2324 | 0.259 | $20\% > \alpha > 10\%$ |
| Lognormal | | | 0.5055 | 0.344 | $1\% > \alpha$ |
| Normal | | | 0.1919 | 0.226 | $\alpha > 20\%$ |
| Rayleigh | | | 0.2048 | 0.226 | $\alpha > 20\%$ |
| Rayleigh-y MLE | | | 0.3221 | 0.344 | $2\% > \alpha > 1\%$ |
| Rayleigh-y MoM | | | 0.2998 | 0.321 | $5\% > \alpha > 2\%$ |
| Rayleigh+1 | | | 0.3545 | 0.344 | $1\% > \alpha$ |
| Beta MLE | 90° | 41 | 0.2087 | 0.212 | $10\% > \alpha > 5\%$ |
| Beta MoM | | | 0.0716 | 0.167 | $\alpha > 20\%$ |
| Weibull MLE | | | 0.3189 | 0.255 | $1\% > \alpha$ |
| Weibull MoM | | | 0.1475 | 0.167 | $\alpha > 20\%$ |
| Lognormal | | | 0.6765 | 0.255 | $1\% > \alpha$ |
| Normal | | | 0.1557 | 0.167 | $\alpha > 20\%$ |
| Rayleigh | | | 0.3405 | 0.255 | $1\% > \alpha$ |
| Rayleigh-y MLE | | | 0.5720 | 0.255 | $1\% > \alpha$ |
| Rayleigh-y MoM | | | 0.5796 | 0.255 | $1\% > \alpha$ |
| Rayleigh+1 | | | 0.2365 | 0.237 | $5\% > \alpha > 2\%$ |
| Beta MLE | 180° | 21 | 0.2377 | 0.259 | $20\% > \alpha > 10\%$ |
| Beta MoM | | | 0.1214 | 0.226 | $\alpha > 20\%$ |
| Weibull MLE | | | 0.2715 | 0.287 | $10\% > \alpha > 5\%$ |
| Weibull MoM | | | 0.1956 | 0.226 | $\alpha > 20\%$ |
| Lognormal | | | 0.3850 | 0.344 | $1\% > \alpha$ |
| Normal | | | 0.2520 | 0.259 | $20\% > \alpha > 10\%$ |
| Rayleigh | | | 0.2887 | 0.321 | $5\% > \alpha > 2\%$ |
| Rayleigh-y MLE | | | 0.2947 | 0.321 | $2\% > \alpha > 1\%$ |
| Rayleigh-y MoM | | | 0.2454 | 0.259 | $20\% > \alpha > 10\%$ |
| Rayleigh+1 | | | 0.3430 | 0.344 | $2\% > \alpha > 1\%$ |

Table A.10. Missile: $\theta = 90^\circ$ Chi-Square Levels of Significance for Window vs. Window, n =number of samples, DoF= Degrees of Freedom, T_1 =Test Statistic, $W_p=1-\alpha$ Quantile

| <i>pdf</i> | <i>Window Center</i> | <i>n</i> | <i>DoF</i> | T_1 | W_p | <i>Level of Significance</i> |
|----------------|----------------------|----------|------------|----------|------------|------------------------------|
| Beta MLE | 0° | 21 | 1 | 4.3333 | 5.024 | 5% > α > 2.5% |
| Beta MoM | | | 1 | 0.5283 | 1.323 | α > 25% |
| Weibull MLE | | | 1 | 6.6190 | 5.0246.635 | 2.5% > α > 1% |
| Weibull MoM | | | 1 | 7.0000 | 7.879 | 1% > α > 0.5% |
| Lognormal | | | 1 | 18.4286 | 10.83 | 0.1% > α |
| Normal | | | 1 | 4.3333 | 5.024 | 5% > α > 2.5% |
| Rayleigh | | | 2 | 8.1429 | 9.210 | 2.5% > α > 1% |
| Rayleigh-y MLE | | | 2 | 5.8571 | 5.991 | 10% > α > 5% |
| Rayleigh-y MoM | | | 2 | 6.2381 | 7.378 | 5% > α > 2.5% |
| Rayleigh+1 | | | 2 | 15.000 | 13.82 | 0.1% > α |
| Beta MLE | 90° | 41 | 2 | 59.8780 | 13.82 | 0.1% > α |
| Beta MoM | | | 2 | 1.5610 | 2.773 | α > 25% |
| Weibull MLE | | | 2 | 16.4310 | 4.605 | 0.1% > α |
| Weibull MoM | | | 2 | 3.5122 | 4.605 | 25% > α > 10% |
| Lognormal | | | 2 | 104.4878 | 13.82 | 0.1% > α |
| Normal | | | 2 | 3.5122 | 4.605 | 25% > α > 10% |
| Rayleigh | | | 3 | 21.5610 | 16.27 | 0.1% > α |
| Rayleigh-y | | | 3 | 75.9512 | 16.27 | 0.1% > α |
| Rayleigh-y | | | 3 | 82.7805 | 16.27 | 0.1% > α |
| Rayleigh+1 | | | 3 | 14.4878 | 16.27 | 0.5% > α > 0.1% |
| Beta MLE | 180° | 21 | 1 | 5.4762 | 6.635 | 2.5% > α > 1% |
| Beta MoM | | | 1 | 1.6667 | 2.706 | 25% > α > 10% |
| Weibull MLE | | | 1 | 5.8571 | 6.635 | 2.5% > α > 1% |
| Weibull MoM | | | 1 | 6.2381 | 6.635 | 2.5% > α > 1% |
| Lognormal | | | 1 | 12.7143 | 10.83 | 0.1% > α |
| Normal | | | 1 | 6.2381 | 6.635 | 2.5% > α > 1% |
| Rayleigh | | | 2 | 8.5238 | 9.210 | 2.5% > α > 1% |
| Rayleigh-y | | | 2 | 12.3333 | 13.82 | 0.5% > α > 0.1% |
| Rayleigh-y | | | 2 | 6.2381 | 7.378 | 5% > α > 2.5% |
| Rayleigh+1 | | | 2 | 8.9048 | 9.210 | 2.5% > α > 1 |

Table A.11. Fighter: $\theta = 90^\circ \pm 5^\circ$ Kolmogorov Levels of Significance for Window vs. Window, n =number of samples, T_1 =Test Statistic, $W_p=1-\alpha$ Quantile

| <i>pdf</i> | <i>Window Center</i> | <i>n</i> | <i>T₁</i> | <i>W_p</i> | <i>Level of Significance</i> |
|----------------|----------------------|----------|----------------------|----------------------|------------------------------|
| Beta MLE | 0° | 121 | 0.1816 | 0.148 | 1% > α |
| Beta MoM | | | 0.1074 | 0.111 | 20% > α > 10% |
| Weibull MLE | | | 0.1943 | 0.148 | 1% > α |
| Weibull MoM | | | 0.1142 | 0.124 | 10% > α > 5% |
| Lognormal | | | 0.5295 | 0.148 | 1% > α |
| Normal | | | 0.1236 | 0.124 | 10% > α > 5% |
| Rayleigh | | | 0.3953 | 0.148 | 1% > α |
| Rayleigh-y MLE | | | 0.5850 | 0.148 | 1% > α |
| Rayleigh-y MoM | | | 0.5735 | 0.148 | 1% > α |
| Rayleigh+1 | | | 0.2376 | 0.148 | 1% > α |
| Beta MLE | 90° | 231 | 0.1576 | 0.107 | 1% > α |
| Beta MoM | | | 0.0780 | 0.080 | 20% > α > 10% |
| Weibull MLE | | | 0.1244 | 0.107 | 1% > α |
| Weibull MoM | | | 0.0758 | 0.080 | 20% > α > 10% |
| Lognormal | | | 0.4818 | 0.107 | 1% > α |
| Normal | | | 0.0898 | 0.090 | 10% > α > 5% |
| Rayleigh | | | 0.3877 | 0.107 | 1% > α |
| Rayleigh-y MLE | | | 0.6199 | 0.107 | 1% > α |
| Rayleigh-y MoM | | | 0.6046 | 0.107 | 1% > α |
| Rayleigh+1 | | | 0.2611 | 0.107 | 1% > α |
| Beta MLE | 180° | 121 | 0.1296 | 0.138 | 5% > α > 2% |
| Beta MoM | | | 0.0679 | 0.097 | α > 20% |
| Weibull MLE | | | 0.1862 | 0.148 | 1% > α |
| Weibull MoM | | | 0.1199 | 0.124 | 10% > α > 5% |
| Lognormal | | | 0.5354 | 0.148 | α > 1% |
| Normal | | | 0.1197 | 0.124 | 10% > α > 5% |
| Rayleigh | | | 0.3212 | 0.148 | 1% > α |
| Rayleigh-y MLE | | | 0.5675 | 0.148 | 1% > α |
| Rayleigh-y MoM | | | 0.5674 | 0.148 | 1% > α |
| Rayleigh+1 | | | 0.2004 | 0.148 | 1% > α |

Table A.12. Fighter: $\theta = 90^\circ \pm 5^\circ$ Chi-Square Levels of Significance for Window vs. Window, n =number of samples, DoF= Degrees of Freedom, T_1 =Test Statistic, $W_p=1-\alpha$ Quantile

| <i>pdf</i> | <i>Window Center</i> | <i>n</i> | <i>DoF</i> | T_1 | W_p | <i>Level of Significance</i> |
|----------------|----------------------|----------|------------|----------|-------|------------------------------|
| Beta MLE | 0° | 121 | 2 | 50.4463 | 13.82 | 0.1% > α |
| Beta MoM | | | 2 | 9.2066 | 9.21 | 2.5% > α > 1% |
| Weibull MLE | | | 2 | 21.6860 | 13.82 | 0.1% > α |
| Weibull MoM | | | 2 | 6.5620 | 7.378 | 5% > α > 2.5% |
| Lognormal | | | 2 | 149.3884 | 13.82 | 0.1% > α |
| Normal | | | 2 | 6.5620 | 7.378 | 5% > α > 2.5% |
| Rayleigh | | | 3 | 78.2975 | 16.27 | 0.1% > α |
| Rayleigh-y MLE | | | 3 | 252.6777 | 16.27 | 0.1% > α |
| Rayleigh-y MoM | | | 3 | 235.0744 | 16.27 | 0.1% > α |
| Rayleigh+1 | | | 3 | 22.0165 | 16.27 | 0.1% > α |
| Beta MLE | 90° | 231 | 2 | 60.7965 | 13.82 | 0.1% > α |
| Beta MoM | | | 2 | 15.7749 | 13.82 | 0.1% > α |
| Weibull MLE | | | 2 | 23.9567 | 13.82 | 0.1% > α |
| Weibull MoM | | | 2 | 15.6883 | 13.82 | 0.1% > α |
| Lognormal | | | 2 | 278.7662 | 13.82 | 0.1% > α |
| Normal | | | 2 | 16.1645 | 13.82 | 0.1% > α |
| Rayleigh | | | 3 | 234.5195 | 16.27 | 0.1% > α |
| Rayleigh-y MLE | | | 3 | 527.5065 | 16.27 | 0.1% > α |
| Rayleigh-y MoM | | | 3 | 484.2597 | 16.27 | 0.1% > α |
| Rayleigh+1 | | | 3 | 118.2857 | 16.27 | 0.1% > α |
| Beta MLE | 180° | 121 | 2 | 24.3306 | 13.82 | 0.1% > α |
| Beta MoM | | | 2 | 8.7107 | 9.210 | 2.5% > α > 1% |
| Weibull MLE | | | 2 | 16.2314 | 13.82 | 0.1% > α |
| Weibull MoM | | | 2 | 8.2975 | 9.210 | 2.5% > α > 1% |
| Lognormal | | | 2 | 188.5950 | 13.82 | 0.1% > α |
| Normal | | | 2 | 8.8760 | 9.210 | 2.5% > α > 1% |
| Rayleigh | | | 3 | 50.1983 | 16.27 | 0.1% > α |
| Rayleigh-y MLE | | | 3 | 211.5207 | 16.27 | 0.1% > α |
| Rayleigh-y MoM | | | 3 | 211.5207 | 16.27 | 0.1% > α |
| Rayleigh+1 | | | 3 | 20.6116 | 16.27 | 0.1% > α |

Appendix B. ASPECT RCS Modeling Program

This appendix presents the APECT RCS modeling program along with the 'newton', 'bmle', 'chi', and 'interp' subroutines. The ASPECT MATLAB code inputs a 2-dimensional array and determines the optimum pdf model.

%ASPECT RCS Modeling Program

```
c=0;
while c~=1
clear
z=input('Input number of file to be used:1=sttm,
2=missile180, 3=wid, 4=missile');
if z==1
load sttm
z=sttm;
elseif z==2
load missile180
z=missile180;
elseif z==3
load wid
z=wid;
elseif z==4
load missile
z=missile;
end
k=0;
t=input('Input number of separate sections to
be included in full-range data.
You will be prompted to input the beginning
and ending sample of each section.')
for o=1:t
beginl=input('Input beginning length sample')
beginw=input('Input beginning width sample')
endl=input('Input ending length sample')
endw=input('Input ending width sample')
for i=beginl:endl
for j=beginw:endw
k=k+1;
z1(k)=z(i,j);
end
end
end
message='Data is now linearized. Window will
be a single row table with length equal to
aspect length multiplied by aspect width.'
z1=z1';
s=(z1-min(z1))/abs(max(z1)-min(z1));
data=k
j=0;
y=0;
lo=input('Input beginning window sample')
hi=input('Input ending window sample')
mag=hi-lo+1
```

```
for i=1:data
if i;lo—i;hi
s0(i)=0;
end
if i;=lo&i;=hi
j=j+1;
s0(i)=s(i);
s0m(j)=s(i);
if s0m(j)==0
s0m(j)=10^(-6);
elseif s0m(j)==1
s0m(j)=1-10^(-6);
end
ns0m(j)=1-s0m(j);
s0m1(j)=s0m(j)^2;
s0m4(j)=s0m(j)^4;
s0mg1(j)=s0m(j)^(1/mag);
s0mg2(j)=ns0m(j)^(1/mag);
end
if i;lo—i;hi
s0u(i)=0;
end
if i;=lo&i;=hi
y=y+1;
s0u(i)=s(i);
s0um(y)=s(i);
end
end
G1=prod(s0mg1)% for beta mle alpha
G2=prod(s0mg2)% for beta mle beta
s0l=s0+10^(-6);
```

%MOMENT GENERATION

```
m=mean(s0m)%sample mean
m2=mean(s0m1)%sample second moment
m4=mean(s0m4)%sample 4th moment
M2=(std(s0m))^2% sample variance
var=m2-m^2% sample variance
d=m^2/m2% for weibull mom interp
med=median(s0m)%sample median

for i=lo:hi% lognormal parameter est
lmean(i)=log(s0l(i));
end
lmean=sum(lmean)/mag % log mean
for i=lo:hi
lvar(i)=(log(s0l(i))-lmean)^2;
```

```

end
lvar=sum(lvar)/mag % log variance

%BETA, WEIBULL, AND RAYLEIGH
PARAMETER DETERMINATION

r1=(3*m2/4)^(0.5)% Rayleigh+1 parameter
r=(m2/2)^(0.5)% Rayleigh parameter
rymle=r% Rayleigh-y=x^2 mle parameter
rymom=(m2/8)^(0.25)% Ry mom parameter
a=m*(m-m2)/(var)%a beta estimate using method of moments
b=(1-m)*(m-m2)/(var)%b beta mom
interp % Determine Weibull MoM Parameters
k=input('If Weibull mle is desired press 1, if mom press RETURN');
if k==1
    newton % Determine Weibull MLE parameters
end
k1=input('If Beta mle is desired press 1, if mom press RETURN');
if k1==1
    bmle % Determine Beta MLE parameters
    val=(gamma(a+b))/(gamma(a)*gamma(b))% beta
end

% PDF FORMATION
for i=1:200
    x(i)=i/200;
    B(i)=val*(x(i)^(a-1))*((1-x(i))^(b-1));
    if B(i)==inf
        B(i)=B(i-1)*4;
    end
    W(i)=(a/be)*(x(i)/be)^(a-1)*exp(-(x(i)/be)^a);
    R(i)=2*(x(i)/m2)*exp(-(x(i)^2)/(m2));
    Rymle(i)=(1/(2*(rymle^2)))*exp(-(x(i)^2)/(2*(rymle^2)));
    Rymom(i)=(1/(2*(rymom^2)))*exp(-(x(i)^2)/(2*(rymom^2)));
    R1(i)=(9*x(i)^3/(2*(r1^4))*exp((-3*x(i)^2)/(2*(r1^2)));
    L(i)=((x(i)*sqrt(lvar)*(2*pi)^(1/2))^(-1))*exp(-(log(x(i))
    -lmean)^2)/(2*lvar);
    N(i)=((1/(2*pi*var))^(1/2))*exp(-((x(i)-m)^2)/(2*var));
end

hold off;
%hold on;
j=0.025:0.05:0.975;
[Data, u]=hist(s0um,i);
hist(s0um,i);
for i=1:200
    for j=1:20
        if (i/200);=10*/200&(i/200);10*(j-1)/200
            Data2(i)=Data(j);
        end
    end
    if i==200
        Data2(i)=0;
    end
end
end
plot(x,Data2);
DataP=[x' Data2'];
save DataP.dat DataP /ascii;

pause;
plot(x,W);
WMLEP=[x' W'];
save WMLEP.dat WMLEP /ascii;
WMoMP=[x' W'];
save WMoMP.dat WMoMP /ascii;
pause;
%hold on;
plot(x,L);
LognormalP=[x' L'];
save LognormalP.dat LognormalP /ascii;
pause;
%hold on;
plot(x,B);
%title('Beta MLE pdf: 0 deg');
BMoMP=[x' B'];
save BMoMP.dat BMoMP /ascii;
BMLEP=[x' B'];
save BMLEP.dat BMLEP /ascii;pause;
%hold on;
plot(x,N);
NormalP=[x' N'];
save NormalP.dat NormalP /ascii;
pause;
%hold on;
plot(x,R);
RayleighP=[x' R'];
save RayleighP.dat RayleighP /ascii;
pause;
%hold on;
plot(x,Rymle);
RayleighyP=[x' Rymle'];
save RayleighyP.dat RayleighyP /ascii;
pause;
plot(x,Rymom);
%hold on;
RayleighyoP=[x' Rymom'];
save RayleighyoP.dat RayleighyoP /ascii;
pause;
%hold on;
plot(x,R1);
Rayleigh1P=[x' R1'];
save Rayleigh1P.dat Rayleigh1P /ascii;
pause;
[Bmax,iB]=max(B)
[Wmax,iW]=max(W)
[Lmax,iL]=max(L)
[Nmax,iN]=max(N)
[Rmax,iR]=max(R)
[Rymlemax,iRymle]=max(Rymle)
[Rymommax,iRymom]=max(Rymom)
[R1max,iR1]=max(R1)

%CDF Formation

j=0;
for i=1:200

```

```

x(i)=i/200;
sP(i)=0;
for j=1:mag
    if s0um(j)==0&i==1
        sP(i)=sP(i)+1;
    end
    if x(i)<=(s0um(j)-1/(400))&x(i)>=(s0um(j)+1/(400))
        sP(i)=sP(i)+1;
    end
end
end
for i=1:200
    if i==1
        sP1(i)=sP(i);
        BP1(i)=B(i);
        WP1(i)=W(i);
        RP1(i)=R(i);
        RymleP1(i)=Rymle(i);
        RymomP1(i)=Rymom(i);
        R1P1(i)=R1(i);
        LP1(i)=L(i);
        NP1(i)=N(i);
    else
        sP1(i)=sP(i)+sP1(i-1);
        BP1(i)=B(i)+BP1(i-1);
        WP1(i)=W(i)+WP1(i-1);
        RP1(i)=R(i)+RP1(i-1);
        RymleP1(i)=Rymle(i)+RymleP1(i-1);
        RymomP1(i)=Rymom(i)+RymomP1(i-1);
        R1P1(i)=R1(i)+R1P1(i-1);
        LP1(i)=L(i)+LP1(i-1);
        NP1(i)=N(i)+NP1(i-1);
    end
end
sP1=sP1/max(sP1);
BP1=BP1/max(BP1);
WP1=WP1/max(WP1);
RP1=RP1/max(RP1);
RymleP1=RymleP1/max(RymleP1);
RymomP1=RymomP1/max(RymomP1);
R1P1=R1P1/max(R1P1);
LP1=LP1/max(LP1);
NP1=NP1/max(NP1);

plot(x,sP1,x,RP1);
title('Rayleigh cdf: 0 deg');
RayleighC=[x' RP1'];
save RayleighC.dat RayleighC /ascii;
%print;
pause;
plot(x,sP1,x,RymleP1);
title('Rayleigh+1 cdf: 0 deg');
%print;
Rayleigh1C=[x' R1P1'];
save Rayleigh1C.dat Rayleigh1C /ascii;
pause;
plot(x,sP1,x,RymleP1);
title('Rayleigh-y mle cdf: 0 deg');

```

```

%print;
RayleighyC=[x' RymleP1'];
save RayleighyC.dat RayleighyC /ascii;
pause;
plot(x,sP1,x,RymomP1);
title('Rayleigh-y mom cdf: 0 deg');
%print;
RayleighyoC=[x' RymomP1'];
save RayleighyoC.dat RayleighyoC /ascii;
pause;
plot(x,sP1,x,LP1);
title('Lognormal cdf: 0 deg');
%print;
LognormalC=[x' LP1'];
save LognormalC.dat LognormalC /ascii;
pause;
plot(x,sP1,x,NP1);
title('Normal cdf: 0 deg');
%print;
NormalC=[x' NP1'];
save NormalC.dat NormalC /ascii;
pause;
plot(x,sP1,x,BP1);
title('Beta MoM cdf: 0 deg');
BMoMC=[x' BP1'];
save BMoMC.dat BMoMC /ascii;
BMLEC=[x' BP1'];
save BMLEC.dat BMLEC /ascii;%print;
pause;
plot(x,sP1,x,WP1);
title('Weibull MoM cdf: 0 deg');
WMoMC=[x' WP1'];
save WMoMC.dat WMoMC /ascii;
WMLEC=[x' WP1'];
save WMLEC.dat WMLEC /ascii;
DataC=[x' sP1'];
save DataC.dat DataC /ascii;
%print;
pause;

%Goodness-Of-Fit

for i=1:200
    gfb(i)=abs(sP1(i)-BP1(i));
    gfw(i)=abs(sP1(i)-WP1(i));
    gfr(i)=abs(sP1(i)-RP1(i));
    gfr1(i)=abs(sP1(i)-R1P1(i));
    gfrymle(i)=abs(sP1(i)-RymleP1(i));
    gfrymom(i)=abs(sP1(i)-RymomP1(i));
    gfl(i)=abs(sP1(i)-LP1(i));
    gfn(i)=abs(sP1(i)-NP1(i));
end

% Kolmogorov Test Statistic

kgfb=max(gfb)
kgfw=max(gfw)
kgfr=max(gfr)

```

```

kgfr1=max(gfr1)
kgfrymle=max(gfrymle)
kgfrymom=max(gfrymom)
kgfl=max(gfl)
kgfn=max(gfn)

pdf=min(kgfb,kgfw);
pdf=min(pdf,kgfr);
pdf=min(pdf,kgfr1);
pdf=min(pdf,kgfrymle);
pdf=min(pdf,kgfrymom);
pdf=min(pdf,kgfl);
pdf=min(pdf,kgfn);
if pdf==kgfb
    message='Beta is the optimum pdf, alpha='
    a
    message='beta='
    b
elseif pdf==kgfw
    message='Weibull is the optimum pdf, alpha='
    al
    message='beta='
    be
elseif pdf==kgfr
    message='Rayleigh is the optimum pdf, alpha='
    (m2/2)^0.5
elseif pdf==kgfr1
    message='One-Dominant-Plus-Rayleigh is the optimum pdf,
alpha='r1
elseif pdf==kgfrymle
    message='Rayleigh-y mle is the optimum pdf, alpha='
    ryml
elseif pdf==kgfrymom
    message='Rayleigh-y mom is the optimum pdf, alpha='
    rymom
elseif pdf==kgfl
    message='Lognormal is the optimum pdf, sigma='
    sqrt(lvar)
    message='mu='
    lmean
elseif pdf==kgfn
    message='Normal is the optimum pdf, sigma='
    var
    message='mu='
    m
end
message='Enter RETURN for Chi-Square GOF'
pause;

% Chi-Square Goodness of Fit
chi

c=input('Enter 1 to quit, enter another number to continue');
if c==[]
    c=0;
end
end
end

```

%INTERP: Weibull MoM Parameter Formation

```

load tablew1.mat
for i=1:100
    diff(i)=d-tablew1(i);
end
k=0;
for i=1:100
    if diff(i)~=0
        k=k+1;
        diffn(k)=diff(i);
    end
end
[o,p]=min(abs(diffn));
y2=(p-1)/100;
y1=(p)/100;
x1=tablew1(p);
x2=tablew1(p+1);
y=(x2-d)^y1/(x2-x1)+(d-x1)^y2/(x2-x1);
almom=1/y
bemom=m/gamma(1+y)
al=almom
be=bemom

```

%NEWTON: Weibull MLE Parameter Formation

```

j=0;

almle=input('Input beginning iteration (al suggested)')
for i=1:hi
    j=j+1;
    sn0m(j)=s(i)+10^(-6);
    lnsn01(j)=log(sn0m(j));
    sn01(j)=sn0m(j);
    sn02(j)=1-sn0m(j);
end
sum2=sum(lnsn01);
sum1=1;
sum3=1;
j=0;
while (sum1/sum3-1/almle)~=sum2/mag
    for i=1:mag
        lnsn0(i)=(sn0m(i)^almle)*log(sn0m(i));
        sn0c0(i)=sn0m(i)^almle;
        lnsn02(i)=(sn0m(i)^almle)*(log(sn0m(i)))^2;
    end
    sum1=sum(lnsn0);
    sum3=sum(sn0c0);
    sum4=sum(lnsn02);

    almle=almle+(sum2/mag+1/almle-(sum1/sum3))/
    ((1/almle)^2+(sum3*sum4-(sum1)^2)/(sum3)^2)
    bemle=(sum3/mag)^(1/almle)
    j=j+1;
    if j==20

```

```

        break;
    end
end
end
al=almle
be=bemle

%BMLE: Beta MLE Parameter Formation

load betat.mat;
if G1==G2&G1==0
    a=0
    b=0
end
if G1<G2
    G1a=G2;
    G2a=G1;

elseif G1==G2&G2~=0
    G1a=G1;
    G2a=G2;
end
if G2~=0
for i=2:122
    if G1a==betat(i,1)&G1a==betat(i-1,1)
        G1x1=betat(i-1,1);
        G1x2=betat(i,1);
    end
    if G1a==0
        G1x1=0.01;
        G1x2=0.05;
    end
end
u=0;
k=0;
for i=2:122
    if betat(i,1)==G1x1
        u=u+1;
        v(u)=i;
        if G2a==betat(i,2)&G2a==betat(i-1,2)
            G2x11=betat(i-1,2);
            G2x12=betat(i,2);
            a11=betat(i-1,3);
            a12=betat(i,3);
            b11=betat(i-1,4);
            b12=betat(i,4);
        end
    end
    if betat(i,1)==G1x2
        k=k+1;
        h(k)=i;
        if G2a==betat(i,2)&G2a==betat(i-1,2)
            G2x21=betat(i-1,2);
            G2x22=betat(i,2);
            a21=betat(i-1,3);
            a22=betat(i,3);
            b21=betat(i-1,4);
            b22=betat(i,4);

```

```

        end
    end
end
if betat(v(u),2);G2a
    G2x11=betat(v(u)-1,2);
    G2x12=betat(v(u),2);
    a11=betat(v(u)-1,3);
    a12=betat(v(u),3);
    b11=betat(v(u)-1,4);
    b12=betat(v(u),4);
end
if betat(h(k),2);G2a
    G2x21=betat(h(k)-1,2);
    G2x22=betat(h(k),2);
    a21=betat(h(k)-1,3);
    a22=betat(h(k),3);
    b21=betat(h(k)-1,4);
    b22=betat(h(k),4);
    x1=G2x11;
    x2=G2x12;
    x=G2a;
    y1=a11;
    y2=a12;
    y=(x2-x)*y1/(x2-x1)+(x-x1)*y2/(x2-x1);
    a1=y
    y1=b11;
    y2=b12;
    y=(x2-x)*y1/(x2-x1)+(x-x1)*y2/(x2-x1);
    b1=y
    x1=G2x21;
    x2=G2x22;
    y1=a21;
    y2=a22;
    y=(x-x1)*y2/(x2-x1)-(x-x2)*y1/(x2-x1);
    a2=y
    y1=b21;
    y2=b22;
    y=(x-x1)*y2/(x2-x1)-(x-x2)*y1/(x2-x1);
    b2=y
    x1=G1x1;
    x2=G1x2;
    x=G1a;
    y1=a1;
    y2=a2;
    y=(x2-x)*y1/(x2-x1)+(x-x1)*y2/(x2-x1);
    a=y
    y1=b1;
    y2=b2;
    y=(x2-x)*y1/(x2-x1)+(x-x1)*y2/(x2-x1);
    b=y
elseif G1a==0
    x1=G2x11;
    x2=G2x12;
    x=G2a;
    y1=a11;
    y2=a12;
    y=(x2-x)*y1/(x2-x1)+(x-x1)*y2/(x2-x1);
    a1=y

```

```

y1=b11;
y2=b12;
y=(x2-x)*y1/(x2-x1)+(x-x1)*y2/(x2-x1);
b1=y
x1=G2x21;
x2=G2x22;
y1=a21;
y2=a22;
y=(x2-x)*y1/(x2-x1)+(x-x1)*y2/(x2-x1);
a2=y
y1=b21;
y2=b22;
y=(x2-x)*y1/(x2-x1)+(x-x1)*y2/(x2-x1);
b2=y
x1=G1x1;
x2=G1x2;
x=G1a;
y1=a1;
y2=a2;
y=(x2-x)*y1/(x2-x1)+(x-x1)*y2/(x2-x1);
a=y
y1=b1;
y2=b2;
y=(x2-x)*y1/(x2-x1)+(x-x1)*y2/(x2-x1);
b=y
else
x1=G2x11;
x2=G2x12;
x=G2a;
y1=a11;
y2=a12;
y=(x2-x)*y1/(x2-x1)+(x-x1)*y2/(x2-x1);
a1=y
y1=b11;
y2=b12;
y=(x2-x)*y1/(x2-x1)+(x-x1)*y2/(x2-x1);
b1=y
x1=G2x21;
x2=G2x22;
y1=a21;
y2=a22;
y=(x2-x)*y1/(x2-x1)+(x-x1)*y2/(x2-x1);
a2=y
y1=b21;
y2=b22;
y=(x2-x)*y1/(x2-x1)+(x-x1)*y2/(x2-x1);
b2=y
x1=G1x1;
x2=G1x2;
x=G1a;
y1=a1;
y2=a2;
y=(x2-x)*y1/(x2-x1)+(x-x1)*y2/(x2-x1);
a=y
y1=b1;
y2=b2;
y=(x2-x)*y1/(x2-x1)+(x-x1)*y2/(x2-x1);
b=y

```

```

end
if G1;G2
bb=a;
aa=b;
b=bb
a=aa
end
end

```

%CHI: Determine Chi-Square Goodness-of-Fit

```

if magi=10&magi15
for i=1:200
bc(i)=abs(BP1(i)-0.5);
wc(i)=abs(WP1(i)-0.5);
rc(i)=abs(RP1(i)-0.5);
rymlec(i)=abs(RymleP1(i)-0.5);
rymomc(i)=abs(RymomP1(i)-0.5);
r1c(i)=abs(R1P1(i)-0.5);
lc(i)=abs(LP1(i)-0.5);
nc(i)=abs(NP1(i)-0.5);
end
[bc,samb]=min(bc);
[wc,samw]=min(wc);
[rc,samr]=min(rc);
[rymlec,samrymle]=min(rymlec);
[rymomc,samrymom]=min(rymomc);
[r1c,samr1]=min(r1c);
[lc,saml]=min(lc);
[nc,samn]=min(nc);
NB1=0;
NB2=0;
NW1=0;
NW2=0;
NR1=0;
NR2=0;
NRymle1=0;
NRymle2=0;
NRymom1=0;
NRymom2=0;
NR11=0;
NR12=0;
NL1=0;
NL2=0;
NN1=0;
NN2=0;
s0um1=sort(s0um);
for i=1:mag
if s0um1(i);samb/200
NB1=NB1+1;
end
if s0um1(i);samw/200
NB2=NB2+1;
end
if s0um1(i);samr/200
NW1=NW1+1;
end
end

```

```

if s0um1(i);samw/200
    NW2=NW2+1;
end
if s0um1(i);samr/200
    NR1=NR1+1;
end
if s0um1(i);samr/200
    NR2=NR2+1;
end
if s0um1(i);samrymle/200
    NRymle1=NRymle1+1;
end
if s0um1(i);samrymle/200
    NRymle2=NRymle2+1;
end
if s0um1(i);samrymom/200
    NRymom1=NRymom1+1;
end
if s0um1(i);samrymom/200
    NRymom2=NRymom2+1;
end
if s0um1(i);samr1/200
    NR11=NR11+1;
end
if s0um1(i);samr1/200
    NR12=NR12+1;
end
if s0um1(i);sam1/200
    NL1=NL1+1;
end
if s0um1(i);sam1/200
    NL2=NL2+1;
end
if s0um1(i);samn/200
    NN1=NN1+1;
end
if s0um1(i);samn/200
    NN2=NN2+1;
end
end
TSB1=((NB1-0.5*mag)^2)/(0.5*mag);
TSB2=((NB2-0.5*mag)^2)/(0.5*mag);
TSB=TSB1+TSB2
TSW1=((NW1-0.5*mag)^2)/(0.5*mag);
TSW2=((NW2-0.5*mag)^2)/(0.5*mag);
TSW=TSW1+TSW2
TSR1=((NR1-0.5*mag)^2)/(0.5*mag);
TSR2=((NR2-0.5*mag)^2)/(0.5*mag);
TSR=TSR1+TSR2
TSRymle1=((NRymle1-0.5*mag)^2)/(0.5*mag);
TSRymle2=((NRymle2-0.5*mag)^2)/(0.5*mag);
TSRymle=TSRymle1+TSRymle2
TSRymom1=((NRymom1-0.5*mag)^2)/(0.5*mag);
TSRymom2=((NRymom2-0.5*mag)^2)/(0.5*mag);
TSRymom=TSRymom1+TSRymom2
TSR11=((NR11-0.5*mag)^2)/(0.5*mag);
TSR12=((NR12-0.5*mag)^2)/(0.5*mag);
TSR1=TSR11+TSR12

TSL1=((NL1-0.5*mag)^2)/(0.5*mag);
TSL2=((NL2-0.5*mag)^2)/(0.5*mag);
TSL=TSL1+TSL2
TSN1=((NN1-0.5*mag)^2)/(0.5*mag);
TSN2=((NN2-0.5*mag)^2)/(0.5*mag);
TSN=TSN1+TSN2
end
%pause;
if 15;=mag&mag;20
    for i=1:200
        bc1(i)=abs(BP1(i)-1/3);
        bc2(i)=abs(BP1(i)-2/3);
        wc1(i)=abs(WP1(i)-1/3);
        wc2(i)=abs(WP1(i)-2/3);
        rc1(i)=abs(RP1(i)-1/3);
        rc2(i)=abs(RP1(i)-2/3);
        rymomc1(i)=abs(RymomP1(i)-1/3);
        rymomc2(i)=abs(RymomP1(i)-2/3);
        rymlec1(i)=abs(RymleP1(i)-1/3);
        rymlec2(i)=abs(RymleP1(i)-2/3);
        r1c1(i)=abs(R1P1(i)-1/3);
        r1c2(i)=abs(R1P1(i)-2/3);
        lc1(i)=abs(LP1(i)-1/3);
        lc2(i)=abs(LP1(i)-2/3);
        nc1(i)=abs(NP1(i)-1/3);
        nc2(i)=abs(NP1(i)-2/3);
    end
    [bc1,samb1]=min(bc1);
    [wc1,samw1]=min(wc1);
    [rc1,samr1]=min(rc1);
    [rymlec1,samrymle1]=min(rymlec1);
    [rymomc1,samrymom1]=min(rymomc1);
    [r1c1,samr11]=min(r1c1);
    [lc1,saml1]=min(lc1);
    [nc1,samn1]=min(nc1);
    [bc2,samb2]=min(bc2);
    [wc2,samw2]=min(wc2);
    [rc2,samr2]=min(rc2);
    [rymomc2,samrymom2]=min(rymomc2);
    [rymlec2,samrymle2]=min(rymlec2);
    [r1c2,samr12]=min(r1c2);
    [lc2,saml2]=min(lc2);
    [nc2,samn2]=min(nc2);
    NB1=0;
    NB2=0;
    NB3=0;
    NW1=0;
    NW2=0;
    NW3=0;
    NR1=0;
    NR2=0;
    NR3=0;
    NRymle1=0;
    NRymle2=0;
    NRymle3=0;
    NRymom1=0;
    NRymom2=0;
    NRymom3=0;

```



```

NR11=0;
NR12=0;
NR13=0;
NL1=0;
NL2=0;
NL3=0;
NN1=0;
NN2=0;
NN3=0;
s0um1=sort(s0um);
for i=1:mag
    if s0um1(i);=samb1/200
        NB1=NB1+1;
    end
    if s0um1(i);=samb1/200&s0um1(i);=samb2/200
        NB2=NB2+1;
    end
    if s0um1(i);=samb2/200
        NB3=NB3+1;
    end
    if s0um1(i);=samw1/200
        NW1=NW1+1;
    end
    if s0um1(i);=samw1/200&s0um1(i);=samw2/200
        NW2=NW2+1;
    end
    if s0um1(i);=samw2/200
        NW3=NW3+1;
    end
    if s0um1(i);=samr1/200
        NR1=NR1+1;
    end
    if s0um1(i);=samr1/200&s0um1(i);=samr2/200
        NR2=NR2+1;
    end
    if s0um1(i);=samr2/200
        NR3=NR3+1;
    end
    if s0um1(i);=samrymle1/200
        NRymle1=NRymle1+1;
    end
    if s0um1(i);=samrymle1/200&s0um1(i);=samrymle2/200
        NRy2=NRy2+1;
    end
    if s0um1(i);=samrymle2/200
        NRymle3=NRymle3+1;
    end
    if s0um1(i);=samrymom1/200
        NRymom1=NRymom1+1;
    end
    if s0um1(i);=samrymom1/200&s0um1(i);=samrymom2/200
        NRymom2=NRymom2+1;
    end
    if s0um1(i);=samrymom2/200
        NRymom3=NRymom3+1;
    end
    if s0um1(i);=samr11/200
        NR11=NR11+1;

```

```

end
if s0um1(i);=samr11/200&s0um1(i);=samr12/200
    NR12=NR12+1;
end
if s0um1(i);=samr12/200
    NR13=NR13+1;
end
if s0um1(i);=sam11/200
    NL1=NL1+1;
end
if s0um1(i);=sam11/200&s0um1(i);=sam12/200
    NL2=NL2+1;
end
if s0um1(i);=sam12/200
    NL3=NL3+1;
end
if s0um1(i);=samn1/200
    NN1=NN1+1;
end
if s0um1(i);=samn1/200&s0um1(i);=samn2/200
    NN2=NN2+1;
end
if s0um1(i);=samn2/200
    NN3=NN3+1;
end
end
TSB1=((NB1-(1/3)^mag)^2)/((1/3)^mag);
TSB2=((NB2-(1/3)^mag)^2)/((1/3)^mag);
TSB3=((NB3-(1/3)^mag)^2)/((1/3)^mag);
TSB=TSB1+TSB2+TSB3
TSW1=((NW1-(1/3)^mag)^2)/((1/3)^mag);
TSW2=((NW2-(1/3)^mag)^2)/((1/3)^mag);
TSW3=((NW3-(1/3)^mag)^2)/((1/3)^mag);
TSW=TSW1+TSW2+TSW3
TSR1=((NR1-(1/3)^mag)^2)/((1/3)^mag);
TSR2=((NR2-(1/3)^mag)^2)/((1/3)^mag);
TSR3=((NR3-(1/3)^mag)^2)/((1/3)^mag);
TSR=TSR1+TSR2+TSR3
TSRymle1=((NRymle1-(1/3)^mag)^2)/((1/3)^mag);
TSRymle2=((NRymle2-(1/3)^mag)^2)/((1/3)^mag);
TSRymle3=((NRymle3-(1/3)^mag)^2)/((1/3)^mag);
TSRymle=TSRymle1+TSRymle2+TSRymle3
TSRymom1=((NRymom1-(1/3)^mag)^2)/((1/3)^mag);
TSRymom2=((NRymom2-(1/3)^mag)^2)/((1/3)^mag);
TSRymom3=((NRymom3-(1/3)^mag)^2)/((1/3)^mag);
TSRymom=TSRymom1+TSRymom2+TSRymom3
TSR11=((NR11-(1/3)^mag)^2)/((1/3)^mag);
TSR12=((NR12-(1/3)^mag)^2)/((1/3)^mag);
TSR13=((NR13-(1/3)^mag)^2)/((1/3)^mag);
TSR1=TSR11+TSR12+TSR13
TSL1=((NL1-(1/3)^mag)^2)/((1/3)^mag);
TSL2=((NL2-(1/3)^mag)^2)/((1/3)^mag);
TSL3=((NL3-(1/3)^mag)^2)/((1/3)^mag);
TSL=TSL1+TSL2+TSL3
TSN1=((NN1-(1/3)^mag)^2)/((1/3)^mag);
TSN2=((NN2-(1/3)^mag)^2)/((1/3)^mag);
TSN3=((NN3-(1/3)^mag)^2)/((1/3)^mag);
TSN=TSN1+TSN2+TSN3

```

```

end
if 20;=mag&n.ag;25
for i=1:200
    bc1(i)=abs(BP1(i)-0.25);
    bc2(i)=abs(BP1(i)-0.5);
    bc3(i)=abs(BP1(i)-0.75);
    wc1(i)=abs(WP1(i)-0.25);
    wc2(i)=abs(WP1(i)-0.5);
    wc3(i)=abs(WP1(i)-0.75);
    rc1(i)=abs(RP1(i)-0.25);
    rc2(i)=abs(RP1(i)-0.5);
    rc3(i)=abs(RP1(i)-0.75);
    rymlec1(i)=abs(RymleP1(i)-0.25);
    rymlec2(i)=abs(RymleP1(i)-0.5);
    rymlec3(i)=abs(RymleP1(i)-0.75);
    rymomc1(i)=abs(RymomP1(i)-0.25);
    rymomc2(i)=abs(RymomP1(i)-0.5);
    rymomc3(i)=abs(RymomP1(i)-0.75);
    rlc1(i)=abs(R1P1(i)-0.25);
    rlc2(i)=abs(R1P1(i)-0.5);
    rlc3(i)=abs(R1P1(i)-0.75);
    lc1(i)=abs(LP1(i)-0.25);
    lc2(i)=abs(LP1(i)-0.5);
    lc3(i)=abs(LP1(i)-0.75);
    nc1(i)=abs(NP1(i)-0.25);
    nc2(i)=abs(NP1(i)-0.5);
    nc3(i)=abs(NP1(i)-0.75);
end
[bc1,samb1]=min(bc1);
[wc1,samw1]=min(wc1);
[rc1,samr1]=min(rc1);
[rymlec1,samrymle1]=min(rymlec1);
[rymomc1,samrymom1]=min(rymomc1);
[rlc1,samr11]=min(rlc1);
[lc1,saml1]=min(lc1);
[nc1,samn1]=min(nc1);
[bc2,samb2]=min(bc2);
[wc2,samw2]=min(wc2);
[rc2,samr2]=min(rc2);
[rymlec2,samrymle2]=min(rymlec2);
[rymomc2,samrymom2]=min(rymomc2);
[rlc2,samr12]=min(rlc2);
[lc2,saml2]=min(lc2);
[nc2,samn2]=min(nc2);
[bc3,samb3]=min(bc3);
[wc3,samw3]=min(wc3);
[rc3,samr3]=min(rc3);
[rymlec3,samrymle3]=min(rymlec3);
[rymomc3,samrymom3]=min(rymomc3);
[rlc3,samr13]=min(rlc3);
[lc3,saml3]=min(lc3);
[nc3,samn3]=min(nc3);
NB1=0;
NB2=0;
NB3=0;
NB4=0;
NW1=0;
NW2=0;

NW3=0;
NW4=0;
NR1=0;
NR2=0;
NR3=0;
NR4=0;
NRymle1=0;
NRymle2=0;
NRymle3=0;
NRymle4=0;
NRymom1=0;
NRymom2=0;
NRymom3=0;
NRymom4=0;
NR11=0;
NR12=0;
NR13=0;
NR14=0;
NL1=0;
NL2=0;
NL3=0;
NL4=0;
NN1=0;
NN2=0;
NN3=0;
NN4=0;
s0um1=sort(s0um);
for i=1:mag
    if s0um1(i);=samb1/200
        NB1=NB1+1;
    end
    if s0um1(i);samb1/200&s0um1(i);=samb2/200
        NB2=NB2+1;
    end
    if s0um1(i);samb2/200&s0um1(i);=samb3/200
        NB3=NB3+1;
    end
    if s0um1(i);samb3/200
        NB4=NB4+1;
    end
    if s0um1(i);=samw1/200
        NW1=NW1+1;
    end
    if s0um1(i);samw1/200&s0um1(i);=-samw2/200
        NW2=NW2+1;
    end
    if s0um1(i);samw2/200&s0um1(i);=samw3/200
        NW3=NW3+1;
    end
    if s0um1(i);samw3/200
        NW4=NW4+1;
    end
    if s0um1(i);=samr1/200
        NR1=NR1+1;
    end
    if s0um1(i);samr1/200&s0um1(i);=samr2/200
        NR2=NR2+1;
    end
end

```

```

if s0um1(i);samr2/200&s0um1(i);=samr3/200
    NR3=NR3+1;
end
if s0um1(i);samr3/200
    NR4=NR4+1;
end
if s0um1(i);samrymle1/200
    NRymle1=NRymle1+1;
end
if s0um1(i);samrymle1/200&s0um1(i);=samrymle2/200
    NRymle2=NRymle2+1;
end
if s0um1(i);samrymle2/200&s0um1(i);=samrymle3/200
    NRymle3=NRymle3+1;
end
if s0um1(i);samrymle3/200
    NRymle4=NRymle4+1;
end
if s0um1(i);samrymom1/200
    NRymom1=NRymom1+1;
end
if s0um1(i);samrymom1/200&s0um1(i);=samrymom2/200
    NRymom2=NRymom2+1;
end
if s0um1(i);samrymom2/200&s0um1(i);=samrymom3/200
    NRymom3=NRymom3+1;
end
if s0um1(i);samrymom3/200
    NRymom4=NRymom4+1;
end
if s0um1(i);samr11/200
    NR11=NR11+1;
end
if s0um1(i);samr11/200&s0um1(i);=samr12/200
    NR12=NR12+1;
end
if s0um1(i);samr12/200&s0um1(i);=samr13/200
    NR13=NR13+1;
end
if s0um1(i);samr13/200
    NR14=NR14+1;
end
if s0um1(i);samr1/200
    NL1=NL1+1;
end
if s0um1(i);samr1/200&s0um1(i);=samr2/200
    NL2=NL2+1;
end
if s0um1(i);samr2/200&s0um1(i);=samr3/200
    NL3=NL3+1;
end
if s0um1(i);samr3/200
    NL4=NL4+1;
end
if s0um1(i);samn1/200
    NN1=NN1+1;
end
if s0um1(i);samn1/200&s0um1(i);=samn2/200

```

```

    NN2=NN2+1;
end
if s0um1(i);samn2/200&s0um1(i);=samn3/200
    NN3=NN3+1;
end
if s0um1(i);samn3/200
    NN4=NN4+1;
end
end
TSB1=((NB1-0.25*mag)^2)/(0.25*mag);
TSB2=((NB2-0.25*mag)^2)/(0.25*mag);
TSB3=((NB3-0.25*mag)^2)/(0.25*mag);
TSB4=((NB4-0.25*mag)^2)/(0.25*mag);
TSB=TSB1+TSB2+TSB3+TSB4
TSW1=((NW1-0.25*mag)^2)/(0.25*mag);
TSW2=((NW2-0.25*mag)^2)/(0.25*mag);
TSW3=((NW3-0.25*mag)^2)/(0.25*mag);
TSW4=((NW4-0.25*mag)^2)/(0.25*mag);
TSW=TSW1+TSW2+TSW3+TSW4
TSR1=((NR1-0.25*mag)^2)/(0.25*mag);
TSR2=((NR2-0.25*mag)^2)/(0.25*mag);
TSR3=((NR3-0.25*mag)^2)/(0.25*mag);
TSR4=((NR4-0.25*mag)^2)/(0.25*mag);
TSR=TSR1+TSR2+TSR3+TSR4
TSRymle1=((NRymle1-0.25*mag)^2)/(0.25*mag);
TSRymle2=((NRymle2-0.25*mag)^2)/(0.25*mag);
TSRymle3=((NRymle3-0.25*mag)^2)/(0.25*mag);
TSRymle4=((NRymle4-0.25*mag)^2)/(0.25*mag);
TSRymle=TSRymle1+TSRymle2+TSRymle3+TSRymle4
TSRymom1=((NRymom1-0.25*mag)^2)/(0.25*mag);
TSRymom2=((NRymom2-0.25*mag)^2)/(0.25*mag);
TSRymom3=((NRymom3-0.25*mag)^2)/(0.25*mag);
TSRymom4=((NRymom4-0.25*mag)^2)/(0.25*mag);
TSRymom=TSRymom1+TSRymom2+TSRymom3+TSRymom4
TSR11=((NR11-0.25*mag)^2)/(0.25*mag);
TSR12=((NR12-0.25*mag)^2)/(0.25*mag);
TSR13=((NR13-0.25*mag)^2)/(0.25*mag);
TSR14=((NR14-0.25*mag)^2)/(0.25*mag);
TSR1=TSR11+TSR12+TSR13+TSR14
TSL1=((NL1-0.25*mag)^2)/(0.25*mag);
TSL2=((NL2-0.25*mag)^2)/(0.25*mag);
TSL3=((NL3-0.25*mag)^2)/(0.25*mag);
TSL4=((NL4-0.25*mag)^2)/(0.25*mag);
TSL=TSL1+TSL2+TSL3+TSL4
TSN1=((NN1-0.25*mag)^2)/(0.25*mag);
TSN2=((NN2-0.25*mag)^2)/(0.25*mag);
TSN3=((NN3-0.25*mag)^2)/(0.25*mag);
TSN4=((NN4-0.25*mag)^2)/(0.25*mag);
TSN=TSN1+TSN2+TSN3+TSN4
end
if mag;=25
    for i=1:200
        bc1(i)=abs(BP1(i)-0.2);
        bc2(i)=abs(BP1(i)-0.4);
        bc3(i)=abs(BP1(i)-0.6);
        bc4(i)=abs(BP1(i)-0.8);
        wc1(i)=abs(WP1(i)-0.2);
        wc2(i)=abs(WP1(i)-0.4);

```

```

wc3(i)=abs(WP1(i)-0.6);
wc4(i)=abs(WP1(i)-0.8);
rc1(i)=abs(RP1(i)-0.2);
rc2(i)=abs(RP1(i)-0.4);
rc3(i)=abs(RP1(i)-0.6);
rc4(i)=abs(RP1(i)-0.8);
rymlec1(i)=abs(RymleP1(i)-0.2);
rymlec2(i)=abs(RymleP1(i)-0.4);
rymlec3(i)=abs(RymleP1(i)-0.6);
rymlec4(i)=abs(RymleP1(i)-0.8);
rymomc1(i)=abs(RymomP1(i)-0.2);
rymomc2(i)=abs(RymomP1(i)-0.4);
rymomc3(i)=abs(RymomP1(i)-0.6);
rymomc4(i)=abs(RymomP1(i)-0.8);
r1c1(i)=abs(R1P1(i)-0.2);
r1c2(i)=abs(R1P1(i)-0.4);
r1c3(i)=abs(R1P1(i)-0.6);
r1c4(i)=abs(R1P1(i)-0.8);
lc1(i)=abs(LP1(i)-0.2);
lc2(i)=abs(LP1(i)-0.4);
lc3(i)=abs(LP1(i)-0.6);
lc4(i)=abs(LP1(i)-0.8);
nc1(i)=abs(NP1(i)-0.2);
nc2(i)=abs(NP1(i)-0.4);
nc3(i)=abs(NP1(i)-0.6);
nc4(i)=abs(NP1(i)-0.8);
end
[bc1,samb1]=min(bc1);
[wc1,samw1]=min(wc1);
[rc1,samr1]=min(rc1);
[rymlec1,samrymle1]=min(rymlec1);
[rymomc1,samrymom1]=min(rymomc1);
[r1c1,samr11]=min(r1c1);
[lc1,saml1]=min(lc1);
[nc1,samn1]=min(nc1);
[bc2,samb2]=min(bc2);
[wc2,samw2]=min(wc2);
[rc2,samr2]=min(rc2);
[rymlec2,samrymle2]=min(rymlec2);
[rymomc2,samrymom2]=min(rymomc2);
[r1c2,samr12]=min(r1c2);
[lc2,saml2]=min(lc2);
[nc2,samn2]=min(nc2);
[bc3,samb3]=min(bc3);
[wc3,samw3]=min(wc3);
[rc3,samr3]=min(rc3);
[rymlec3,samrymle3]=min(rymlec3);
[rymomc3,samrymom3]=min(rymomc3);
[r1c3,samr13]=min(r1c3);
[lc3,saml3]=min(lc3);
[nc3,samn3]=min(nc3);
[bc4,samb4]=min(bc4);
[wc4,samw4]=min(wc4);
[rc4,samr4]=min(rc4);
[rymlec4,samrymle4]=min(rymlec4);
[rymomc4,samrymom4]=min(rymomc4);
[r1c4,samr14]=min(r1c4);
[lc4,saml4]=min(lc4);

```

```

[nc4,samn4]=min(nc4);
NB1=0;
NB2=0;
NB3=0;
NB4=0;
NB5=0;
NW1=0;
NW2=0;
NW3=0;
NW4=0;
NW5=0;
NR1=0;
NR2=0;
NR3=0;
NR4=0;
NR5=0;
NRymle1=0;
NRymle2=0;
NRymle3=0;
NRymle4=0;
NRymle5=0;
NRymom1=0;
NRymom2=0;
NRymom3=0;
NRymom4=0;
NRymom5=0;
NR11=0;
NR12=0;
NR13=0;
NR14=0;
NR15=0;
NL1=0;
NL2=0;
NL3=0;
NL4=0;
NL5=0;
NN1=0;
NN2=0;
NN3=0;
NN4=0;
NN5=0;
s0um1=sort(s0um);
for i=1:mag
    if s0um1(i);=samb1/200
        NB1=NB1+1;
    end
    if s0um1(i);samb1/200&s0um1(i);=samb2/200
        NB2=NB2+1;
    end
    if s0um1(i);samb2/200&s0um1(i);=samb3/200
        NB3=NB3+1;
    end
    if s0um1(i);samb3/200&s0um1(i);=samb4/200
        NB4=NB4+1;
    end
    if s0um1(i);samb2/200
        NB5=NB5+1;
    end
end

```

```

if s0um1(i);=samw1/200
  NW1=NW1+1;
end
if s0um1(i);samw1/200&s0um1(i);=samw2/200
  NW2=NW2+1;
end
if s0um1(i);samw2/200&s0um1(i);=samw3/200
  NW3=NW3+1;
end
if s0um1(i);samw3/200&s0um1(i);=samw4/200
  NW4=NW4+1;
end
if s0um1(i);samw4/200
  NW5=NW5+1;
end
if s0um1(i);=samr1/200
  NR1=NR1+1;
end
if s0um1(i);samr1/200&s0um1(i);=samr2/200
  NR2=NR2+1;
end
if s0um1(i);samr2/200&s0um1(i);=samr3/200
  NR3=NR3+1;
end
if s0um1(i);samr3/200&s0um1(i);=samr4/200
  NR4=NR4+1;
end
if s0um1(i);samr4/200
  NR5=NR5+1;
end
if s0um1(i);=samrymle1/200
  NRymle1=NRymle1+1;
end
if s0um1(i);samrymle1/200&s0um1(i);=samrymle2/200
  NRymle2=NRymle2+1;
end
if s0um1(i);samrymle2/200&s0um1(i);=samrymle3/200
  NRymle3=NRymle3+1;
end
if s0um1(i);samrymle3/200&s0um1(i);=samrymle4/200
  NRymle4=NRymle4+1;
end
if s0um1(i);samrymle4/200
  NRymle5=NRymle5+1;
end
if s0um1(i);=samrymom1/200
  NRymom1=NRymom1+1;
end
if s0um1(i);samrymom1/200&s0um1(i);=samrymom2/200
  NRymom2=NRymom2+1;
end
if s0um1(i);samrymom2/200&s0um1(i);=samrymom3/200
  NRymom3=NRymom3+1;
end
if s0um1(i);samrymom3/200&s0um1(i);=samrymom4/200
  NRymom4=NRymom4+1;
end
if s0um1(i);samrymom4/200

```

```

  NRymom5=NRymom5+1;
end
if s0um1(i);=samr11/200
  NR11=NR11+1;
end
if s0um1(i);samr11/200&s0um1(i);=samr12/200
  NR12=NR12+1;
end
if s0um1(i);samr12/200&s0um1(i);=samr13/200
  NR13=NR13+1;
end
if s0um1(i);samr13/200&s0um1(i);=samr14/200
  NR14=NR14+1;
end
if s0um1(i);samr14/200
  NR15=NR15+1;
end
if s0um1(i);=sam11/200
  NL1=NL1+1;
end
if s0um1(i);sam11/200&s0um1(i);=sam12/200
  NL2=NL2+1;
end
if s0um1(i);sam12/200&s0um1(i);=sam13/200
  NL=NL3+1;
end
if s0um1(i);sam13/200&s0um1(i);=sam14/200
  NL4=NL4+1;
end
if s0um1(i);sam14/200
  NL5=NL5+1;
end
if s0um1(i);=samn1/200
  NN1=NN1+1;
end
if s0um1(i);samn1/200&s0um1(i);=samn2/200
  NN2=NN2+1;
end
if s0um1(i);samn2/200&s0um1(i);=samn3/200
  NN3=NN3+1;
end
if s0um1(i);samn3/200&s0um1(i);=samn4/200
  NN4=NN4+1;
end
if s0um1(i);samn4/200
  NN5=NN5+1;
end
end
TSB1=((NB1-0.2*mag)^2)/(0.2*mag);
TSB2=((NB2-0.2*mag)^2)/(0.2*mag);
TSB3=((NB3-0.2*mag)^2)/(0.2*mag);
TSB4=((NB4-0.2*mag)^2)/(0.2*mag);
TSB5=((NB5-0.2*mag)^2)/(0.2*mag);
TSB=TSB1+TSB2+TSB3+TSB4+TSB5
TSW1=((NW1-0.2*mag)^2)/(0.2*mag);
TSW2=((NW2-0.2*mag)^2)/(0.2*mag);
TSW3=((NW3-0.2*mag)^2)/(0.2*mag);
TSW4=((NW4-0.2*mag)^2)/(0.2*mag);

```

```

TSW5=((NW5-0.2*mag)^2)/(0.2*mag);
TSW=TSW1+TSW2+TSW3+TSW4+TSW5
TSR1=((NR1-0.2*mag)^2)/(0.2*mag);
TSR2=((NR2-0.2*mag)^2)/(0.2*mag);
TSR3=((NR3-0.2*mag)^2)/(0.2*mag);
TSR4=((NR4-0.2*mag)^2)/(0.2*mag);
TSR5=((NR5-0.2*mag)^2)/(0.2*mag);
TSR=TSR1+TSR2+TSR3+TSR4+TSR5
TSRymle1=((NRymle1-0.2*mag)^2)/(0.2*mag);
TSRymle2=((NRymle2-0.2*mag)^2)/(0.2*mag);
TSRymle3=((NRymle3-0.2*mag)^2)/(0.2*mag);
TSRymle4=((NRymle4-0.2*mag)^2)/(0.2*mag);
TSRymle5=((NRymle5-0.2*mag)^2)/(0.2*mag);
TSRymle=TSRymle1+TSRymle2+TSRymle3
+TSRymle4+TSRymle5
TSRymom1=((NRymom1-0.2*mag)^2)/(0.2*mag);
TSRymom2=((NRymom2-0.2*mag)^2)/(0.2*mag);
TSRymom3=((NRymom3-0.2*mag)^2)/(0.2*mag);
TSRymom4=((NRymom4-0.2*mag)^2)/(0.2*mag);
TSRymom5=((NRymom5-0.2*mag)^2)/(0.2*mag);
TSRymom=TSRymom1+TSRymom2+TSRymom3

```

```

+TSRymom4+TSRymom5
TSR11=((NR11-0.2*mag)^2)/(0.2*mag);
TSR12=((NR12-0.2*mag)^2)/(0.2*mag);
TSR13=((NR13-0.2*mag)^2)/(0.2*mag);
TSR14=((NR14-0.2*mag)^2)/(0.2*mag);
TSR15=((NR15-0.2*mag)^2)/(0.2*mag);
TSR1=TSR11+TSR12+TSR13+TSR14+TSR15
TSL1=((NL1-0.2*mag)^2)/(0.2*mag);
TSL2=((NL2-0.2*mag)^2)/(0.2*mag);
TSL3=((NL3-0.2*mag)^2)/(0.2*mag);
TSL4=((NL4-0.2*mag)^2)/(0.2*mag);
TSL5=((NL5-0.2*mag)^2)/(0.2*mag);
TSL=TSL1+TSL2+TSL3+TSL4+TSL5
TSN1=((NN1-0.2*mag)^2)/(0.2*mag);
TSN2=((NN2-0.2*mag)^2)/(0.2*mag);
TSN3=((NN3-0.2*mag)^2)/(0.2*mag);
TSN4=((NN4-0.2*mag)^2)/(0.2*mag);
TSN5=((NN5-0.2*mag)^2)/(0.2*mag);
TSN=TSN1+TSN2+TSN3+TSN4+TSN5
end

```

Bibliography

1. Beckman, R. J. "Maximum Likelihood Estimation for the Beta Distribution," *Journal of Statistical Computer Simulation*, 7:253-258 (1978).
2. Breiman, Leo. *Statistics With a View Toward Applications*. Houghton Mifflin, 1973.
3. Chernoff, H. and E.L. Lehmann. "The Use of Maximum Likelihood Estimates in Chi-Square Tests for Goodness of Fit," *Annals of Mathematical Statistics*, 25:579-586 (1954).
4. Conover, W. J. *Practical Nonparametric Statistics*. John Wiley and Sons, 1980.
5. Cramer, Harald. *Mathematical Methods of Statistics*. Princeton Press, 1946.
6. Crispin, J.W. and K.M. Siegel. *Methods of Radar Cross Section Analysis*. Academic Press, 1968.
7. Derman, Cyrus et al. *A Guide to Probability Theory and Application*. Holt, Rinehart, and Winston, 1973.
8. DiFranco, J.V. and W.L. Rubin. *Radar Detection*. Prentice-Hall, 1980.
9. Dowdy, Patrick C. "RCS Probability Distribution Function Modeling of a Fluctuating Target," *IEEE*:164-168 (1991).
10. Fisher, R.A. *Statistical Methods for Research Workers*. Princeton Press, 1946.
11. Knott, Eugene F. et al. *Radar Cross Section, Its Prediction, Measurement, and Reduction*. Artec House, 1986.
12. Kraus, John D. *Electromagnetics*. McGraw-Hill, 1984.
13. Kulp, R. L. "Detection Probabilities for Beta-Distributed Scattering Cross Sections," *Electromagnetics*, 4:165-183 (1984).
14. Law, Averill M. and W. David Kelton. *Simulation Modeling and Analysis*. McGraw-Hill, 1982.
15. Lewis, P.A.W. and E.J. Orav. *Simulation Methodology for Statisticians, Operations, and Engineers*. Wadsworth and Brooks, 1988.
16. Link, 2Lt Jon N. *Accuracy Estimate for Radar Cross Section Measurements of Targets Modelled by Multiple Independent Scatterers in Constant Clutter*. MS Thesis, AFIT/GE/EE/83D-39, School of Engineering, Air Force Institute of Technology (AU), Wright-Patterson AFB OH, December 1983. DTIC Number AD-A138075.
17. Maffett, Andrew L. *Topics for a Statistical Description of Radar Cross Section*. John Wiley and Sons, 1989.
18. Melsa, James L. and David L. Cohn. *Decision and Estimation Theory*. McGraw-Hill, 1980.
19. Otnes, Robert K. and Loren Enochson. *Applied Time Series Analysis*. John Wiley and Sons, 1978.

20. Sandhu, G.S. and A.V. Saylor. "A Real-Time Statistical Radar Target Model," *IEEE Transactions on Aerospace and Electronics Systems*, AES-21:490-507 (1985).
21. Shenton, L.R. and K.O. Bowman. *Maximum Likelihood Estimates in Small Samples*. McMillan, 1977.

Vita

Mark Clayton Robinson was born 24 June 1959 in Seattle, WA. In 1981 he enlisted in the Air Force and was assigned to the 2nd Strategic Bombardment Wing at Barksdale AFB, LA as an Electronic Warfare Technician. He entered AECP and graduated from Louisiana Tech University with a BSEE in November, 1987. After completing OTS, he was assigned to the 341st Strategic Missile Wing at Malmstrom AFB, MT as a Technical Engineer for Minuteman II and III ICBM systems. He separated from the Air Force in September, 1992 and begins work as a Communications Engineer for Pacific Power of Portland, OR in December, 1992.

REPORT DOCUMENTATION PAGE

Form Approved
OMB No. 0704-0188

Public reporting burden for this collection of information is estimated to average 1 hour per response, including the time for reviewing instructions, searching existing data sources, gathering and maintaining the data needed, and completing and reviewing the collection of information. Send comments regarding this burden estimate or any other aspect of this collection of information, including suggestions for reducing this burden, to Washington Headquarters Services, Directorate for Information Operations and Reports, 1215 Jefferson Davis Highway, Suite 1204, Arlington, VA 22202-4302, and to the Office of Management and Budget, Paperwork Reduction Project (0704-0188), Washington, DC 20503.

| | | | | | |
|---|---|--|----------------------------------|---|--|
| 1. AGENCY USE ONLY (Leave blank) | | 2. REPORT DATE December, 1992 | | 3. REPORT TYPE AND DATES COVERED Master's Thesis | |
| 4. TITLE AND SUBTITLE Radar Cross Section Models for Limited Aspect Angle Windows | | | | 5. FUNDING NUMBERS | |
| 6. AUTHOR(S) Mark C. Robinson, Captain, USAFR | | | | | |
| 7. PERFORMING ORGANIZATION NAME(S) AND ADDRESS(ES) Air Force Institute of Technology WPAFB, OH 45433-6583 | | | | 8. PERFORMING ORGANIZATION REPORT NUMBER AFIT/GE/ENG/92D-32 | |
| 9. SPONSORING/MONITORING AGENCY NAME(S) AND ADDRESS(ES) Mr. Lee Bishop, RATSCAT Technical Director 6585 West Group/RX Holloman AFB, NM 88330-5000 | | | | 10. SPONSORING/MONITORING AGENCY REPORT NUMBER | |
| 11. SUPPLEMENTARY NOTES | | | | | |
| 12a. DISTRIBUTION/AVAILABILITY STATEMENT Approved for public release; distribution unlimited | | | | 12b. DISTRIBUTION CODE | |
| 13. ABSTRACT (Maximum 200 words) This thesis presents a method for building Radar Cross Section (RCS) models of aircraft based on static data taken from limited aspect angle windows. These models statistically characterize static RCS. This is done to show that a limited number of samples can be used to effectively characterize static aircraft RCS. The optimum models are determined by performing both a Kolmogorov and a Chi-Square goodness-of-fit test comparing the static RCS data with a variety of probability density functions (pdf) that are known to be effective at approximating the static RCS of aircraft. The optimum parameter estimator is also determined by the goodness of-fit tests if there is a difference in pdf parameters obtained by the Maximum Likelihood Estimator (MLE) and the Method of Moments (MoM) estimators. | | | | | |
| 14. SUBJECT TERMS Radar Cross Section, Statistical Modeling | | | | 15. NUMBER OF PAGES 129 | |
| | | | | 16. PRICE CODE | |
| 17. SECURITY CLASSIFICATION OF REPORT Unclassified | 18. SECURITY CLASSIFICATION OF THIS PAGE Unclassified | 19. SECURITY CLASSIFICATION OF ABSTRACT Unclassified | 20. LIMITATION OF ABSTRACT UL | | |